

**APPLICATION OF A FINE MESH NUMERICAL MODEL OF
THE NORTH SEA TO THE CALCULATION OF STORM
SURGE ELEVATIONS AND CURRENTS**

by

A. M. DAVIES

REPORT NO 28

1976

**NATURAL ENVIRONMENT
INSTITUTE OF OCEANOGRAPHIC
SCIENCES
RESEARCH COUNCIL**

INSTITUTE OF OCEANOGRAPHIC SCIENCES

Wormley, Godalming,
Surrey, GU8 5UB.
(0428 - 79 - 4141)

(Director: Professor H. Charnock)

Bidston Observatory,
Birkenhead,
Merseyside, L43 7RA.
(051-653-8633)

(Assistant Director: Dr. D. E. Cartwright)

Crossway,
Taunton,
Somerset, TA1 2DW.
(0823-86211)

(Assistant Director: M.J. Tucker)

Marine Scientific Equipment Service
Research Vessel Base,
No. 1 Dock,
Barry,
South Glamorgan, CF6 6UZ.
(04462-77451)
(Officer-in-Charge: Dr. L.M. Skinner)

*On citing this report in a bibliography the reference should be followed by
the words UNPUBLISHED MANUSCRIPT.*

APPLICATION OF A FINE MESH NUMERICAL MODEL OF
THE NORTH SEA TO THE CALCULATION OF STORM
SURGE ELEVATIONS AND CURRENTS

A. M. DAVIES

REPORT NO.28

1976

Institute of Oceanographic Sciences
Bidston Observatory
Birkenhead
Merseyside L43 7RA

CONTENTS

	Page
1. Introduction	1
2. Numerical model	2
3. The meteorological data	6
4. Calculation of the vertical profile of storm surge current.	7
5. The storm surge period of 4 November to 18 December 1973.	12
5.1 Comparison of results at various coastal gauges.	12
5.2 The negative surge of 12 November.	18
6. Concluding Remarks	23
References	25
Tables 1-2	28
Captions	30
Figures 1-7	

1. INTRODUCTION

This paper compares computed sea surface elevations and depth mean currents for the period 4 November to 18 December 1973 from a fine mesh two-dimensional hydrodynamic model of the North Sea (DAVIES 1976a) with results for the same period computed by FLATHER (1976a) using a model of the continental shelf (FLATHER 1976b). The North Sea model has a mesh resolution of $1/9^{\circ}$ latitude by $1/6^{\circ}$ longitude compared with $1/3^{\circ}$ latitude by $1/2^{\circ}$ longitude for the coarser shelf model. The finite difference grids used in the two models are shown in Figures 1 and 2.

The resolution of the present North Sea model is considerably finer than that used in earlier models of the North Sea (DUUN-CHRISTENSEN 1971, HANSEN 1961), so that the shallow coastal regions may be modelled more accurately than hitherto. The continental shelf model, covers a sufficiently large sea area to the north-west of Scotland, for the calculation of external surges, generated by meteorological forces in this region (HEAPS 1969, TIMMERMAN 1975) to be satisfactorily computed.

The M_2 and S_2 components of the tide are introduced along the open boundaries of our North Sea model, together with storm surge residual elevations computed by the shelf model, interpolated in two dimensions onto the finer mesh of the North Sea model. Along the northern open boundary of the model, observed residual elevations at Wick are used to improve the values obtained from the shelf model.

Comparing surge profiles calculated by the two models at various ports, the effect of introducing observed residuals at Wick, on the

model's northern boundary, may be considered.

An improvement in computed surge elevation was obtained for a number of surge periods, where boundary conditions were important, although during other periods when meteorological effects were dominant, little or no improvement occurred.

Contours of sea surface elevation, calculated by the model are shown, and comparing these spatial distributions with those computed by FLATHER (1976a) it is possible to illustrate the differences arising from the more detailed representation of bottomtopography within the finer mesh model, and the influence of the shallow coastal regions upon the surge magnitude.

Storm surge depth-mean residual currents are also calculated, and using an inverse Laplace transform (JELESNIANSKI 1970, FORRISTALL 1974) the wind induced current profiles at a number of selected points are determined.

2. NUMERICAL MODEL

The vertically integrated equations for storm surges, in polar coordinates, incorporating a quadratic law of bottom friction and including the non-linear advective terms are taken in the form :

(i) Continuity

$$\frac{\partial \xi}{\partial t} + \frac{1}{R \cos \phi} \left\{ \frac{\partial (dU)}{\partial \lambda} + \frac{\partial (dV \cos \phi)}{\partial \phi} \right\} = 0 \quad (1)$$

(ii) U equation of motion

$$\begin{aligned} \frac{\partial U}{\partial t} - 2\omega \sin\phi V + \frac{U}{R \cos\phi} \frac{\partial U}{\partial \lambda} + \frac{V}{R \cos\phi} \frac{\partial (U \cos\phi)}{\partial \phi} \\ = \frac{-g}{R \cos\phi} \frac{\partial \xi}{\partial \lambda} - \frac{1}{\rho R \cos\phi} \frac{\partial P}{\partial \lambda} - \frac{\rho U (U^2 + V^2)^{1/2}}{d} + \frac{F^{(s)}}{\rho d} \end{aligned} \quad (2)$$

(iii) V equation of motion

$$\begin{aligned} \frac{\partial V}{\partial t} + 2\omega \sin\phi U + \frac{U}{R \cos\phi} \frac{\partial V}{\partial \lambda} + \frac{V}{R} \frac{\partial V}{\partial \phi} \\ = -\frac{g}{R} \frac{\partial \xi}{\partial \phi} - \frac{1}{\rho R} \frac{\partial P}{\partial \phi} - \frac{\rho V (U^2 + V^2)^{1/2}}{d} + \frac{G^{(s)}}{\rho d} \end{aligned} \quad (3)$$

where the notation is :

λ, ϕ east-longitude and latitude, respectively,

t time,

ξ elevation of sea surface above the undisturbed level,

h undisturbed depth of water,

$d = h + \xi$ total depth of water,

R radius of the Earth,

ω angular speed of the Earth's rotation,
 g acceleration due to gravity,
 $F^{(s)}, G^{(s)}$ components of wind stress on sea surface to the east and the north respectively,

P atmospheric pressure at the sea surface,

U, V components of depth mean current given by

$$U = \frac{1}{h+\xi} \int_{-h}^{\xi} U(z) dz, \quad V = \frac{1}{h+\xi} \int_{-h}^{\xi} V(z) dz \quad (4)$$

$U(z), V(z)$ components of current in the directions of increasing x, ϕ respectively, at a depth z below the undisturbed sea surface,

R the coefficient of quadratic bottom friction.

We take $R = 0.0035$ close to the Dutch coast and $R = 0.0025$ away from this sea region (DAVIES 1976a). In the shelf model, $R = 0.0025$ (FLATHER 1976b).

Equations (1), (2) and (3) are discretized in the time and space domain, using a simple one-step forward time difference, and a staggered spatial grid in which ξ, U and V are calculated at different grid points. This grid scheme has been used previously (FLATHER and DAVIES 1975, DAVIES 1976a) in discretizing the hydrodynamic equations.

The non-linear advective terms are incorporated using the 'angled-derivative' method (ROBERTS and WEISS 1966), a computationally stable technique used by a number of authors (FLATHER and HEAPS, 1975, FLATHER 1976a, DAVIES 1976a) in solving the non-linear hydro-

dynamic equations. The method centres the advective terms in the time domain, effectively damping the high frequency waves generated by the non-linearities.

In order to solve equations (1) to (3), it is necessary to specify both initial conditions and boundary conditions. In the hindcasting of storm surges, the calculation is usually started from a state of rest, $\xi = U = V = 0$, at least 36 hours before the period of interest; this allows sufficient time for the meteorological forces and friction to remove the influence of the initial conditions in the solution. At land boundaries, the component of current normal to the boundary is set to zero, and on open boundaries the sea surface elevation is specified as a function of position and time, given by :

$$\xi(\phi, \lambda, t) = \xi_T(\phi, \lambda, t) + \xi_M(\phi, \lambda, t) \quad (5)$$

where ξ_T , the tidal input along the open boundary given by :

$$\xi_T(\phi, \lambda, t) = Z_0(\phi, \lambda) + \sum_{i=1}^3 F_i H_i(\phi, \lambda) \cos(V_i + \sigma_i t + U_i - q_i(\phi, \lambda)) \quad (6)$$

where

Z_0 is mean sea level,

F_i, U_i nodal factors, which allow for the 18.6 year variation in amplitude and phase,

H_i the amplitude of constituent i ,

σ_i the speed of the constituent,

V_i the phase of the corresponding equilibrium constituent at time $t = 0$, at Greenwich,

q_i the phase lag of the tidal constituent behind the equilibrium constituent.

Only the M_2 and S_2 constituents are used in calculating tidal input to the model, mean sea level Z_0 being set to zero. Nodal factors F_i and U_i are calculated for the first day of the 44 day period considered. Since these nodal factors are time dependent, strictly they should be recalculated throughout the period, however their variation over 44 days is negligible. In any operational system they would be recalculated, probably each month.

The change in sea surface elevation on the open boundaries due to meteorological effects $\xi_M(\phi, \lambda, t)$, are computed using a two-dimensional linear interpolation technique, from storm surge residuals derived from the continental shelf model (FLATHER 1976a). Observed residuals at Wick are used in this interpolation (DAVIES and FLATHER 1976) in an attempt to correct errors in boundary data coming from the shelf model.

3. THE METEOROLOGICAL DATA

In order to solve equations (1), (2) and (3), it is necessary to calculate atmospheric pressure gradients and sea surface wind stresses at each grid point of the sea model, throughout the time period of interest. These forcing functions are calculated from hourly values of the geopotential height H , of the 1000 mb surface. The height data H is obtained from hours 6 to 18 of the twice daily routine weather forecasts produced by the 10-level numerical model of atmosphere (BENWELL et al 1971) at the Meteorological Office, Bracknell. Hence the computed pressure gradients and wind stresses are truly predicted quantities with associated errors.

Using the geostrophic balance equations, the geostrophic wind is

calculated from the geopotential height data. Surface winds are calculated from the geostrophic winds using the formula of HASSE and WAGNER (1971) with a cross-isobar angle (the angle between the directions of surface wind and geostrophic wind) of 20° . The cross-isobar angle, however, depends on air sea temperature differences (FINDLATER et al 1966, HASSE 1975) and it is important to take its variation into account (DUUN-CHRISTENSEN 1975). Unfortunately for the period considered here this data was not available, although in future work its variation will be considered. Details of the techniques involved in calculating surface winds and wind stresses are given in FLATHER and DAVIES (1975).

4. CALCULATION OF THE VERTICAL PROFILE OF STORM SURGE CURRENT

Since equations (1), (2) and (3) are formulated in terms of depth mean currents, their solution through time, though yielding information on the transport of water under the influence of the wind field, gives no information about the current structure through depth. However, the magnitude and direction of currents induced by wind fields, can change substantially with depth, as shown for example in the classic Ekman spiral, and in order to calculate such current profiles, a number of three-dimensional numerical modelling techniques have been published in the literature. LEENDERTSE (1973) has developed a finite-difference "grid box" method, in which values of the two components of horizontal current are calculated at grid points in the vertical. A method of determining the vertical profile of current, by using an analytic transform, for both linear and non-linear problems

has been given by HEAPS (1971, 1976), while DAVIES (1976b, 1976c) has developed a method using spline functions to represent the vertical profile of current. All these methods involve the computation of the full three-dimensional current distribution through time, necessary information in studying wind-induced circulation, although for problems in which the primary requirement is the current profile at a few points in the space domain, for a small number of selected moments in time, these methods are expensive in computer time.

However, using a Laplace transform technique (JELESNIANSKI 1970) it is possible to extract the current profile at a limited number of points in space and time from gradients of sea surface elevation computed by a two-dimensional model, overcoming the problem of solving the full three-dimensional problem. In calculating the maximum stress on off-shore structures, the current profile at the structure during the period of maximum storm has to be determined, and FORRISTALL (1974) has applied the method of JELESNIANSKI (1970) in this situation.

The details of the application of the Laplace transform method have been given by JELESNIANSKI (1970) and FORRISTALL (1974) for a linear, cartesian coordinate system. A brief indication of the method is given here, and the assumptions made in applying it to results calculated by the present model are discussed.

Using a cartesian coordinate system, with x increasing eastward, y northward, and z a normalised vertical coordinate, with $z = -1$ at the sea bed, $z = 0$ at the sea surface, neglecting non-linear terms, and horizontal eddy viscosity, the

two equations of horizontal motion can be written using complex notation as :

$$\frac{\partial W}{\partial t} = -i F W + q + \frac{N}{h^2} \frac{\partial^2 W}{\partial z^2} \quad (7)$$

where

$$W = U + i V$$

$$q = g \left[\frac{\partial \xi}{\partial x} + i \frac{\partial \xi}{\partial y} \right]$$

g = acceleration due to gravity,

$\frac{\partial \xi}{\partial x}, \frac{\partial \xi}{\partial y}$ gradients of sea surface elevation to the east and the north respectively,

U, V east and north components of current at depth z ,

F Coriolis parameter,

N coefficient of vertical eddy viscosity,

h undisturbed depth of water.

The total flow can be considered as the linear combination of that produced by the wind stress on the surface, a drift flow, and that produced by the gradient of sea surface elevation, induced by the wind field.

For a drift flow, $q = 0$:

$$\frac{\partial W}{\partial t} = -i F W + \frac{N}{h^2} \frac{\partial^2 W}{\partial z^2} \quad (8)$$

with boundary conditions

$$W(-1, t) = 0, \quad \left. \frac{N}{h} \frac{\partial W}{\partial z} \right|_{z=0} = F(t), \quad \left. \frac{\partial W^n}{\partial t^n} \right|_{t=0} = 0 \text{ for all } n \quad (9)$$

where,

z is in the domain $-1 \leq z \leq 0$, a no slip bottom condition is used, and $F(t) = (F^S(t) + i G^S(t)) / \rho$ is the wind stress acting on the surface.

Using the Laplace transform technique, equation (8) can be solved subject to boundary conditions (9) giving :

$$W(z, t) = \frac{2}{h} \sum_{n=0}^{\infty} \cos\left[\left(n + \frac{1}{2}\right)\pi z\right] \cdot \int_0^t F(t-\tau) \exp(-\Theta_n \tau) d\tau \quad (10)$$

where $\Theta_n = iF + N\beta_n^2$

with $\beta_n = (n + \frac{1}{2})\pi/h$

From equation (10) it is possible to determine the drift current contribution to U and V at any time t and depth z , at any grid point in the horizontal domain of the numerical model provided the time history of the surface wind stress $F(t-\tau)$ is known.

For a slope current W ,

$$\frac{\partial W}{\partial t} = -iFW + \frac{N}{h^2} \frac{\partial^2 W}{\partial z^2} + q \quad (11)$$

with boundary conditions

$$W(-1, t) = 0, \quad \left. \frac{\partial W}{\partial z} \right|_{z=0} = 0, \quad \left. \frac{\partial W^n}{\partial t^n} \right|_{t=0} = 0 \quad \text{for all } n \quad (12)$$

The solution of (11) subject to boundary conditions (12) gives :

$$W(z, t) = \frac{2}{h} \sum_{n=0}^{\infty} \frac{(-1)^n}{\beta_n} \cos\left[\left(n + \frac{1}{2}\right)\pi z\right] \cdot \int_0^t q(t-\tau) \exp(-\sigma_n \tau) d\tau \quad (13)$$

In order to evaluate W from equation (13) it is necessary to compute a time history of sea surface slopes produced by the wind field. This time history is here calculated by the numerical two dimensional model described previously.

Although the evaluation of W given by equations (10) and (13) in theory involves an infinite number of terms n , and a complete time series of both surface slopes and wind stresses, in practice the solution converges rapidly requiring only 20 terms in n , and values of sea surface slope and wind stress for a 10 hour period. The necessary sea surface slopes were computed from elevations calculated by the two-dimensional polar model, transformed into Cartesian coordinates.

The model used to calculate the current profile, however, is not strictly compatible with the two-dimensional model, in that the former is linear, with a no slip bottom boundary condition, the latter being non-linear with a bottom slip condition. The difference produced by the non-linear terms will certainly be small except in shallow water, where these terms become important

(BRETTSCHEIDER 1967), and differences produced by the use of a slip and a no slip bottom boundary condition are an inherent limitation of the method.

5. THE STORM SURGE PERIOD OF 4 NOVEMBER TO 18 DECEMBER 1973

5.1 COMPARISONS OF RESULTS AT VARIOUS COASTAL GAUGES

The period 4 November to 18 December 1973 was particularly stormy, and to ascertain how well the North Sea model would perform with respect to stability and accuracy when run in an operational mode on a routine basis, the complete 44 days were simulated by the model, starting from a state of rest some 36 hours before the beginning of the period. The model was also run for over 44 days with M_2 and S_2 boundary tides as the only input, in order to obtain a tidal regime which was subtracted from the field of surge plus tide values to yield the storm surge residuals.

The period contained some large positive and negative storm surges, occurring during days 6-7 November, 12-13 November, 15-20 November, 5-8 December, 12-15 December and 15-18 December, and the meteorological charts for these periods are shown in Figures 3a to 3g.

Plots of computed storm surge residuals against available observations are given in Figures 4a - 4 ℓ , for both continental and east coast English ports. Input residuals on the open boundaries of the model were obtained from a continental shelf model (FLATHER 1976a) these input residuals being modified by observed residuals at Wick. Residuals from the shelf model are interpolated in two dimensions on to the grid of the North Sea model. The difference between the observed residual at Wick

and that obtained from the shelf model, the error, being determined. This error is linearly interpolated along the line between Wick and the northern boundary grid point ($59^{\circ}20'N$, $0^{\circ}0'W$), at which the error is assumed to be zero, and the interpolated residuals from the shelf model, along this section of boundary adjusted using the interpolated error.

Comparing present results with those of FLATHER (1976a), the effect of introducing the Wick residuals upon the magnitude of the computed surge, particularly along the east coast of England, and the influence on surge heights of shallow water areas close to the Dutch, German and Danish coasts, represented in the present model, but not in the shelf model, can be studied.

Results for the positive surge of 6 November are very similar in both models. The major difference being at Cuxhaven where the North Sea model calculated the maximum of the surge approximately 0.4m higher than the shelf model, which gave near perfect agreement. At Terschelling, Cuxhaven and Esbjerg residual elevations computed by the North Sea model for the surge of 13-14 November are the order of 0.3m higher than the corresponding residual elevations calculated by the shelf model, producing an improvement in the calculated result, although the computed maximum still underestimates the observed. The maximum of this surge at Terschelling and Cuxhaven is split into an initial high peak, and a small second peak. This structure is present in the results from the fine mesh model (Figure 4b), although the shelf model produces two peaks of near equal intensity (FLATHER 1976b Figure 9b). The improvement in the finer detail presumably being due to a better representation

of tide surge interaction in the shallow coastal regions.

The consistent increase in the magnitude of the computed storm surge, above that obtained by the shelf model, in this region must be due to the ability of the finer mesh model to resolve the coastal shallow regions, which are particularly important, in producing a local intensification of the magnitude of the surge.

The negative surge of 12 November, is underestimated in both models by approximately 0.4m at Southend, suggesting some deficiency in the meteorological data. This negative surge is associated with strong off shore winds, and the passage of a front over southern England at approximately 1200 on 12/11/73 (Figure 3b).

The effect of introducing observations at Wick, is clearly demonstrated by the surge of 19-20 November. The shelf model being in error by approximately 0.25m at Wick at the surge peak, this error propagates into the North Sea, intensifying, and producing a surge peak error at Southend of over 0.5m. The effect of introducing observations at Wick into the North Sea model is to effectively remove this error, obtaining near perfect agreement between the calculated and the observed maximum of the surge, along the east coast of England. The improvement in results suggests that, at least over this period, the difference between observed residuals and those calculated by the shelf model, is associated with errors occurring on or near the shelf edge to the north-west of Scotland, which propagate into the North Sea, rather than local errors in the computed wind field associated

with a front moving across the region.

A similar improvement in results occurs (compare Figure 4h, with FLATHER (1976a) Figure 12a) for the positive surge of 7 December, where introducing observations at Wick, produces a marked improvement in the computed storm surge at Southend.

The magnitude of the negative surge of 12-13 November, is accurately computed by both models at Immingham and Inner Dowsing, although the models underestimate by 0.5m its magnitude at Southend. This deficiency in both results presumably stems from errors in the meteorological data. The meteorological situation is shown in Figure 3f.

A slight improvement of the negative surge of 15-16 December at north-east English coastal ports is obtained by introducing observational data at Wick, although the major effect producing this surge is the off shore wind system in the Southern Bight, Figure 3g, and results at Southend, dominated by these winds are nearly identical in both models, and in excellent agreement with observation.

The positive surge of the 17 December is severely overestimated by both models, although observations introduced at Wick help to reduce this error, originating one supposes from the meteorological data.

The performance of the model over each 10 day period, and the four day period 14-18 December, may be determined from Table I, where the root mean square error for each port is given. Errors for the four ten-day periods, at ports along the north-east coast of England being approximately 5 cm lower than those of the shelf

model (FLATHER 1976a), an improvement produced by introducing residuals at Wick. During these periods results computed by the shelf model at Wick were good, however for the period 14-18 December, the shelf model overestimated the surge at Wick by up to 40 cm. An improvement of the order of 20 cm in the root mean square error is obtained in the North Sea model, by inclusion of the Wick residuals.

Consistent errors in the models performance, can be detected using a simple linear regression formula of the form

$$\xi_{\text{observed}} = C_1 \xi_{\text{predicted}} + C_0 \quad (14)$$

Consistent non zero values of C_0 , indicate a possible datum error, values of C_1 , varying from unity indicate the degree to which the model is consistently overestimating or underestimating the surge. Table II gives results for the five storm surge periods, for each port. Values of C_1 fluctuate above and below unity not only for an individual port, for each surge period, but from port to port, and no statistically meaningful variation of C_1 is evident.

For C_0 , however, a consistent value of the order of +20 cm is apparent at Ostende, and -20 cm at Helgoland. This could represent errors in datum in computing the observed storm surge residuals, or deficiencies within the numerical model. Simple consistent differences of this type can easily be removed in an operational system, by applying a simple correction to the model results.

Comparing computed results for the major storm surges of the period, obtained by the two models, a number of effects which produce errors can be distinguished.

For surges generated in the area to the north-west of the North Sea, which subsequently propagate into the North Sea, increasing in magnitude, any small errors produced in the shelf model, in the area to the north-west of Scotland lead generally to large errors in the Southern Bight. Introducing observational data along the boundaries of the North Sea model, appears at present to be the only means of removing this error. For internal storm surges, particularly in the Southern Bight, both models appear to give very similar results. This suggests that the dominant effect is meteorological. FLATHER (1976a) has shown for the negative storm surge of 4 April 1973, that an improvement of the order of 0.5m in computed results is obtained by changing the cross-isobar angle from 0° to 20° . The variation of cross-isobar angle with air-sea temperature difference is well known (DUUN-CHRISTENSEN 1975, HASSE 1975). In the present calculation both models used surface winds derived from geostrophic winds with a constant cross-isobar angle of 20° , and the use of this constant angle may introduce an appreciable error into the surface wind field. Errors in the wind field introduced by the simple differencing technique used to derive pressure gradients, and the unavoidable smoothing produced in interpolation from atmospheric sea model points are other sources of meteorological error which must be present in addition to any deficiencies within the meteorological

model itself.

Deficiencies in representing the complex shallow water area, close to Cuxhaven, lead, despite the high coefficient of friction in this region, to a slight overestimation of the magnitude of the computed surge. However, as can be seen from Figure 6c, the contours of sea surface elevation during the maximum of a storm surge are particularly close, and in the shallow coastal waters, a change of over 50 cm can occur between adjacent grid boxes of the fine mesh model.

5.2 THE NEGATIVE SURGE OF 12 NOVEMBER

The meteorological situation which existed during this storm is shown in Figure 3b, and Figures 5a - 5g, show contours of storm surge residual elevation (cm.), and associated depth mean currents (cm/sec), plotted at every third model grid point, at 6 hourly intervals.

The meteorological situation from 00h 12 November to 12h 13 November is characterised by two low pressure systems passing to the north of Scotland, moving in an easterly direction across the north of the North Sea and over Sweden.

Between 00h and 06h on 12 November a depression near Iceland moved into a position to the north of Scotland, producing off-shore winds of the order of 30 knots along the east coast of Scotland and off-shore winds along the south west coast of England; on-shore winds on the continental coast were light. Figures 5a, 5b and 5c show the progress of the external negative surge down the east coast of England. The external surge increases in magnitude during this period,

enhanced by the increasing magnitude of the off shore winds within the Southern Bight. On the continental coast residual elevations produced by the positive external surge of 11 November continue to decline.

At 12h on 12 November strong off shore winds, in the vicinity of the Wash, produced a negative surge in this region of over 100 cm (Figure 5c). The dominant wind field over the North Sea, at this time, was in a westerly direction in the Southern Bight, with north-west winds blowing along the English coast and local south-west winds close to the Norwegian coast. These conditions produced a southward flow along the Scottish coast, a strong north east flow from the Southern Bight into the Skagerrak, and a flow out of the North Sea, in the central region of the northern boundary, outward flow close to the Norwegian coast being inhibited by the northerly winds (Figure 5c).

By 18h the depression had moved over Sweden, and a north westerly airstream dominated the northern part of the North Sea, producing an inflow of water along the east coast of England, and an associated positive surge. During this period, there were strong westerly winds along the continental coast, producing the positive surge of over 150 cm at Cuxhaven. Subsequently the strong westerly and north westerly winds reduced, as the system of depressions moved eastward over Sweden. Current magnitudes over the North Sea diminished, and residual elevations in the Cuxhaven region, decreased in magnitude as the water flowed along the Danish coast (Figures 5e, 5f), and into the Skagerrak. The flow into the Skagerrak along the Danish coast is particularly high (up to 75

cm/sec). However, elevations in the Skagerrak did not increase appreciably, presumably due to the large volume flow out of this region, in the Norwegian trench.

5.3 THE STORM SURGE OF 06h 19 NOVEMBER TO 18h 20 NOVEMBER

A depression passing to the north of the Shetlands in the early hours of 19 November, produced a change in direction of the wind to the north of Scotland from westerly to north-westerly, producing a positive surge, which progressed down the east coast of England, with increasing magnitude. A residual elevation of over 125 cm occurred in the Wash (Figure 6a).

South-easterly going depth mean residual currents of magnitude up to 50 cm/sec occurred in the central region of the North Sea, and residual depth mean easterly flows of the order of 75 cm/sec were present close to the German coast (Figure 6a). This flow of water into the North Sea produced residual elevations in the Southern Bight in excess of 175 cm (Figure 6c), though in the channel they remained at 25 cm. The associated pressure gradient producing a flow through the Straits of Dover up to 100 cm/sec (Figure 6c).

Residual sea surface elevations in the shallow region near Cuxhaven rose rapidly during this period, and residual elevations along a number of coastal areas exceeded 3.5m. Results of residual sea surface elevation given by FLATHER (1976, Figure 14h) are similar to those given in Figure 6c, except in the region close to Cuxhaven, where residual elevation increases rapidly due to the inclusion of the shallow coastal waters within the present model. A similar distribution of residual currents is produced by both

models, though with a marked difference close to the Danish coast, where the shelf model (FLATHER 1976a, Figure 14h) computed a strong northward flow, in contrast to the small southerly flow depicted in Figure 6c, though a strong north flow can be observed along the north-west Danish coast. The importance of the Skagerrak and Kattegat upon the magnitude of this flow has been described by FISCHER (1959). A closed boundary across the entrance to the Skagerrak would not appear to be physically realistic. The radiation condition used by FLATHER (1976) though producing at times a higher flow than that obtained in the North Sea model, does give a realistic representation of the flow in this region.

At 00h on the 20 November the positive surge travelling down the east coast of England reached Southend, giving a residual elevation of over 170 cm.

During the early hours of 20 November, the depression moved into the Baltic; winds over the North Sea diminishing in magnitude. Residual sea surface elevations decreased and current directions within the North Sea changed from a southward (Figure 6c) to a northward flow (Figure 6e), though with a continuing flow of up to 50 cm/sec through the Straits of Dover, despite the low wind field in the Southern Bight.

Figures 6f and 6g, show the return of residual sea surface elevations to near -zero. The current distribution in Figure 6f, is very similar to that computed by FLATHER (1976a, Figure 14k), showing a strong southward flow close to the west coast of Denmark, turning west in the German Bight, and flowing northward out of the

North Sea, along a line approximating to the zero elevation contour. At this time the wind field over the North Sea was particularly light.

Using the method of JELESNIANSKI (1970), described previously, it is possible to determine the variation of residual current structure with depth, by solving equations (10) and (13). A coefficient of vertical eddy viscosity $N = 650 \text{ cm}^2/\text{sec}$ being used (HEAPS 1971). Figures 7a, 7b and 7c, give the change in the U and V components of current (in cm/sec), with a normalised depth going from sea surface to sea bed, at three points along the line of latitude from the Inner Dowsing to the continental coast at time 12h 19/11/73. The exact positions of the points being ($53^{\circ}10'N$, $1^{\circ}0'E$), ($53^{\circ}10'N$, $2^{\circ}0'E$), ($53^{\circ}10'N$, $3^{\circ}30'E$).

These three plots show a near linear variation in current magnitude with depth, the maximum current occurring at the sea surface where the wind has the greatest effect. The V component of current (Figure 7b) having a maximum value at the surface of 111 cm/sec, compared with a depth mean value of approximately 50 cm/sec, emphasising the inability of a two-dimensional model to calculate maximum currents. A more complex distribution of current with depth is shown in Figure 7d, for a point just south of the southern tip of Norway ($57^{\circ}40'N$, $7^{\circ}0'E$): showing a southward surface flow in the V component of current, and a northward bottom flow of current. The wind field in this region is not particularly strong but the water is very deep. Any change in surface wind field, producing a response in the surface current, though having little effect upon the current at greater depth, in

contrast to the previous points, where the positions lie in much shallower water, in a region of much stronger winds, where the influence of the wind field can extend much closer to the sea bed.

CONCLUDING REMARKS

Results obtained by running the North Sea model in conjunction with the shelf model, for a 44 day period, clearly demonstrate that the models are stable and do not suffer from any accumulation of error. By introducing observational data into the fine mesh model, errors propagating into the North Sea, from the region to the north-west of Scotland can be reduced. In some instances no improvement is obtained by the introduction of observational data, both shelf and North Sea model exhibiting errors of similar magnitude. In these cases we conclude that the major source of error is in the meteorological data.

The use of a constant cross isobar angle, must contribute to errors in determining the direction of the surface wind, and work is presently in progress to take account of variations in this parameter with air sea temperature difference. The present method of obtaining derivatives of the pressure field, by differencing over the meteorological grid, introduces a high degree of smoothing, and a better method being considered is to fit in two dimensions, spline functions to the pressure field, and differentiate analytically these functions, yielding the pressure gradients at any desired point.

The ability of the North Sea model to resolve the shallow coastal regions produces the major differences between the two models in the Cuxhaven - Esbjerg region, where there is a large

expanse of shallow water. Despite the higher coefficient of friction in this region residual elevations at Cuxhaven are too high.

When tidal data becomes available from the JONSDAP '76 exercise, more tidal constituents can be used along the open boundaries of the model, giving a better representation of tide surge interaction.

By using observed residuals at Wick, and any off-shore residuals from data-buoys or off-shore structures in the northern part of the North Sea, as input to the model, a real time operational system would be feasible using this model, giving up to a 12 hour forecast.

ACKNOWLEDGEMENTS

The author is indebted to Dr. N. S. Heaps for many useful comments and suggestions during the course of this work. The care and effort taken by the Meteorological Office in extracting the meteorological data from their atmospheric model is much appreciated, as is the work performed by Mr. R. Smith in preparing the diagrams presented in this report.

The work described in this report was funded by a Consortium consisting of the Natural Environment Research Council, the Ministry of Agriculture Fisheries and Food, and the Departments of Energy, Environment and Industry.

REFERENCES

BENWELL, G.R.R., GADD, A.J., KEERS, J.F., TIMPSON, M.S. & WHITE, P.W. 1971. The Bushby-Timpson 10 level model on a fine mesh. Meteorological Office, London, Scientific Papers, No.32, 23 pp.

BRETTSCHNEIDER, G. 1967. Anwendung des Hydrodynamisch-Numerischen Verfahrens zur Ermittlung der M_2 Mitschwingungszeit der Nordsee. Mitteilungen des Instituts für Meereskunde der Universität Hamburg, 7, 65 pp.

DAVIES, A.M. 1976a. A numerical model of the North Sea and its use in choosing locations for the deployment of offshore tide gauges in the Jonsdap '76 oceanographic experiment. Deutsche Hydrographische Zeitschrift - in press.

DAVIES, A.M. 1976b. The numerical solution of the three-dimensional hydrodynamic equations, using a B-spline representation of the vertical current profile. Mémoires de la Société Royale des Sciences de Liège - in press.

DAVIES, A.M. 1976c. Three dimensional model with depth-varying eddy viscosity. Mémoires de la Société Royale des Sciences de Liège - in press.

DAVIES, A.M. and FLATHER, R.A. 1976 - in preparation

DUUN-CHRISTENSEN, J.T. 1971. Investigations on the practical use of a hydrodynamic numeric model for calculation of sea level variations in the North Sea, the Skagerrak and Kattegat. Deutsche Hydrographische Zeitschrift, 24, 210-227.

DUUN-CHRISTENSEN, J.T. 1975. The representation of the surface pressure field in a two-dimensional hydrodynamic numeric model for the North Sea, the Skagerrak and the Kattegat. Deutsche Hydrographische Zeitschrift, 28, 97-116.

- FINDLATER, J., HARROWER, T.N.S., HOWKINS, G.A. and WRIGHT, H.L. 1966. Surface and 900 mb wind relationships. Scientific Papers of the Meteorological Office, London, 23, 41 pp.
- FISHER, G. 1959. Ein numerisches Verfahren zur Errechnung von Windstau und Gezeiten in Randmeeren. Tellus, 11 60-76.
- FLATHER, R.A. 1976a. Results from a storm surge prediction model of the north-west European continental shelf for April, November and December 1973. Institute of Oceanographic Sciences Report No.24. 33 pp + figs.
- FLATHER, R.A. 1976b. A tidal model of the north-west European continental shelf. Mémoires de la Société Royale des Sciences de Liège, ser.6, 10, 141-164.
- FLATHER, R.A. and DAVIES, A.M. 1975. The application of numerical models to storm surge prediction. Institute of Oceanographic Sciences Report No.16. 23 pp + figs.
- FLATHER, R.A. and HEAPS, N.S. 1975. Tidal computations for Morecambe Bay, Geophysical Journal of the Royal Astronomical Society, 42, 489-517.
- FORRISTALL, G.Z. 1974. Three-dimensional structure of storm-generated currents. Journal of Geophysical Research, 79, 2721-2729.
- HANSEN, W. 1961. Hydrodynamical methods applied to oceanographic problems. Mitt. Inst. Meeresk. Univ. Hamburg. No.1; Proc. Symp. Math.-hydrodyn. Meth. phys. Oceanogr. Sept 1961.
- HASSE, L. and WAGNER, V. 1971. On the relationship between geostrophic and surface wind at sea. Monthly Weather Review, 99, 255-260.
- HASSE, L. 1974. On the surface to geostrophic wind relationship at sea and the stability dependence of the resistance law. Beitrage zur Physik der Atmosphere, 45, 45-55.

- HEAPS, N.S. 1969. A two-dimensional numerical sea model. Philosophical Transactions of the Royal Society, A, 265, 93-137.
- HEAPS, N.S. 1971. On the numerical solution of the three-dimensional hydrodynamical equations for tides and storm surges. Mémoires de la Société Royale des Sciences de Liège, ser.6, 2, 143-180.
- HEAPS, N.S. 1976. On formulating a non-linear numerical model in three dimensions for tides and storm surges. Second International Meeting on Computing Methods in Applied Science and Engineering, Paris, Dec. 1975, Springer-Verlag, in press.
- JELESNIANSKI, C.P. 1970. Bottom stress time-history in linearized equations of motion for storm surges. Monthly Weather Review, 98, 462-478.
- LEENDERTSE, J.J., ALEXANDER, R.C., and LIU, S.K. 1973. A three-dimensional model for estuaries and coastal seas : Volume 1 Principles of Computation. Rand Corporation Report R-1417-OWRR pp.57.
- ROBERTS, K.V. and WEISS, N.O. 1966. Convective difference schemes, Mathematics of Computation, 20, 272-299.
- TIMMERMANN, H. 1975. On the importance of atmospheric pressure gradients for the generation of external surges in the North Sea. Deutsche Hydrographische Zeitschrift, 28, 62-71.

Table 1 : Root Mean square errors (cm) calculated from hourly values
of predicted and observed surge residuals for the period
4 November - 18 December 1973

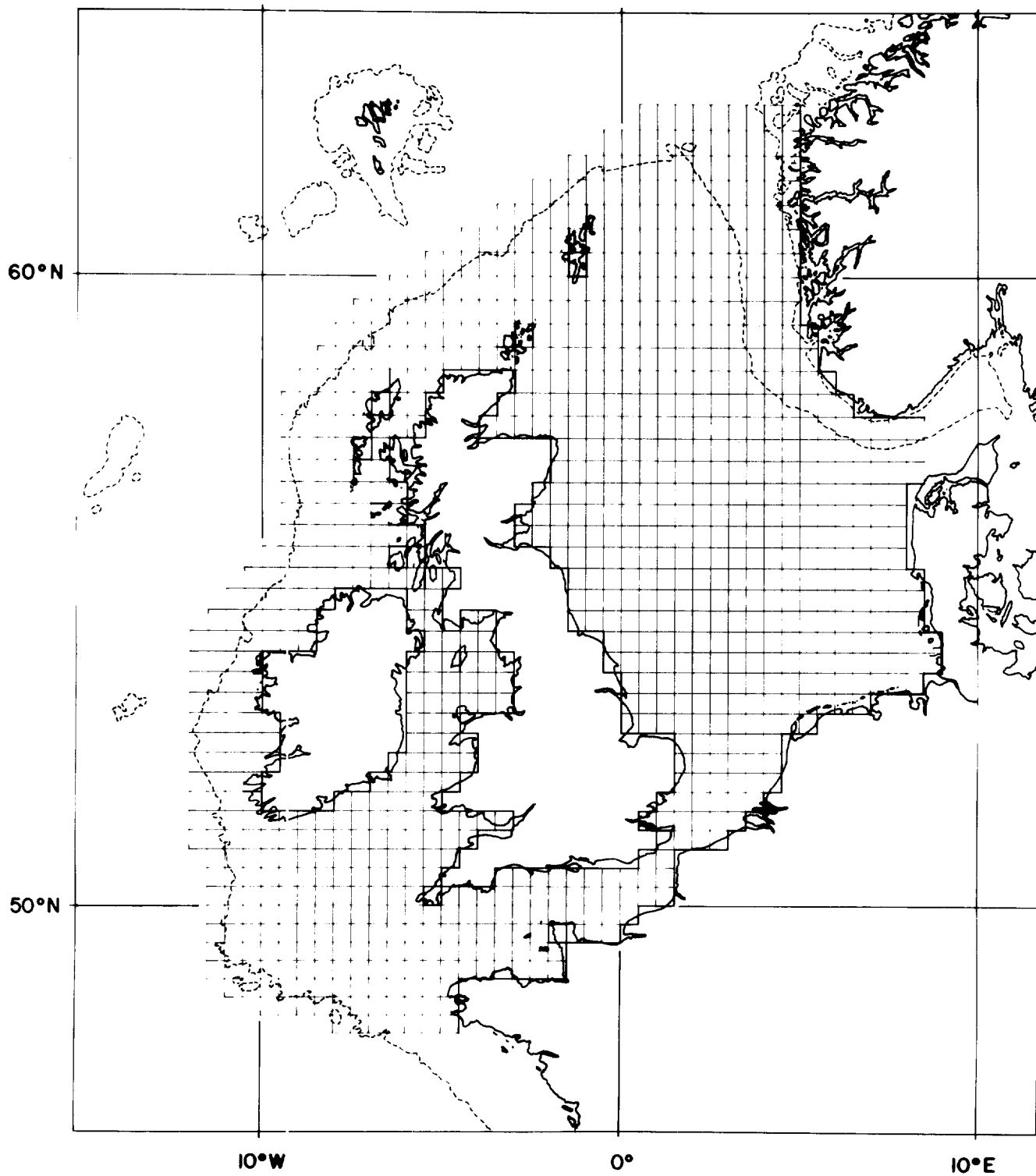
Port	4-14 Nov	14-24 Nov	24 Nov-4 Dec	4-14 Dec	14-18 Dec	Overall	Samples
Aberdeen	11.0	13.1	14.7	14.1	11.9	13.0	1056
North Shields	19.1	16.1	14.1	16.7	9.5	16.1	1056
Immingham	18.4	25.4	16.7	26.0	20.3	21.3	1056
Inner Dowsing	16.8	26.4	16.5	28.3	19.8	21.0	1039
Lowestoft	16.8	20.4	19.9	28.6	18.7	20.8	1056
Walton-on-Naze	21.1	27.3	19.2	32.0	24.5	24.5	580
Southend	24.3	30.5	22.7	33.9	29.8	27.9	580
Dover	15.6	19.7	20.2	30.6	24.7	21.4	1056
Ostende	30.0	33.3	34.2	-	-	32.8	592
Hoek van Holland	-	19.8	-	38.3	-	30.1	360
Ijmuiden	22.7	25.6	21.5	-	-	23.7	673
Terschelling	20.5	23.3	17.7	40.6	16.9	24.5	866
Helgoland	-	32.9	-	55.9	-	46.2	360
Cuxhaven	36.5	37.9	28.5	62.1	31.2	40.1	895
Esbjerg	26.6	34.0	28.0	40.6	28.7	31.9	1049
Tregde-Mandal	-	13.5	-	17.1	-	15.3	360
Stavanger	-	13.8	-	17.4	-	15.6	360
Oslo	-	36.0	-	30.9	-	33.5	360

Table 2 : Linear regression coefficients C_1 and C_0 , where ξ observed = $C_1 x$
 ξ predicted + C_0 determined from the results of the period
 4 November - 18 December 1973

Port	4-14 Nov		14-24 Nov		24 Nov-4 Dec		4-14 Dec		14-18 Dec	
	C_1	C_0	C_1	C_0	C_1	C_0	C_1	C_0	C_1	C_0
Aberdeen	1.00	- 4.0	0.93	0.0	1.36	- 6.6	0.91	- 9.4	0.92	- 6.7
North Shields	1.01	6.0	0.95	7.3	1.30	7.4	0.94	1.6	0.85	4.1
Immingham	0.93	- 2.0	0.86	3.2	1.32	- 5.4	0.81	- 3.3	0.88	- 2.6
Inner Dowsing	1.13	5.1	0.95	8.2	1.28	5.1	0.87	5.7	0.93	3.8
Lowestoft	1.21	1.2	0.98	3.8	1.19	0.5	0.87	2.3	0.86	- 2.0
Walton-on-Naze	1.16	1.3	0.93	3.2	1.14	6.7	0.81	1.6	0.88	-12.8
Southend	1.10	4.2	0.95	0.5	1.14	5.8	0.78	1.3	0.82	-12.1
Dover	1.17	5.1	0.95	- 5.5	1.03	- 8.6	0.80	-12.0	0.84	-15.4
Ostende	1.22	21.0	1.03	25.1	1.27	22.9	-	-	-	-
Hoek van Holland	-	-	0.94	8.0	-	-	0.75	6.8	-	-
Ijmuiden	1.12	3.1	1.02	4.4	1.37	- 7.9	-	-	-	-
Terschelling	1.07	- 1.0	0.98	0.4	1.53	-10.9	0.76	- 5.0	1.14	-15.7
Helgoland	-	-	0.93	-17.5	-	-	0.76	-21.6	-	-
Cuxhaven	0.89	11.2	0.86	16.9	1.34	- 8.8	0.70	9.4	0.61	8.1
Esbjerg	0.97	-10.0	0.86	3.6	1.11	-14.1	0.81	- 8.8	0.74	0.0
Tregde-Mandal	-	-	0.55	4.4	-	-	0.43	4.2	-	-
Stavanger	-	-	0.98	-11.0	-	-	0.67	- 6.8	-	-
Oslo	-	-	0.24	- 9.6	-	-	0.41	- 9.5	-	-

CAPTIONS

- Figure 1 : Finite difference grid for the North Sea and continental shelf.
- Figure 2 : Finite difference grid of the North Sea model.
- Figure 3a : Weather chart for 0600h 6/11/73 with the track of the depression (- x - - x -); crosses indicate the position of the low every 12 hours.
- Figure 3b : Weather charts for 0600h 12 and 13/11/73.
- Figure 3c : Weather charts for 15 - 17/11/73.
- Figure 3d : Weather charts for 17 - 20/11/73.
- Figure 3e : Weather charts for 5 - 8/12/73.
- Figure 3f : Weather charts for 12 - 15/12/73.
- Figure 3g : Weather charts for 15 - 18/12/73.
- Figures 4a-4 ℓ : Comparisons of computed (—●—●—●—●—) and observed (▲ ▲ ▲ ▲) storm surges at a number of ports.
- Figures 5a-5g : Contours of surface elevation (cm) and current vectors for the storm surge 12 - 13/11/73.
- Figures 6a-6g : Contours of surface elevation (cm) and current vectors for the storm surge 19/11/73 - 20/11/73.
- Figures 7a-7d : Vertical profiles of storm surge induced currents.



REVISED FINITE DIFFERENCE GRID FOR THE NORTH SEA AND CONTINENTAL SHELF ;
----- 100 FATHOM DEPTH CONTOUR.

FIGURE 1

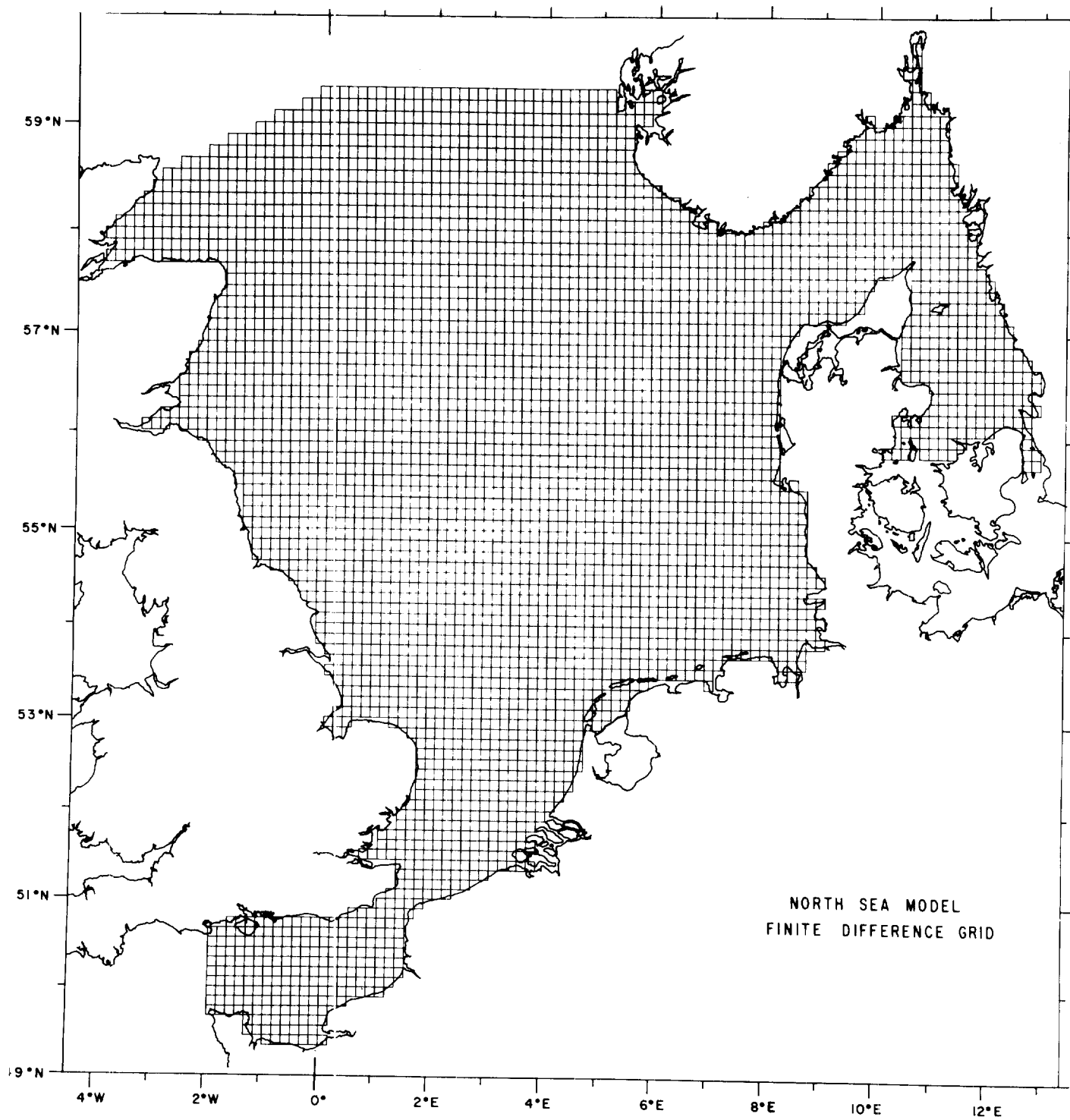


FIGURE 2: FINITE DIFFERENCE GRID OF NORTH SEA MODEL

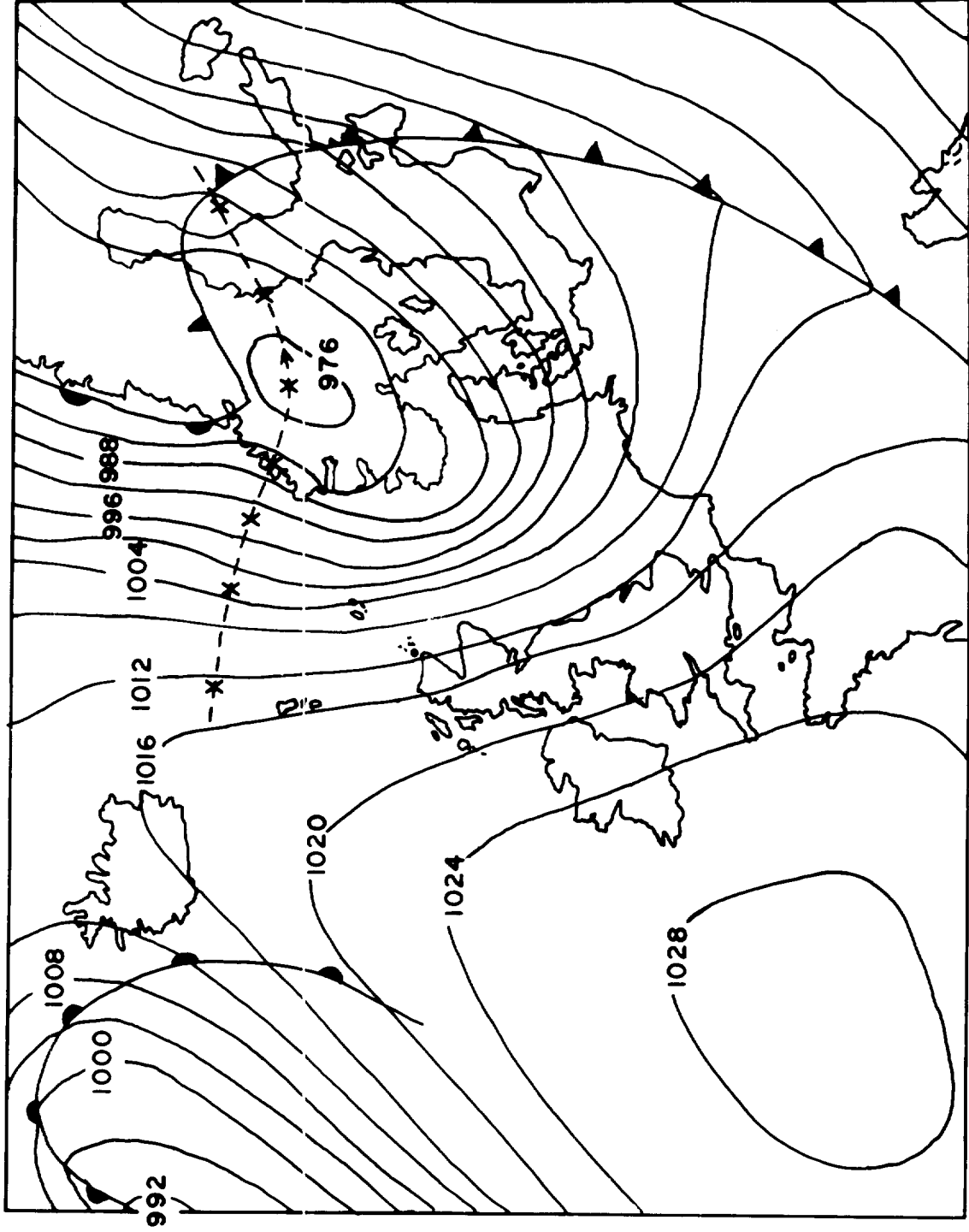


FIGURE 3a : WEATHER CHART FOR 0600h 6/11/73 WITH THE TRACK OF THE DEPRESSION (*--*--*--*); CROSSES INDICATE THE POSITION OF THE LOW EVERY 12 HOURS.

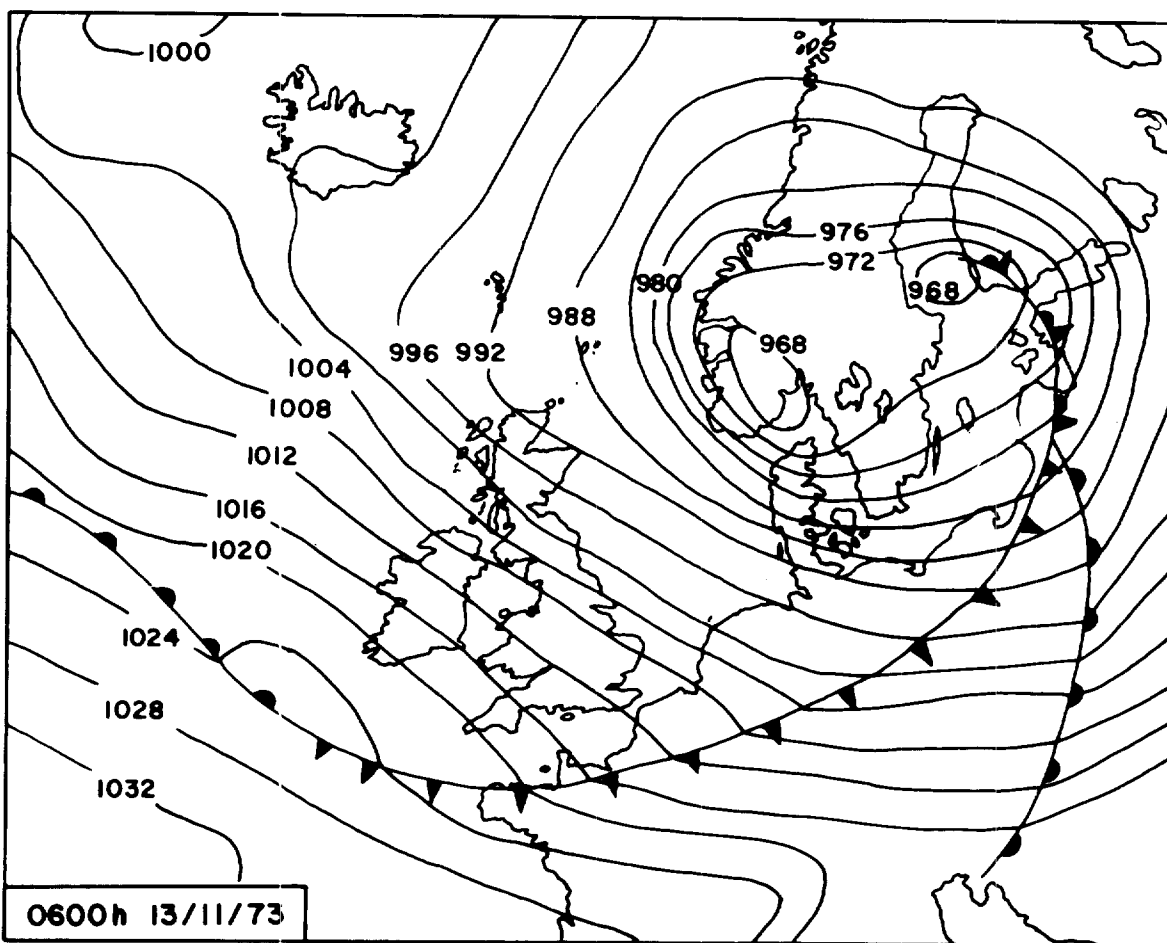
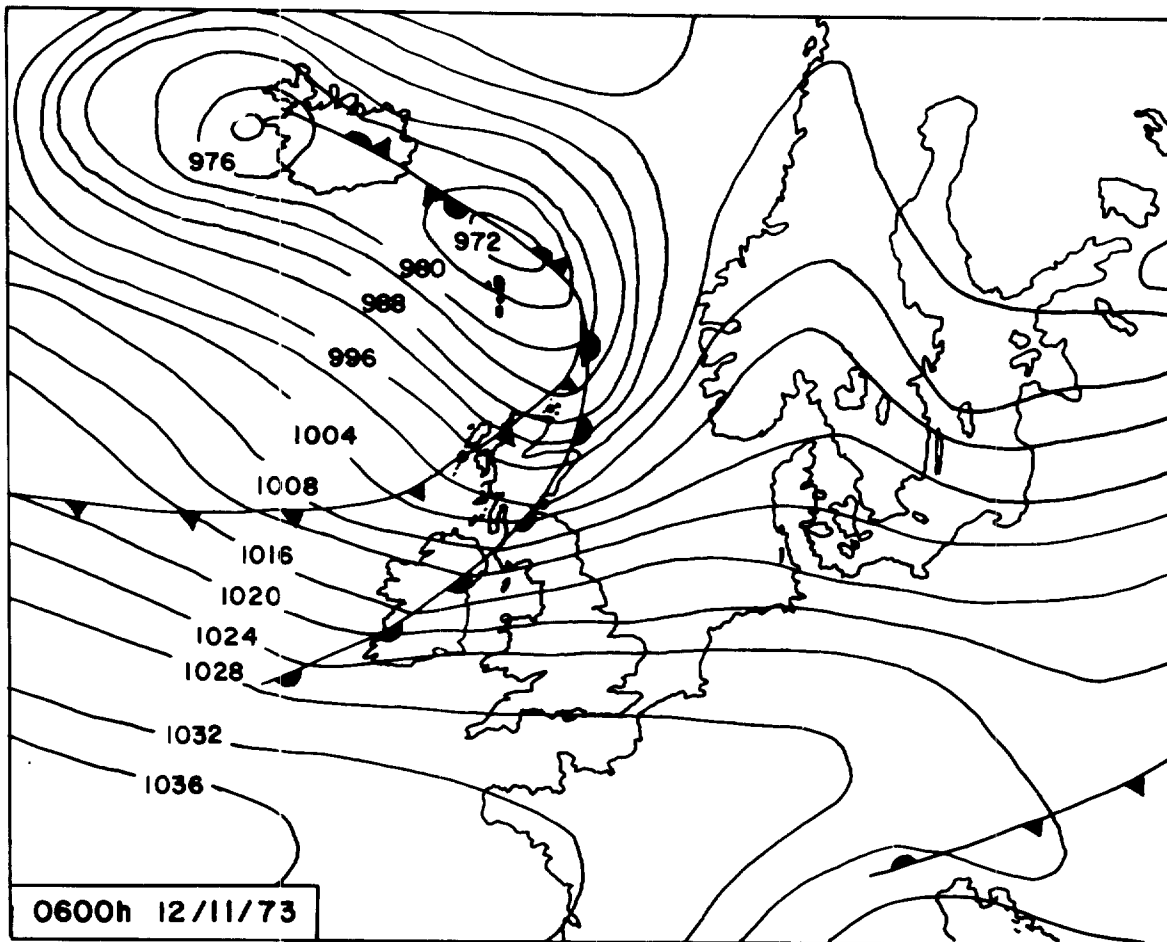


FIGURE 3b: WEATHER CHARTS FOR 0600h 12 & 13/11/73

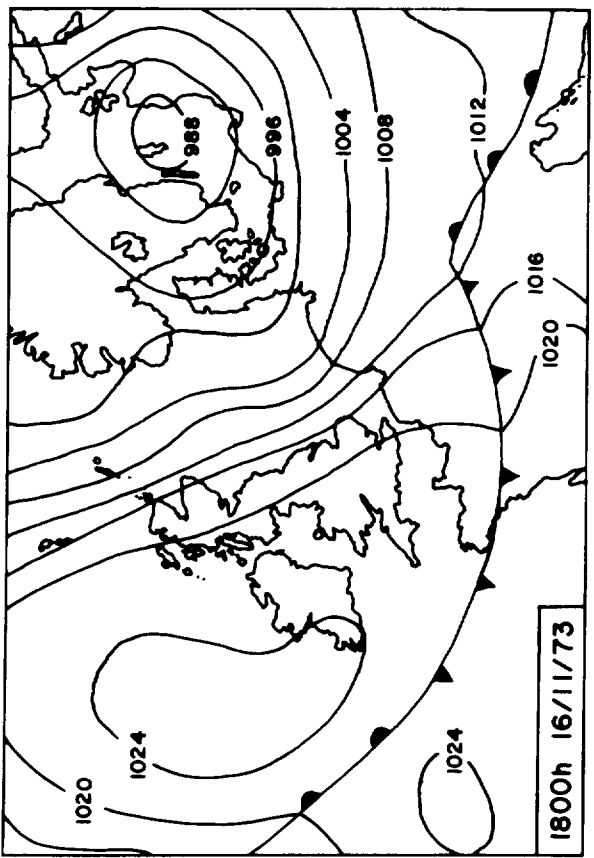
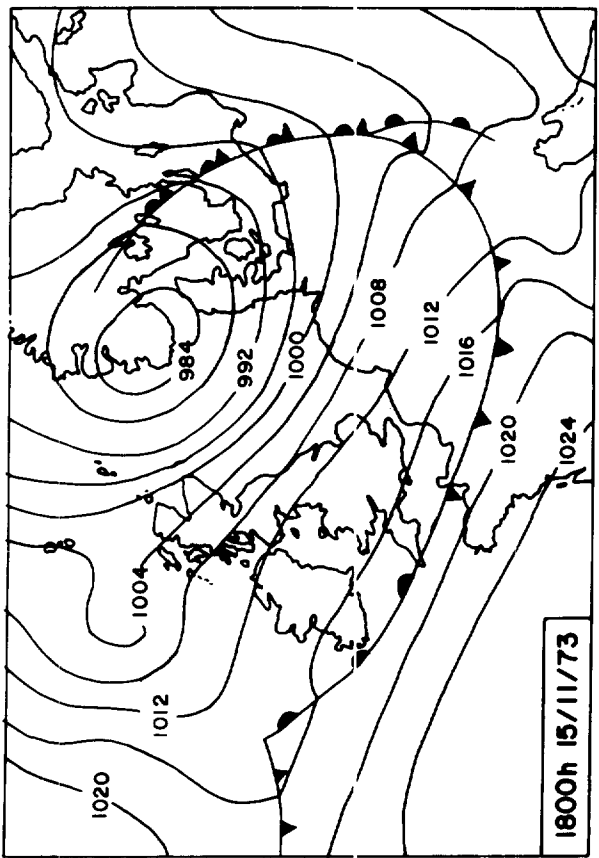
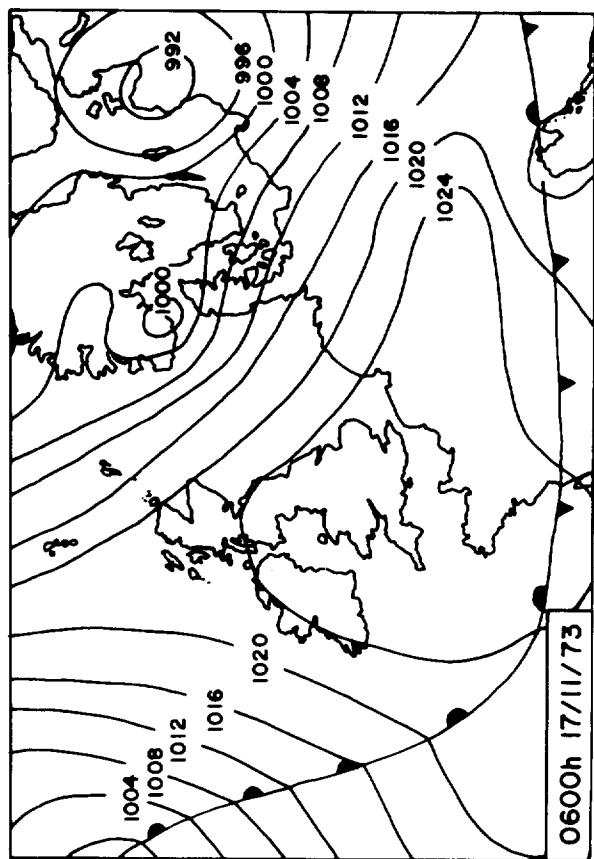
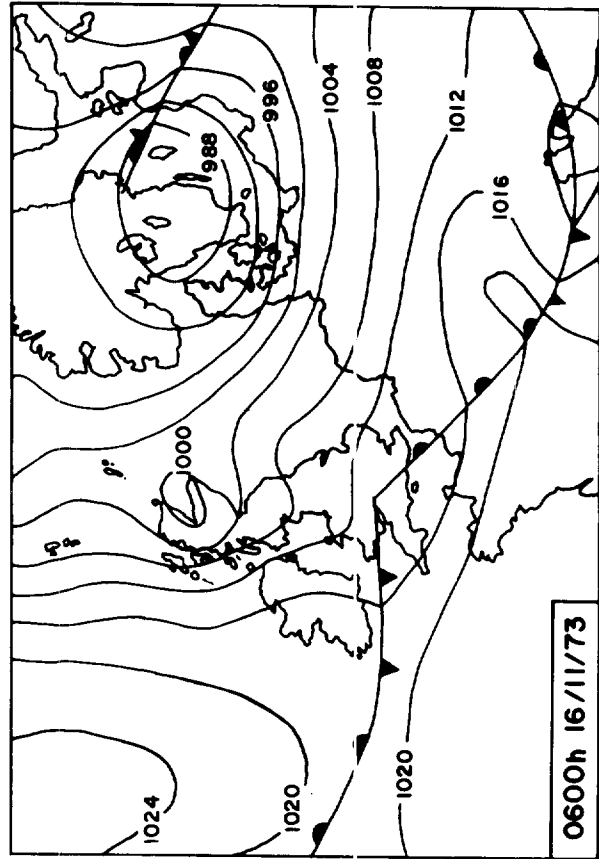


FIGURE 3c: WEATHER CHARTS FOR 15-17/11/73

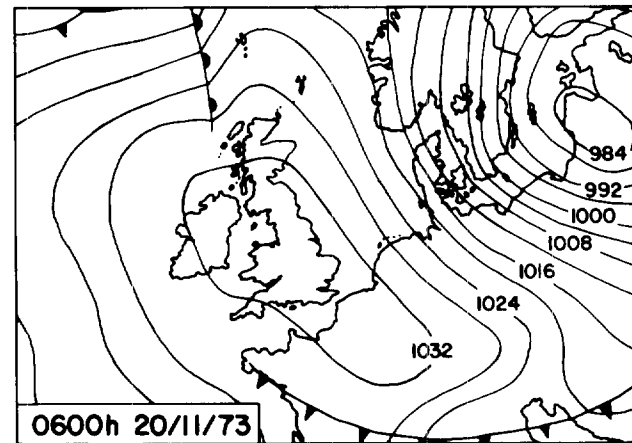
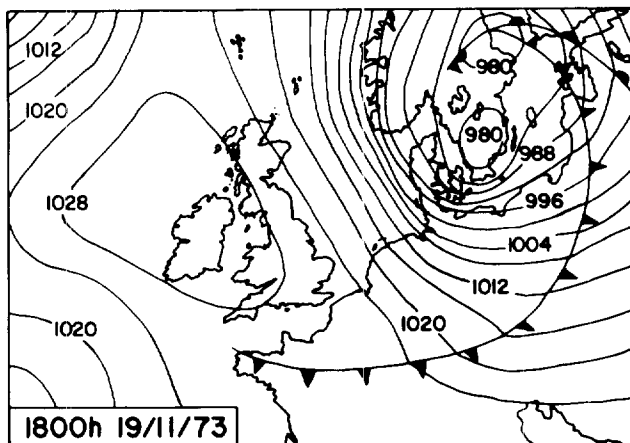
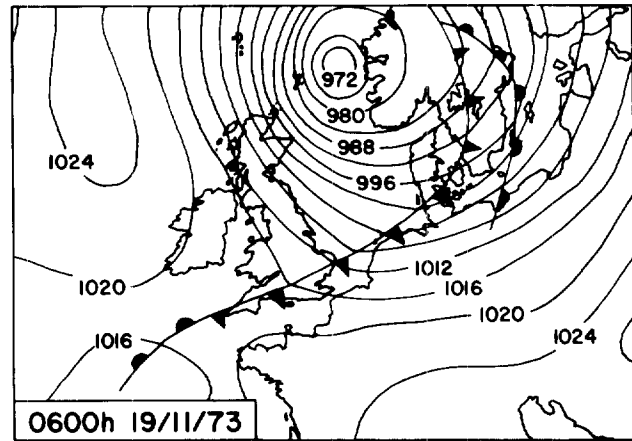
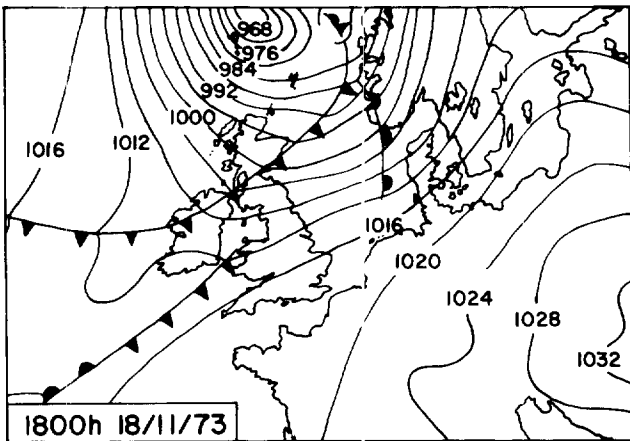
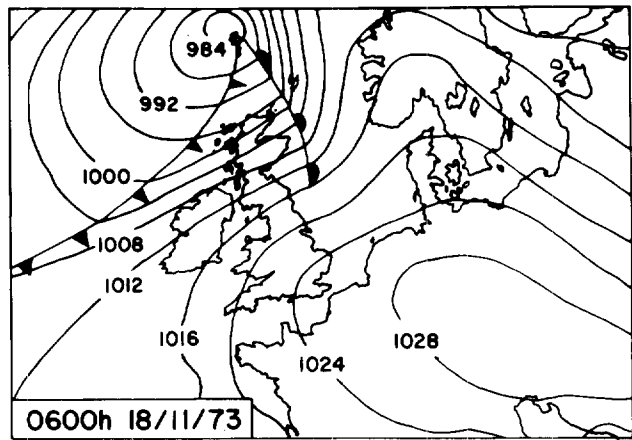
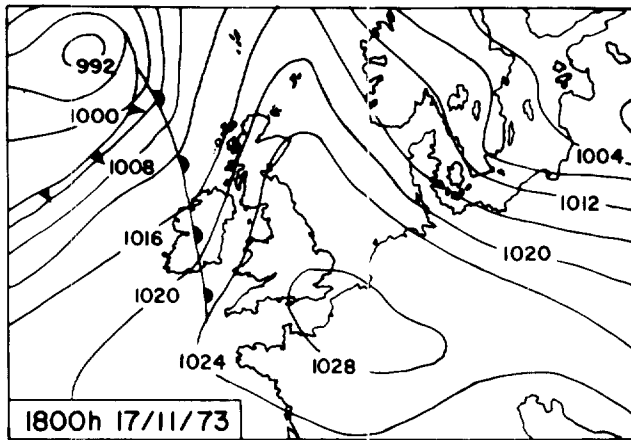


FIGURE 3d: WEATHER CHARTS FOR 17-20/11/73

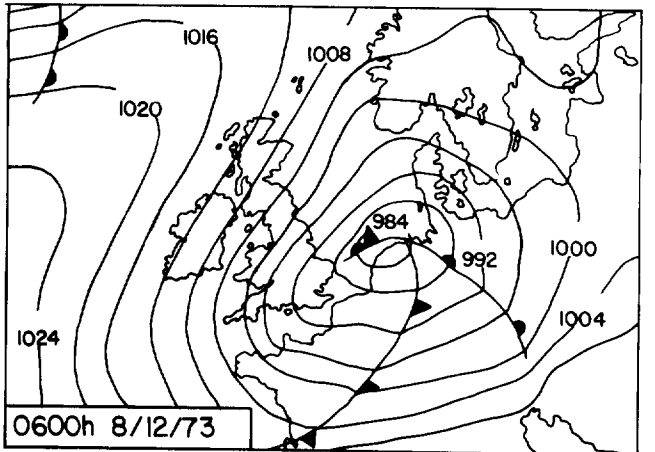
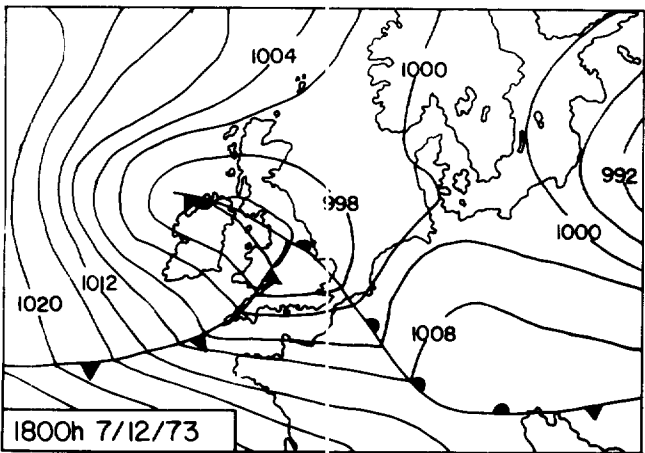
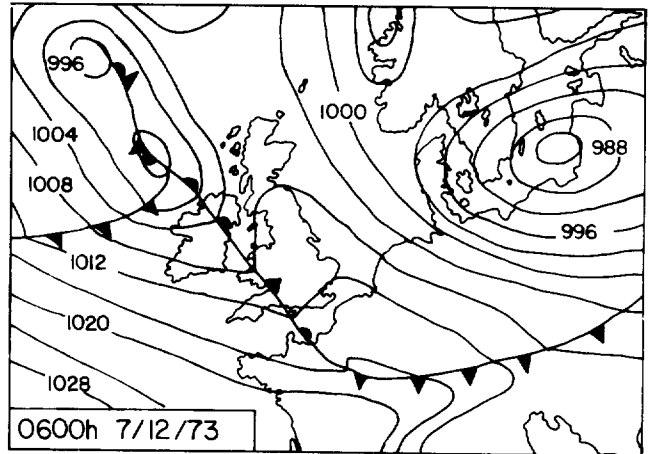
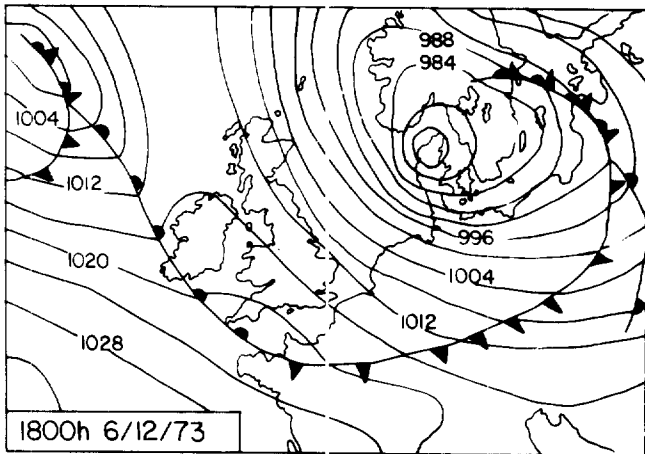
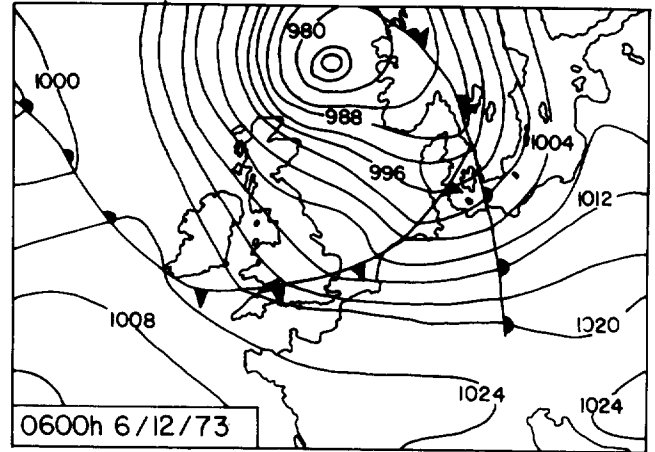
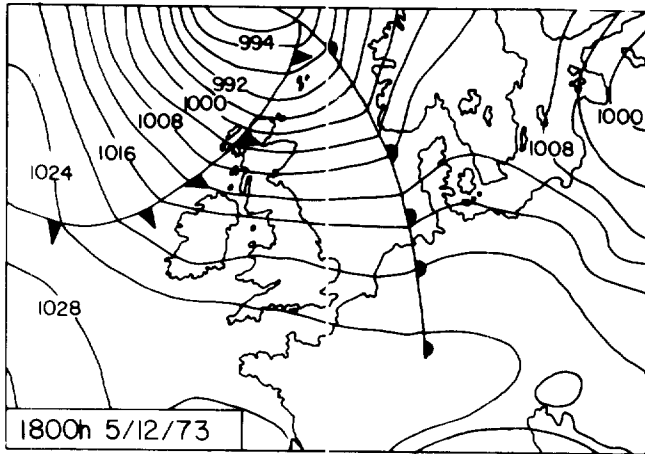


FIGURE 3e: WEATHER CHARTS FOR 5-8/12/73

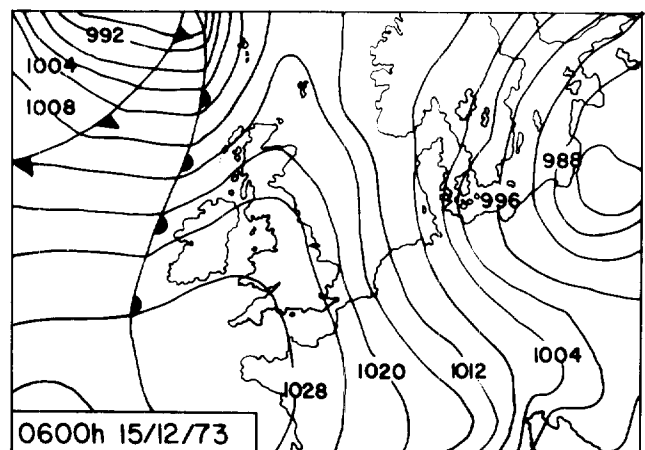
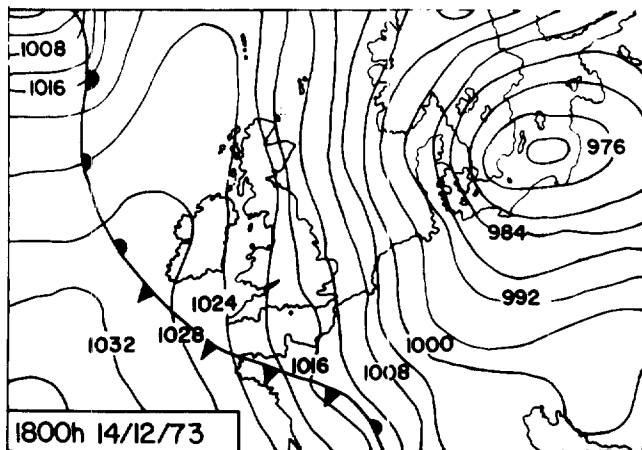
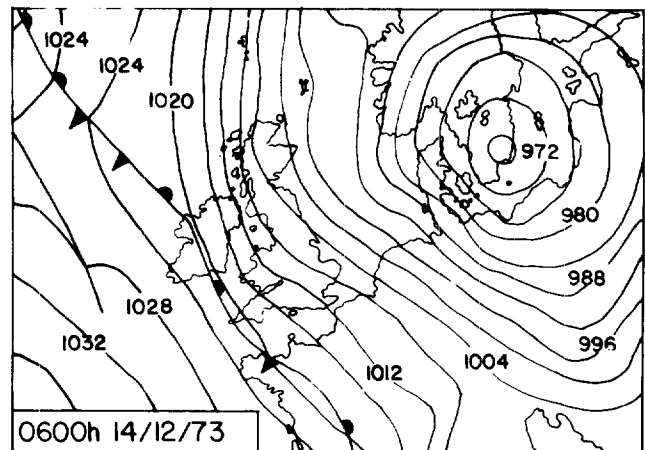
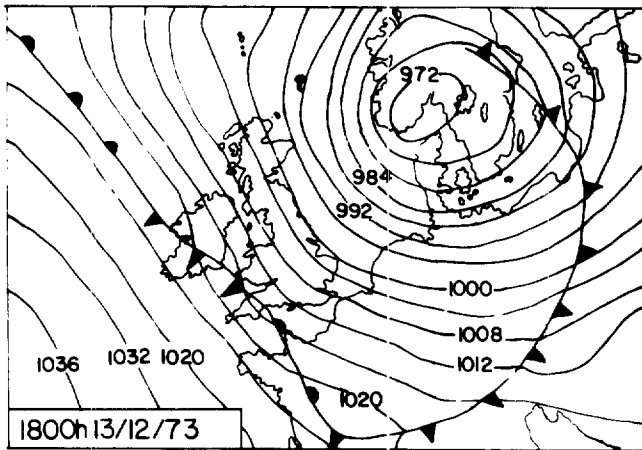
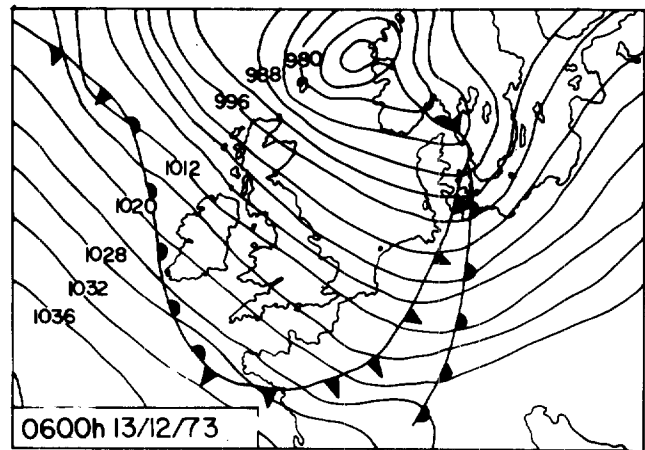
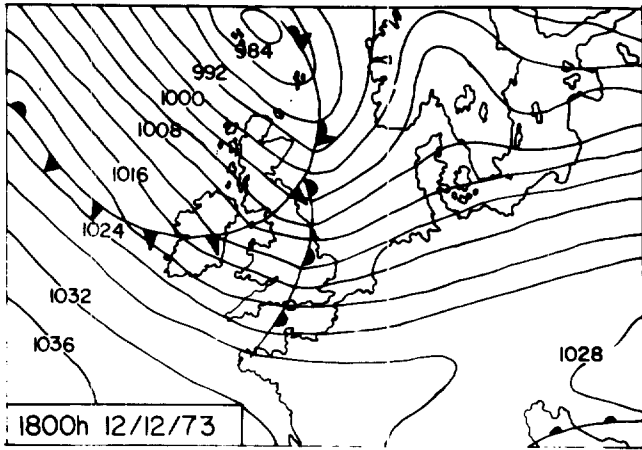


FIGURE 3f: WEATHER CHARTS FOR 12-15/12/73

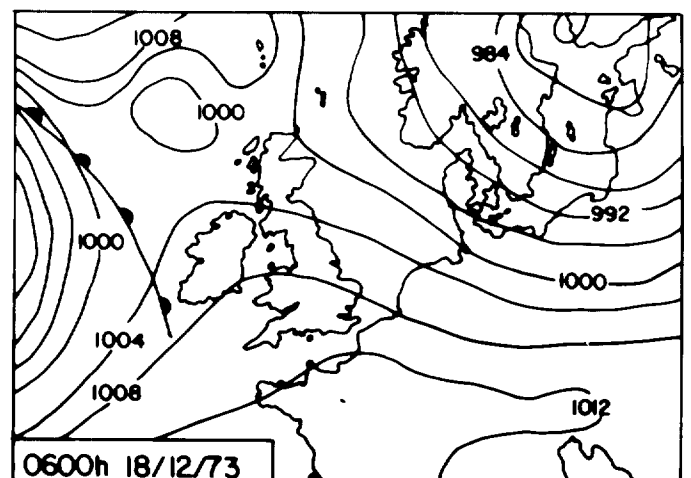
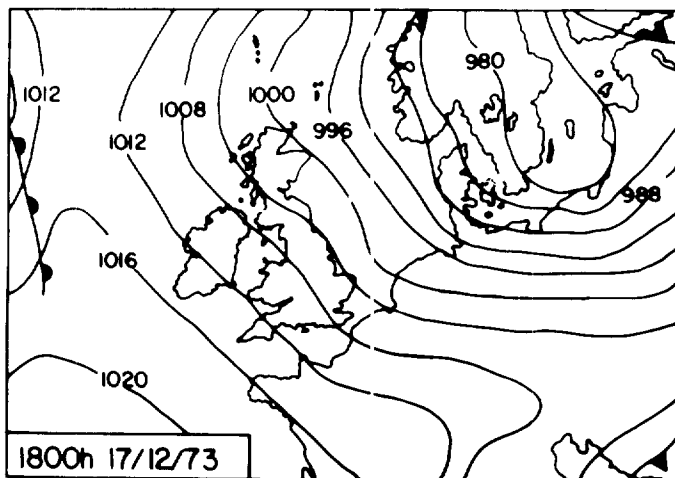
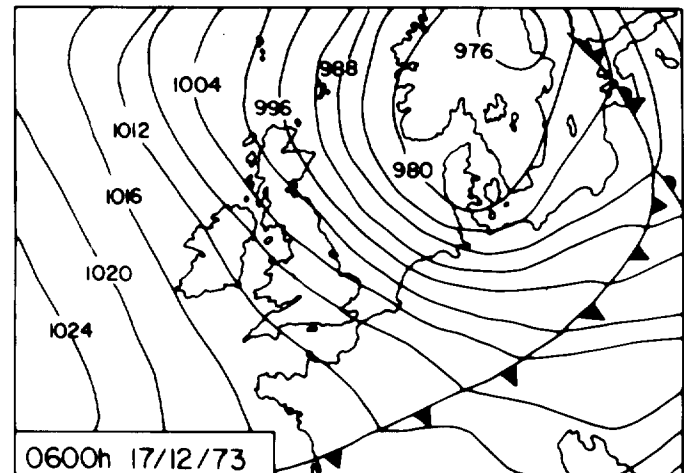
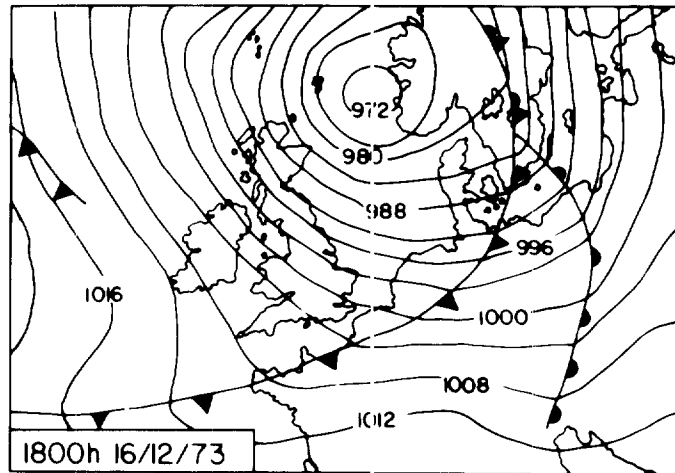
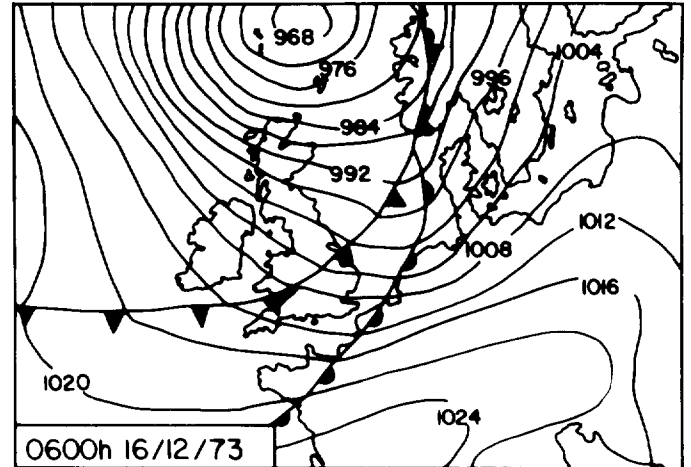
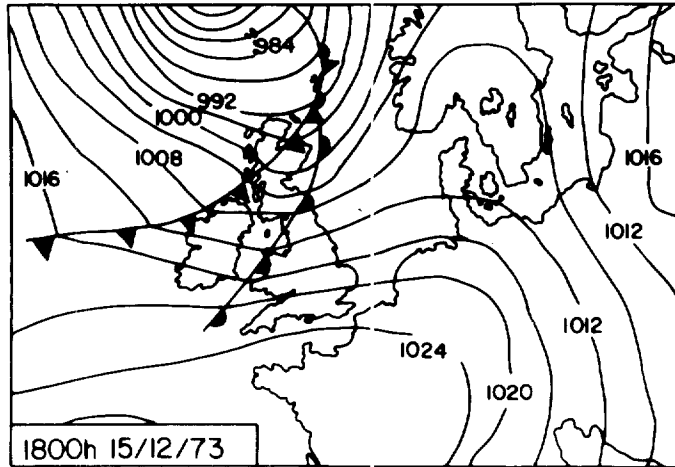


FIGURE 3g: WEATHER CHARTS FOR 15-18/12/73

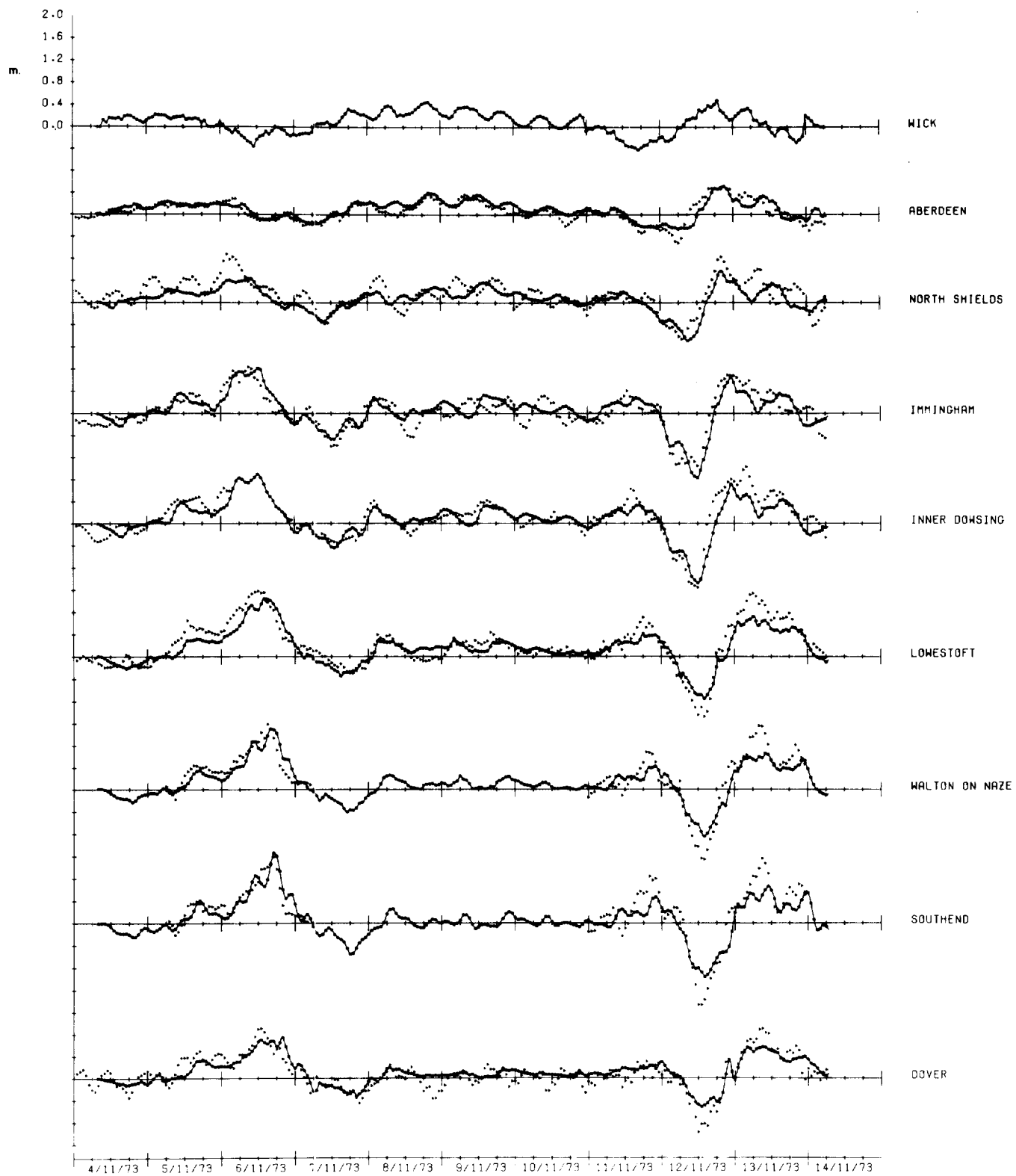


FIGURE 4a: COMPARISON OF COMPUTED (—●—●—●) AND OBSERVED (▴ ▴ ▴ ▴) STORM SURGES AT A NUMBER OF PORTS

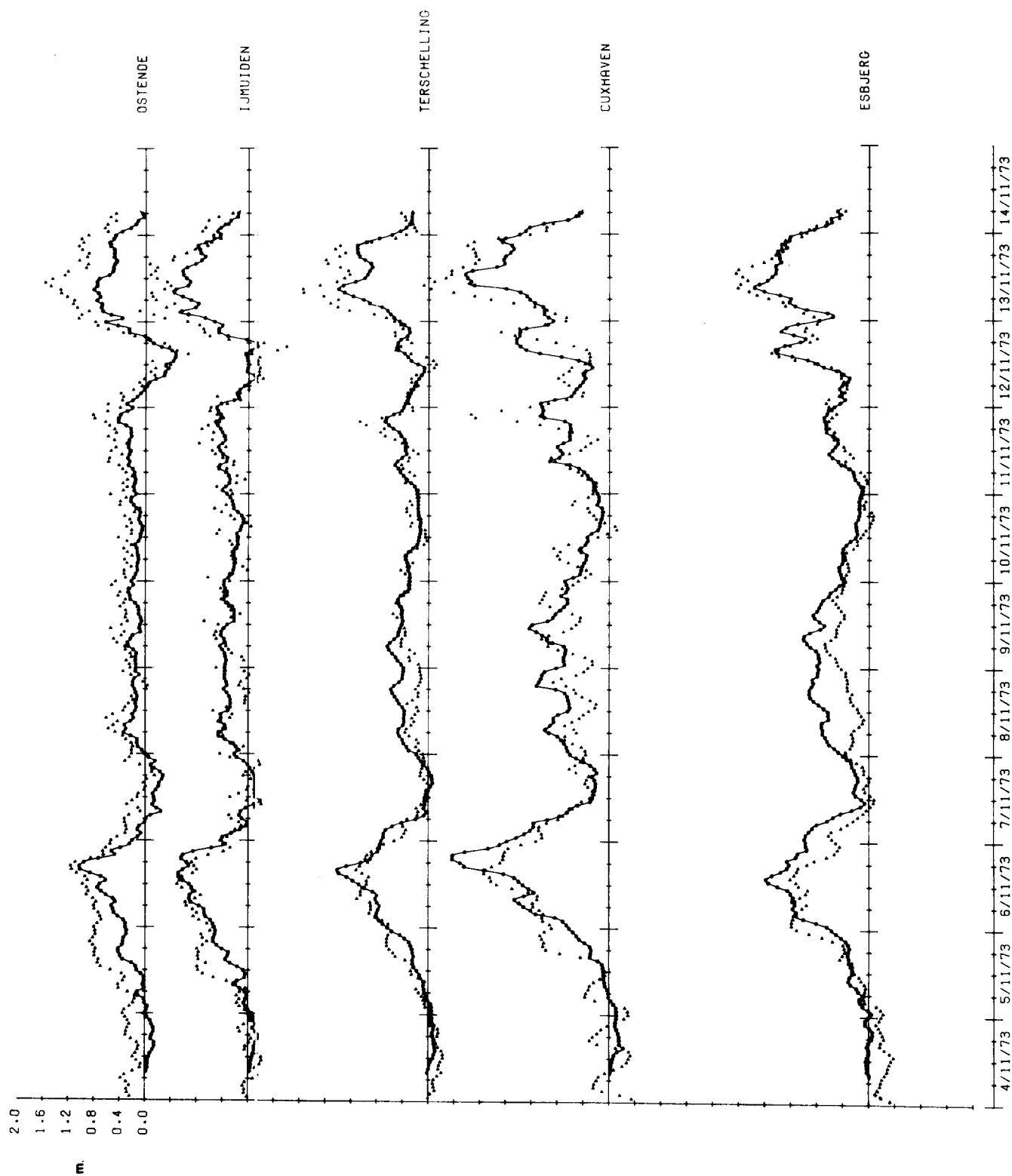


FIGURE 4b

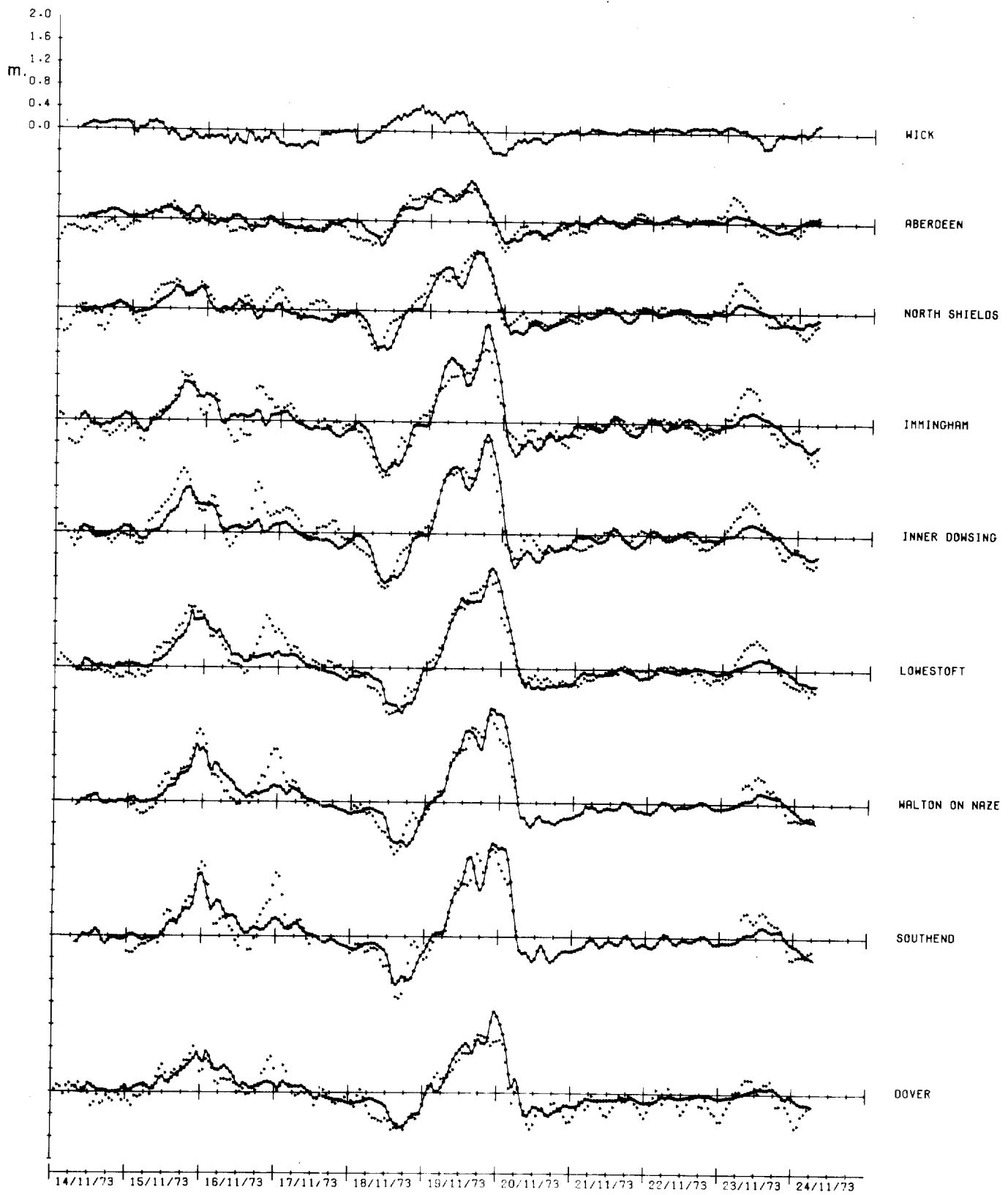


FIGURE 4c

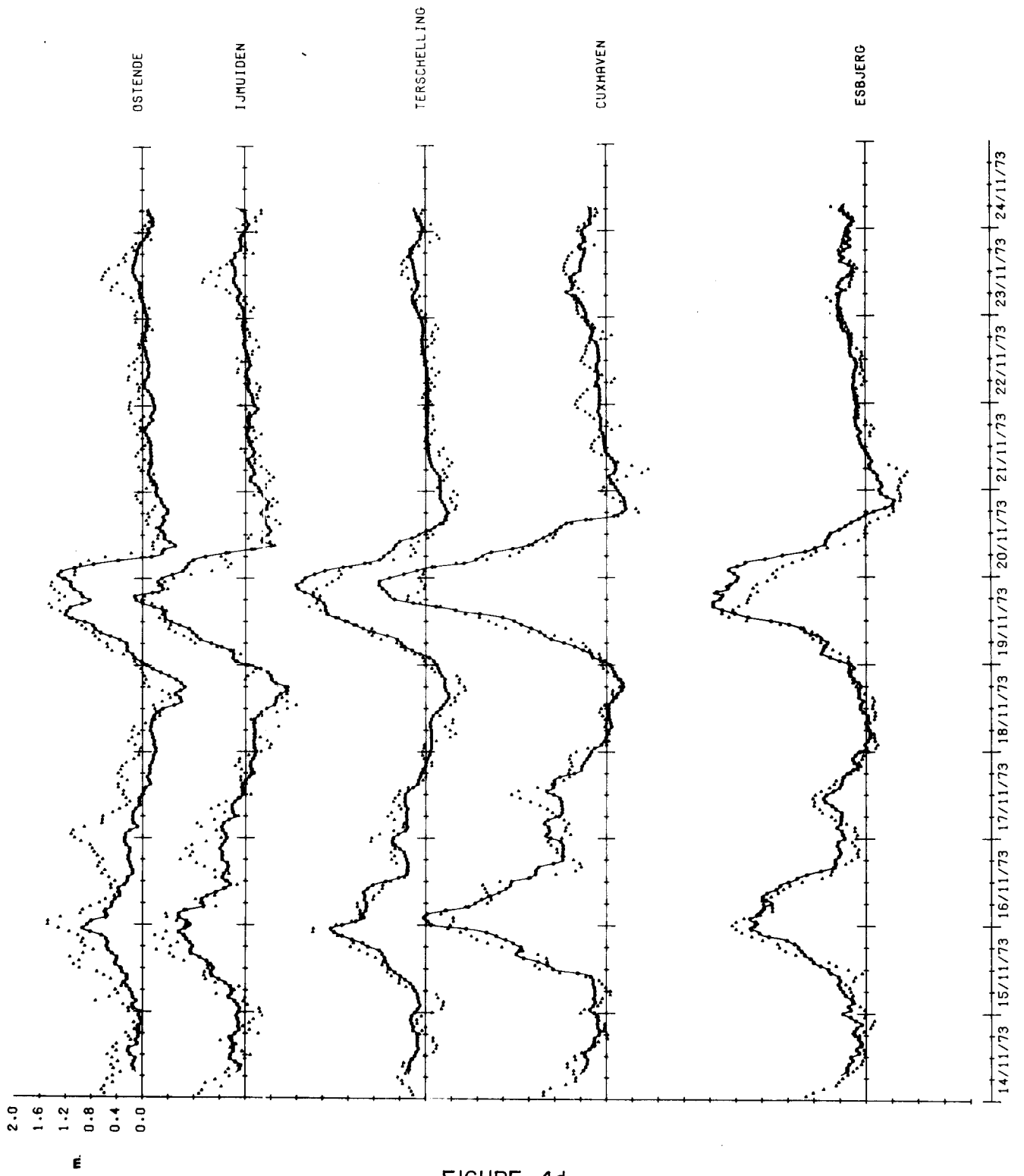


FIGURE 4d

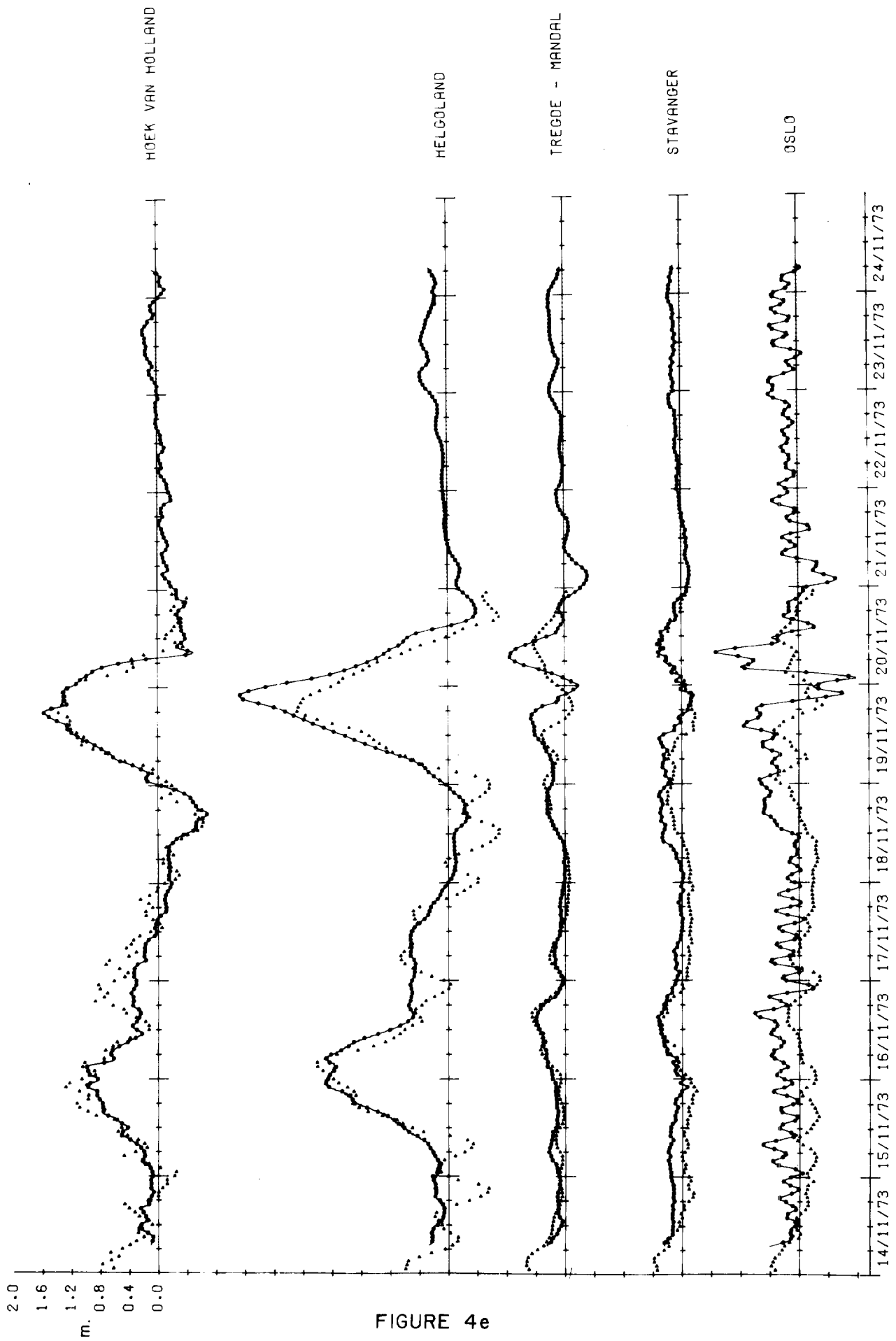


FIGURE 4e

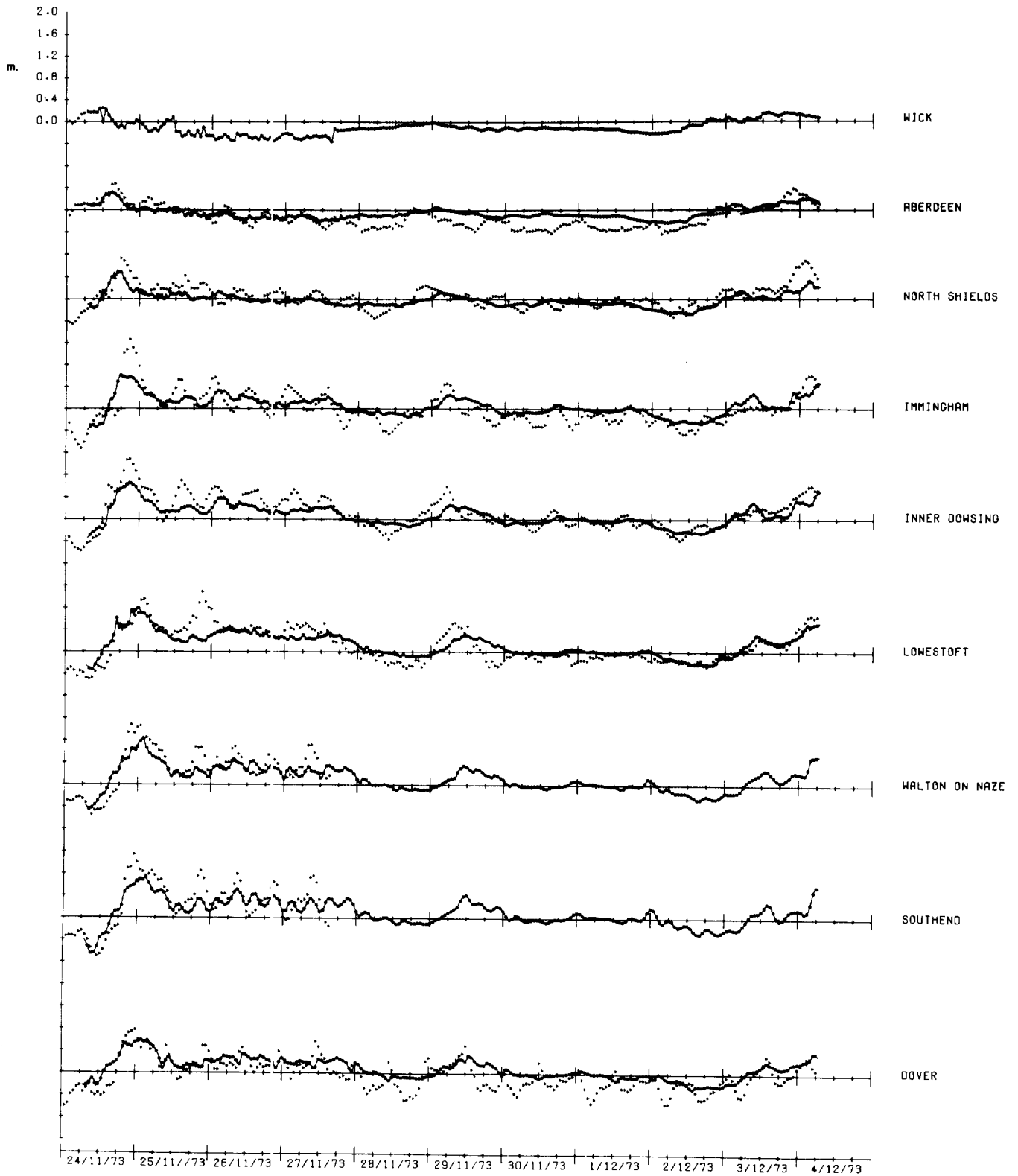


FIGURE 4f

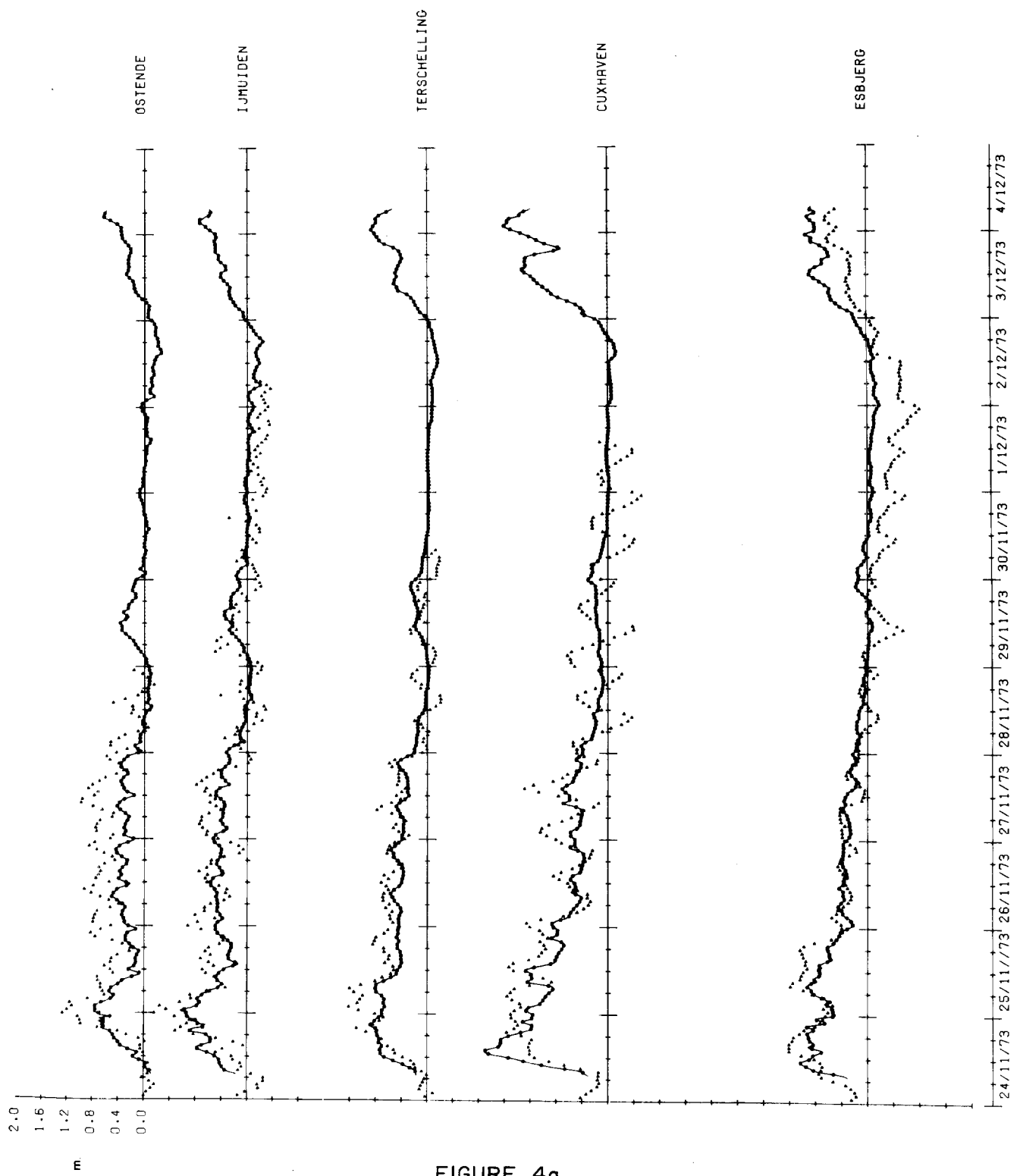


FIGURE 4g

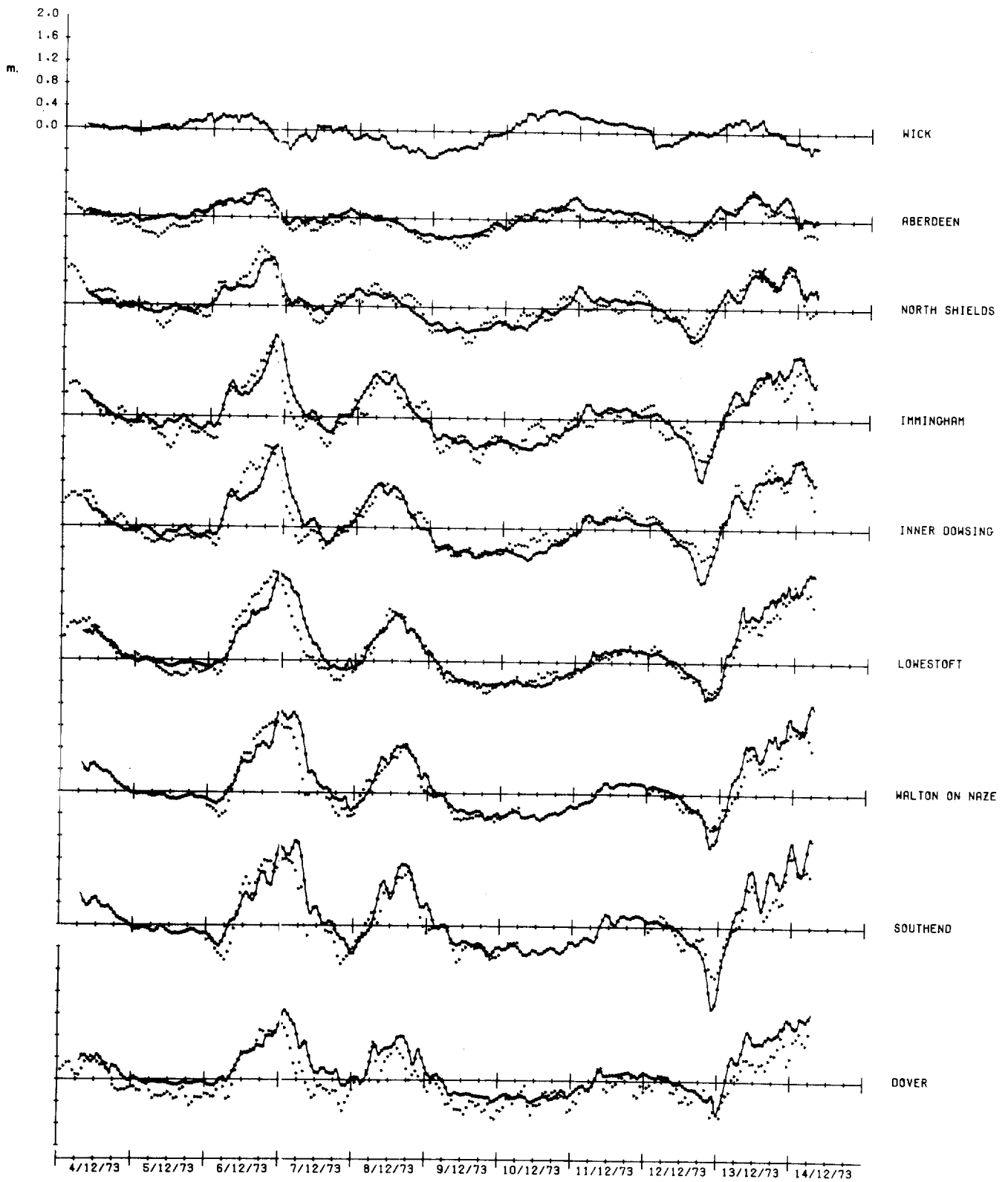


FIGURE 4h

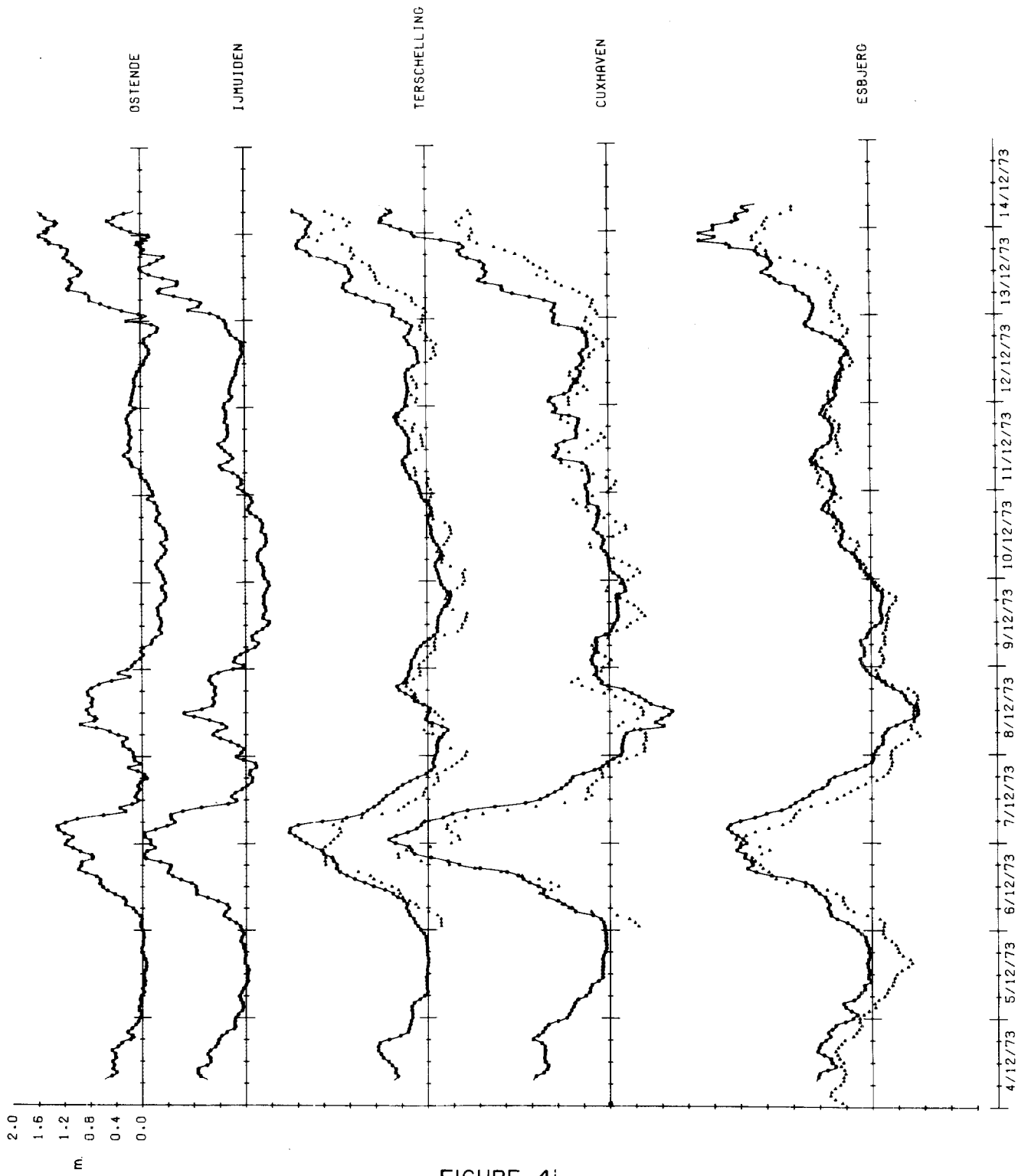


FIGURE 4i

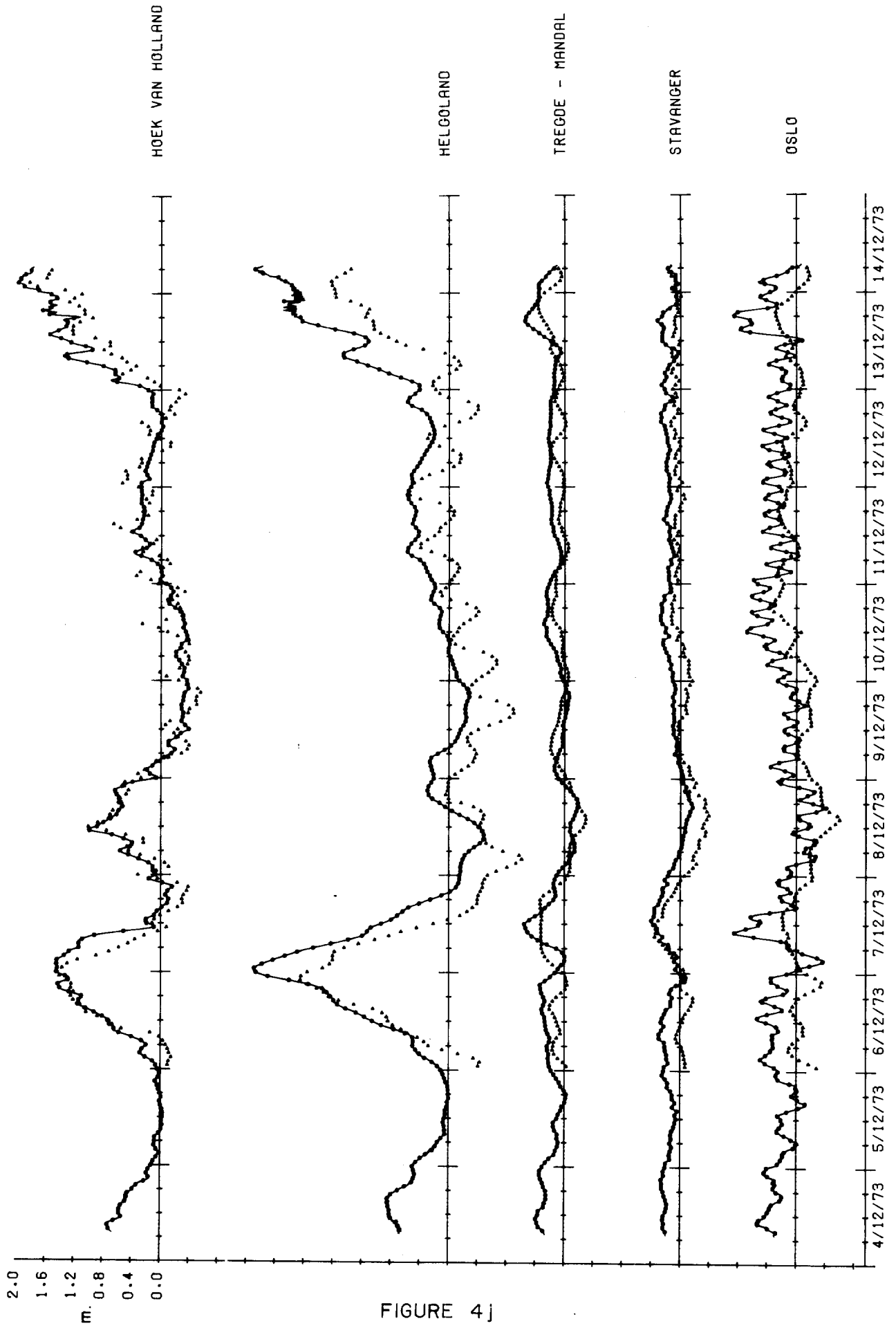


FIGURE 4j

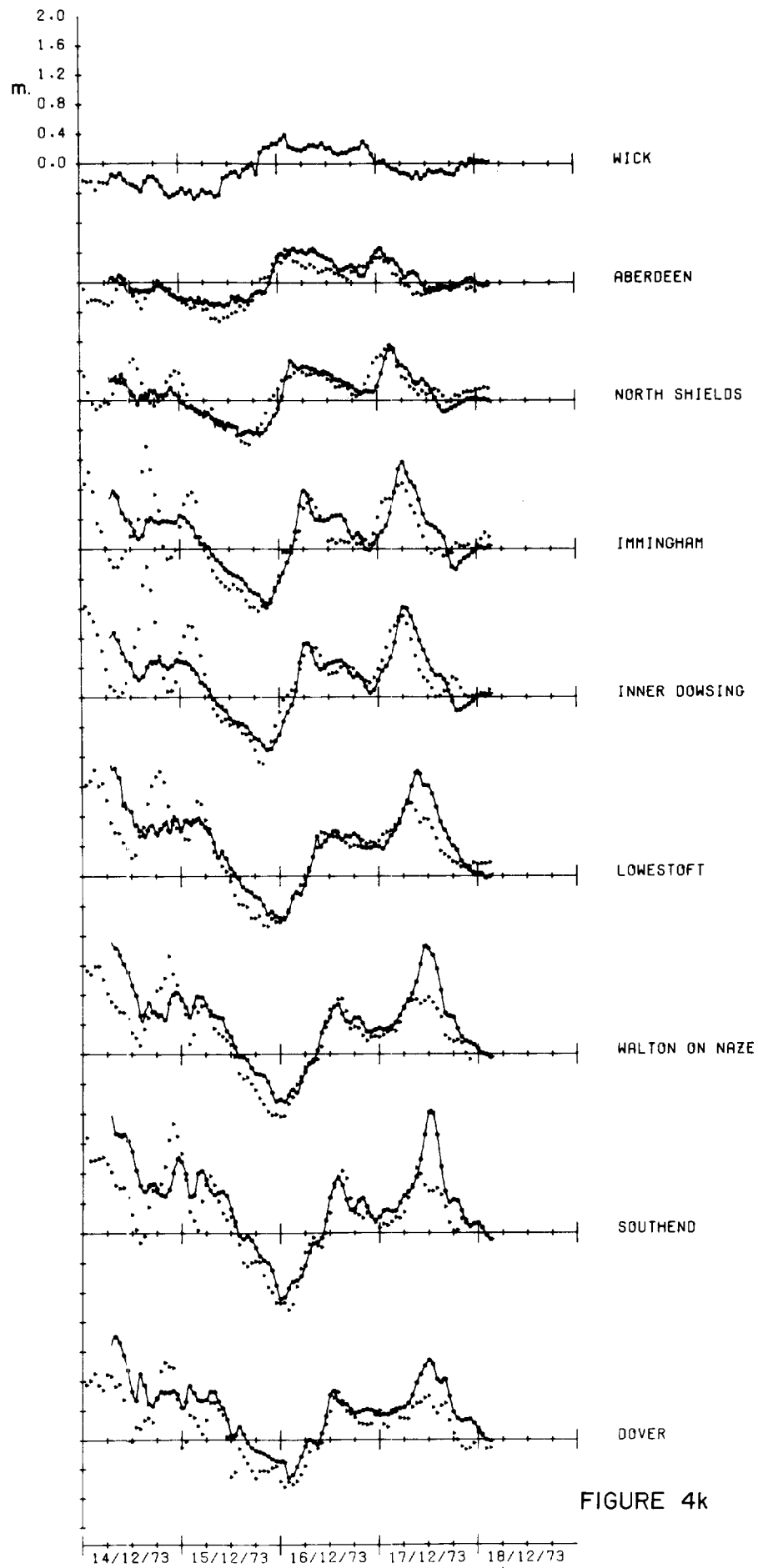


FIGURE 4k

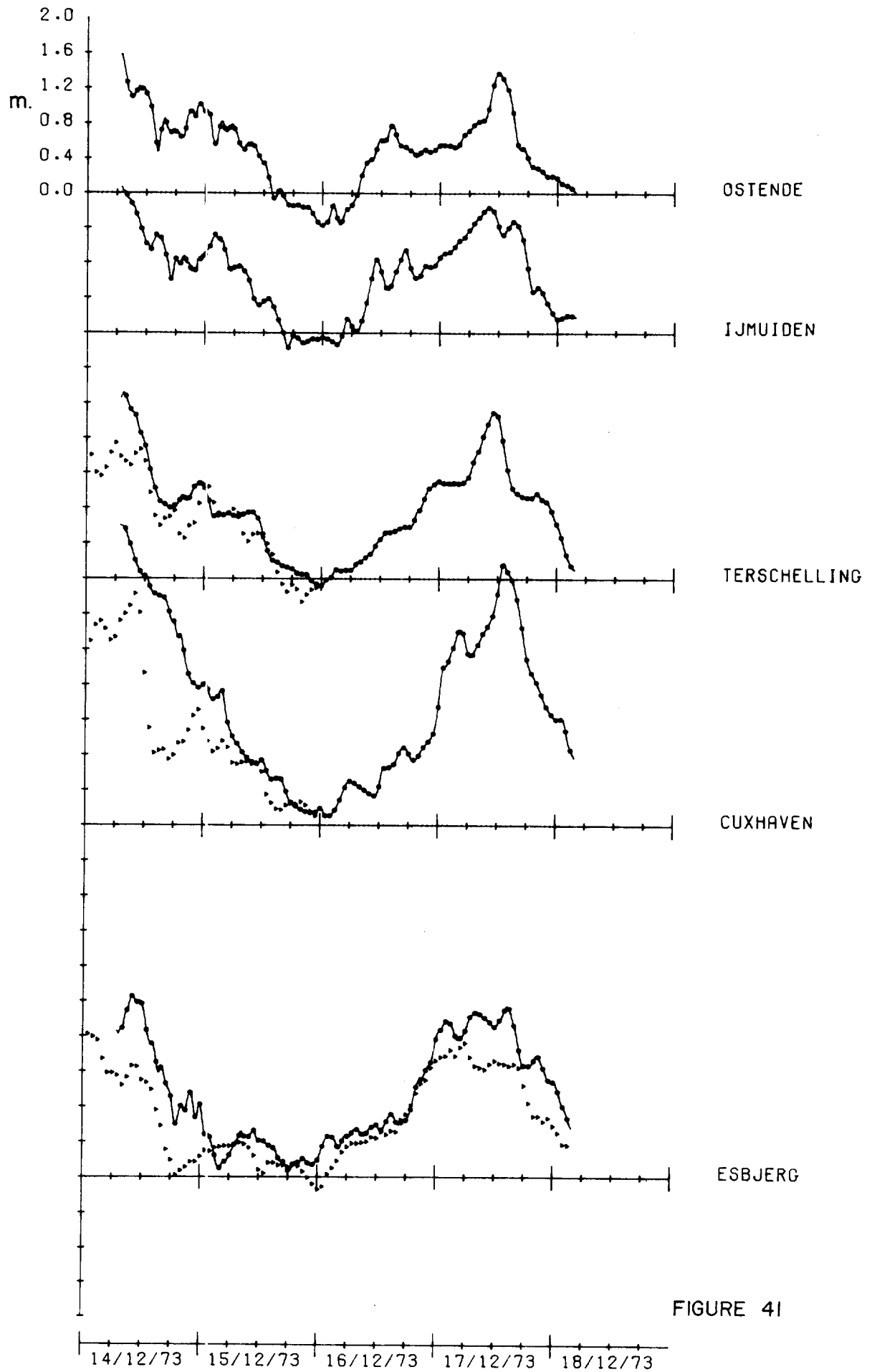


FIGURE 41

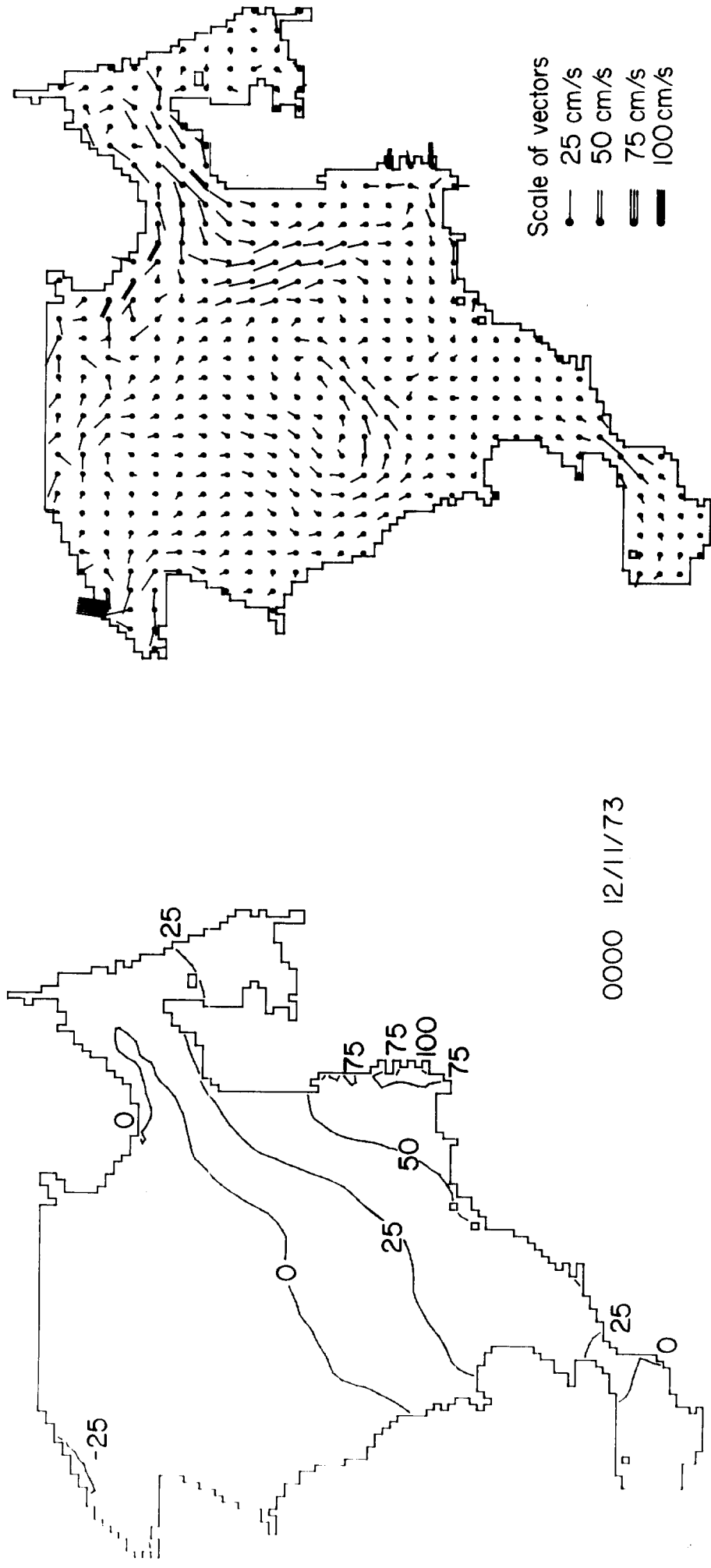
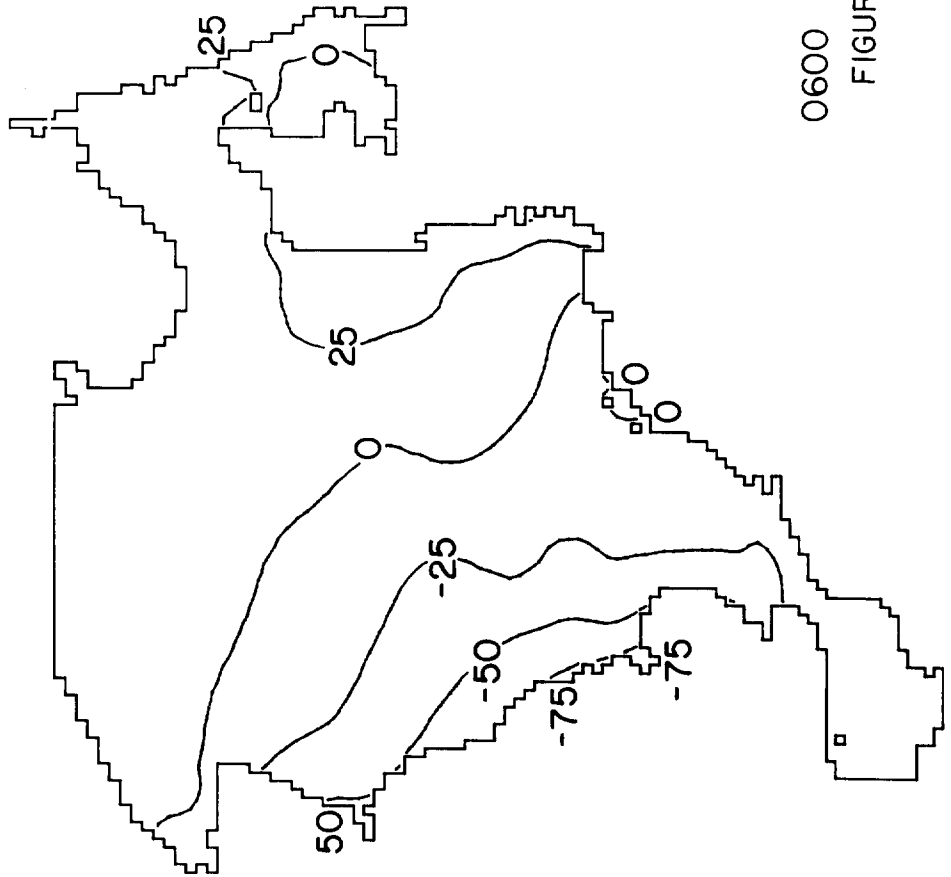
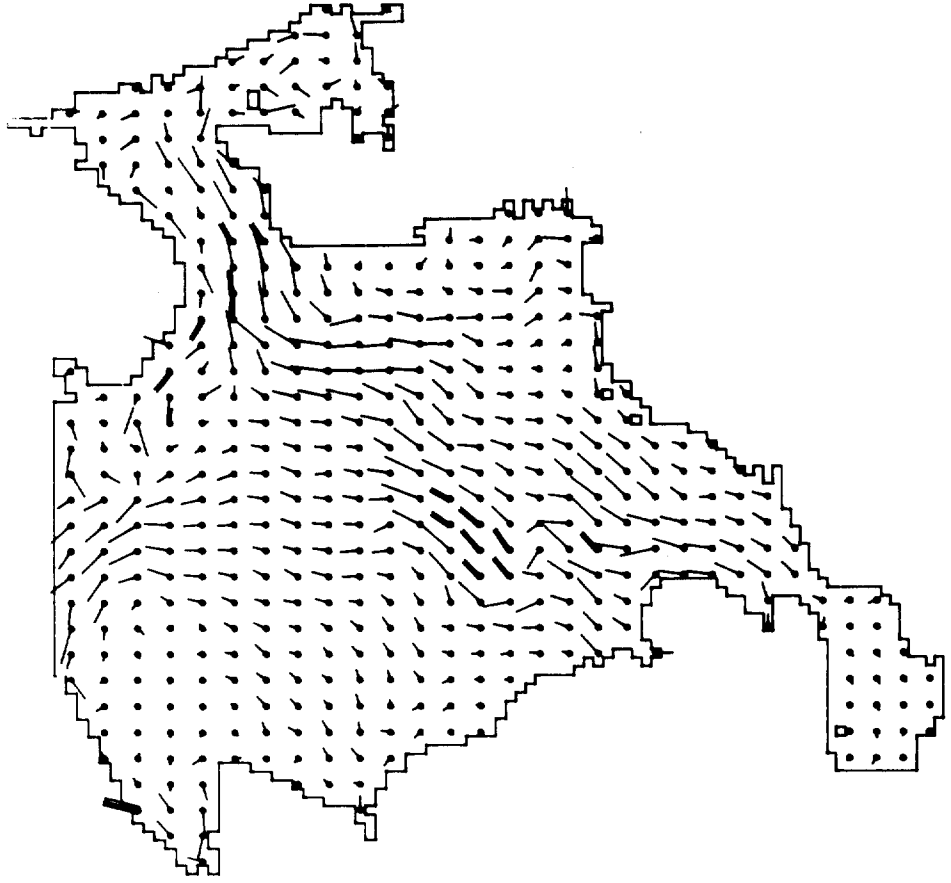
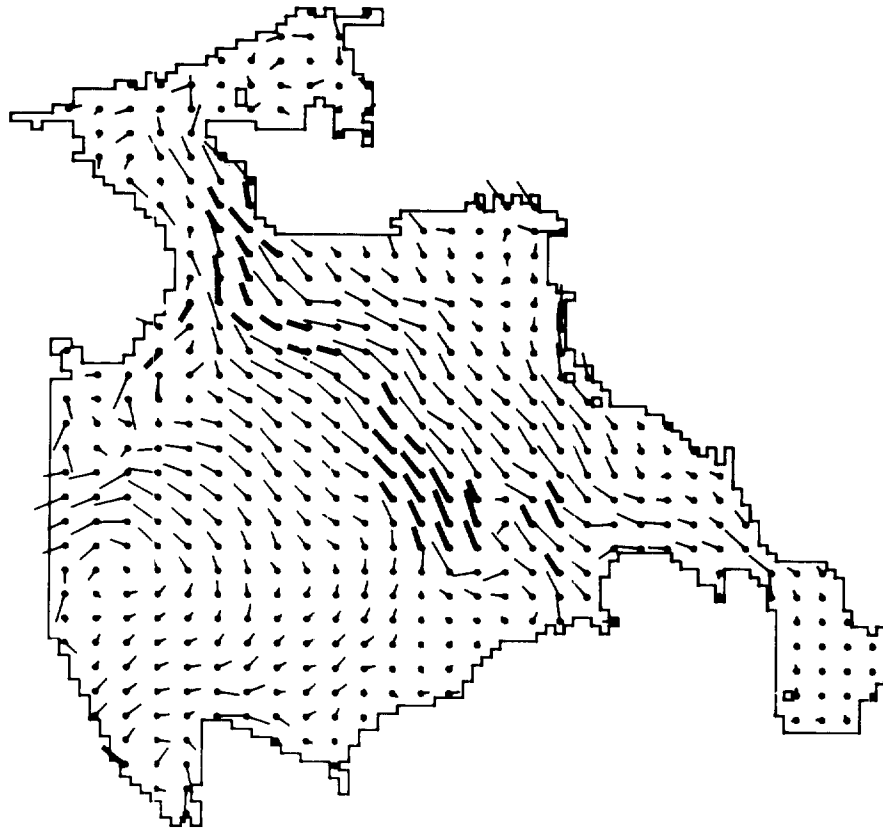
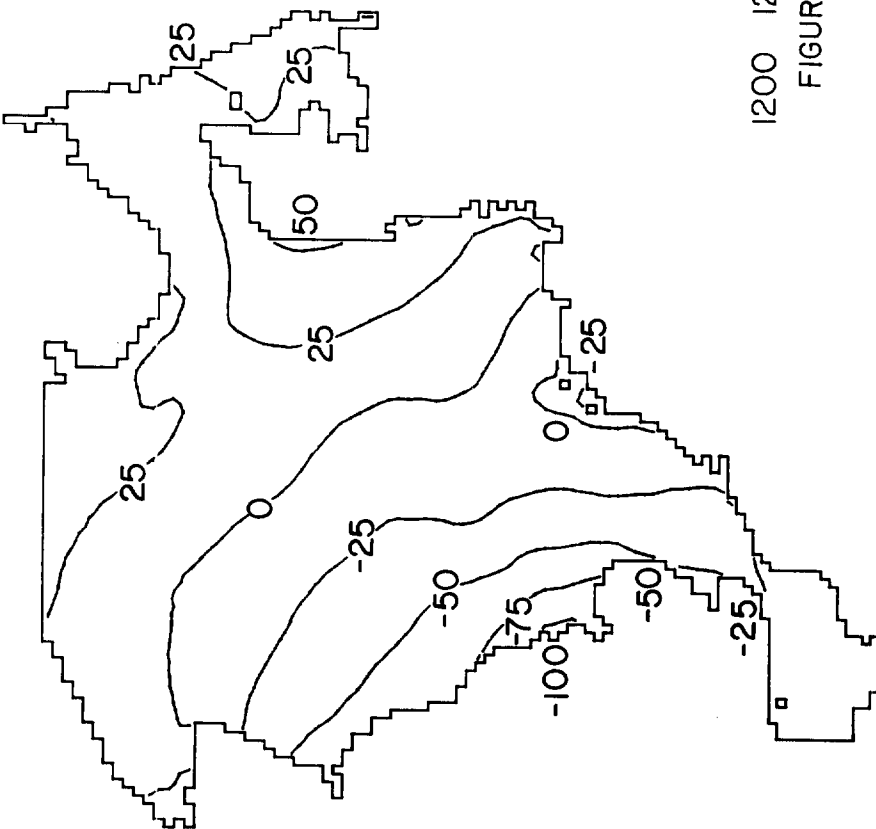


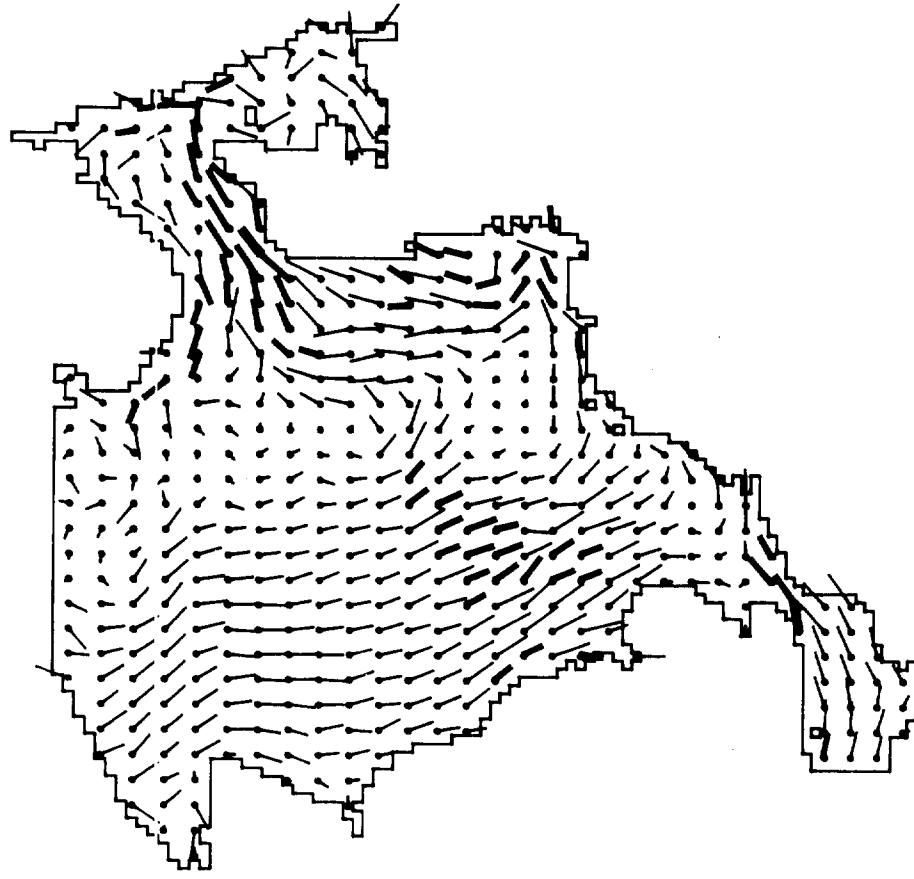
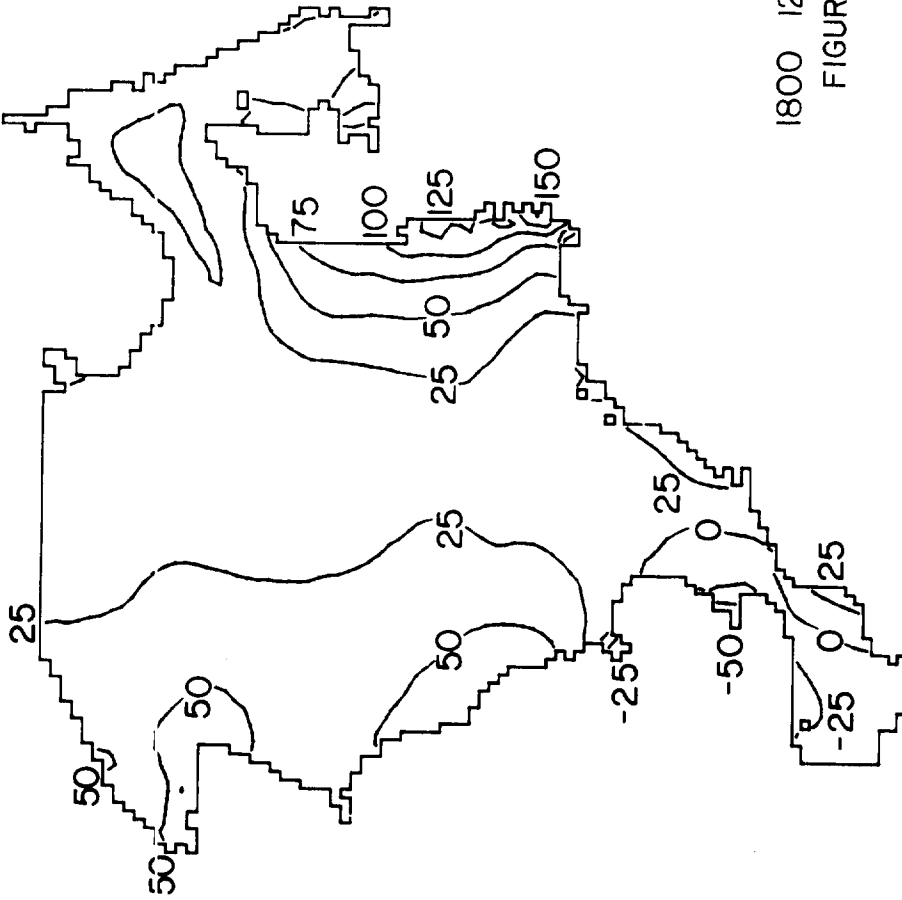
FIGURE 5a: CONTOURS OF SURFACE ELEVATION (cm.) AND CURRENT VECTORS FOR STORM SURGE 12-13/11/73



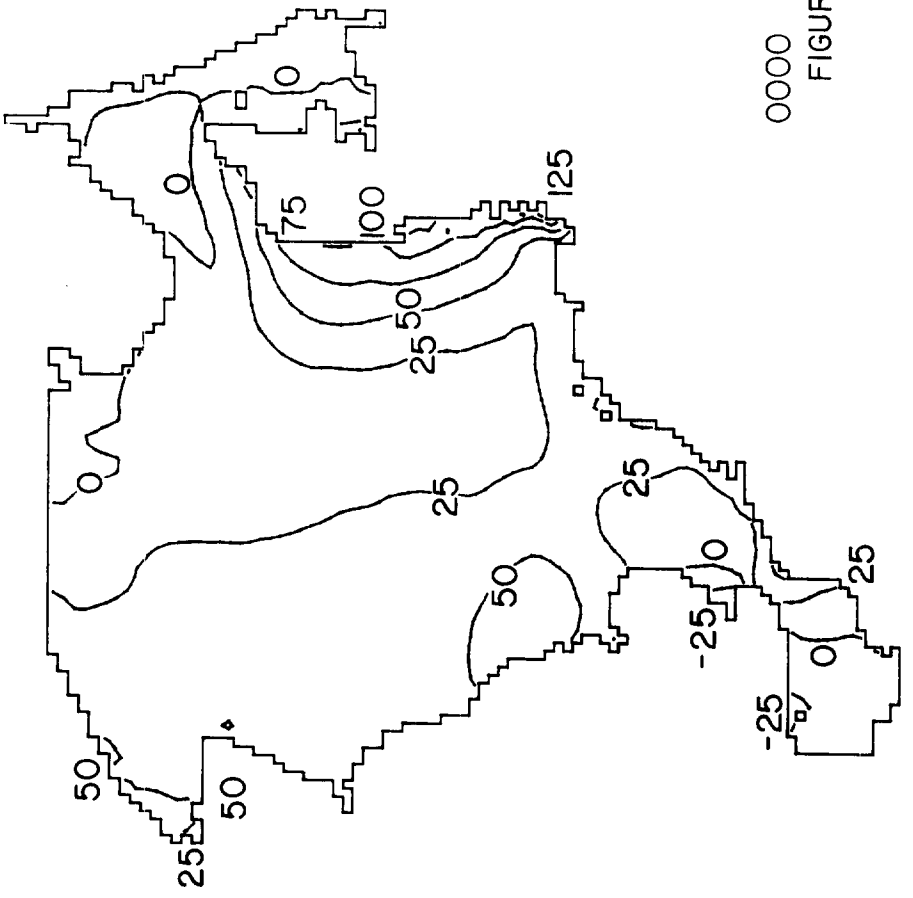
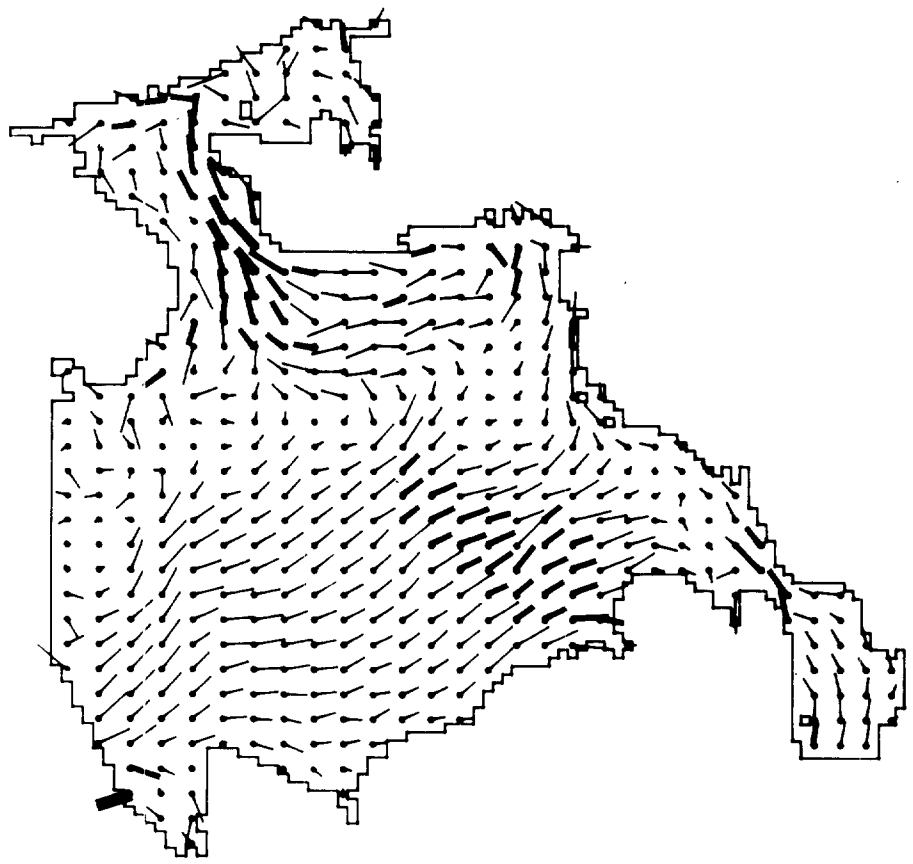
0600 12/11/73
FIGURE 5b



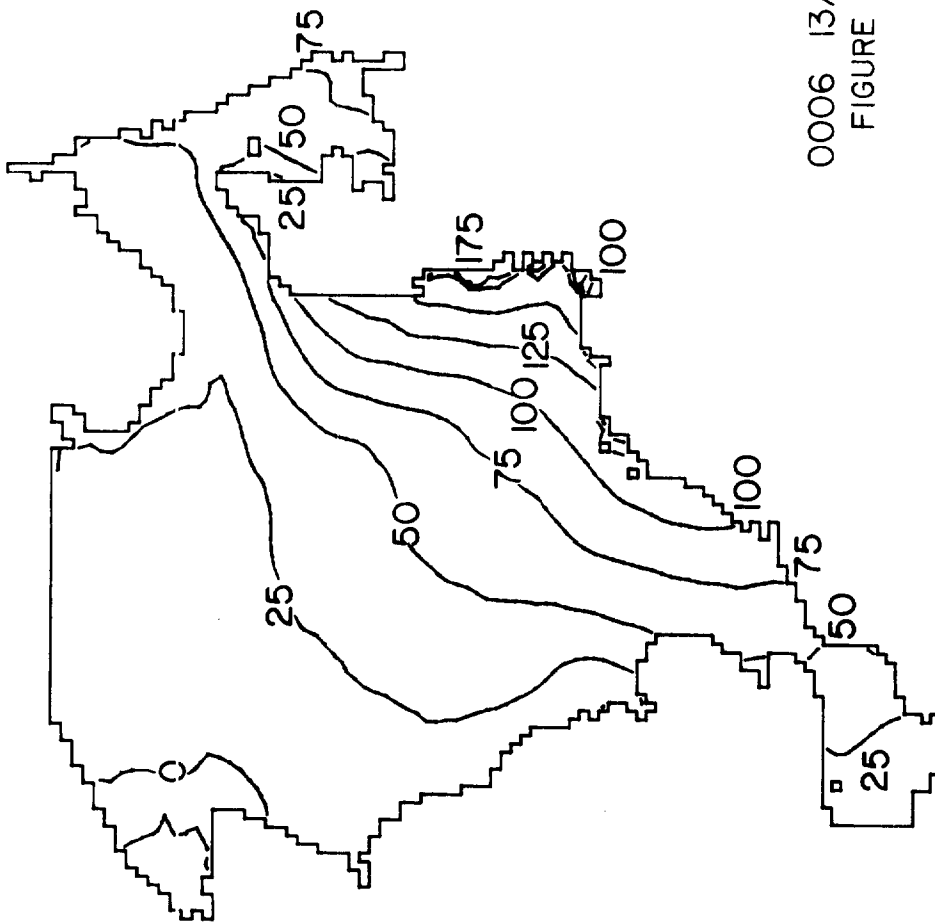
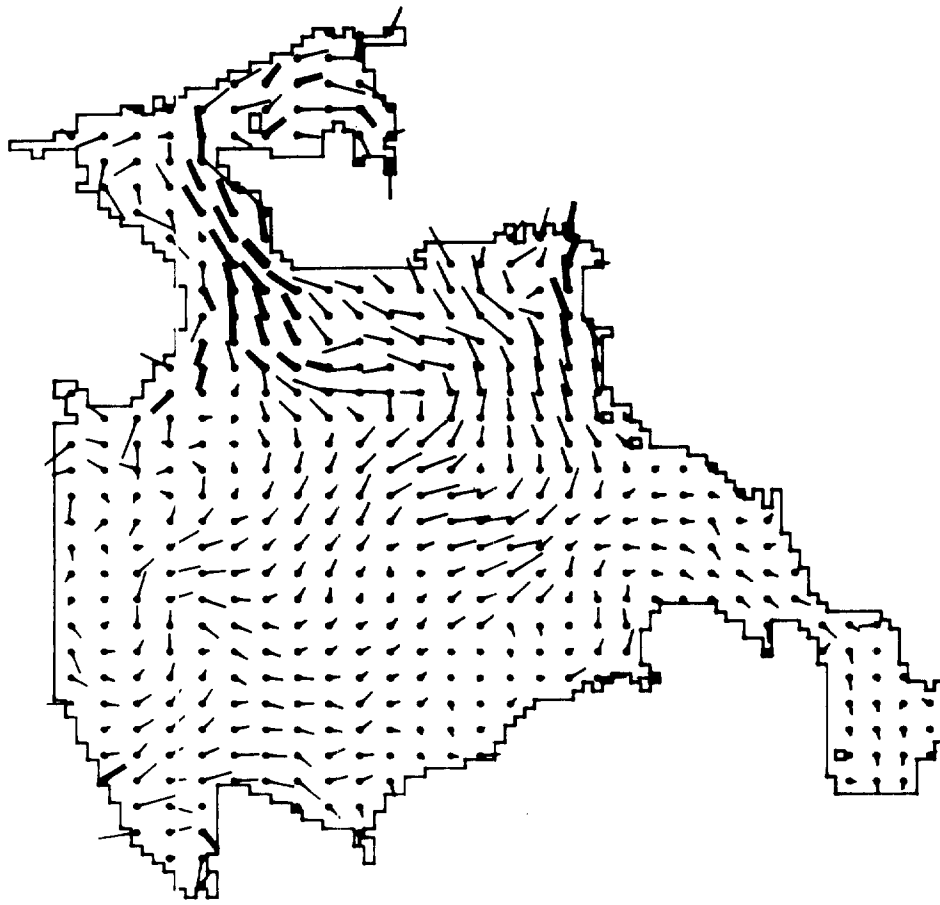
1200 12/11/73
FIGURE 5c



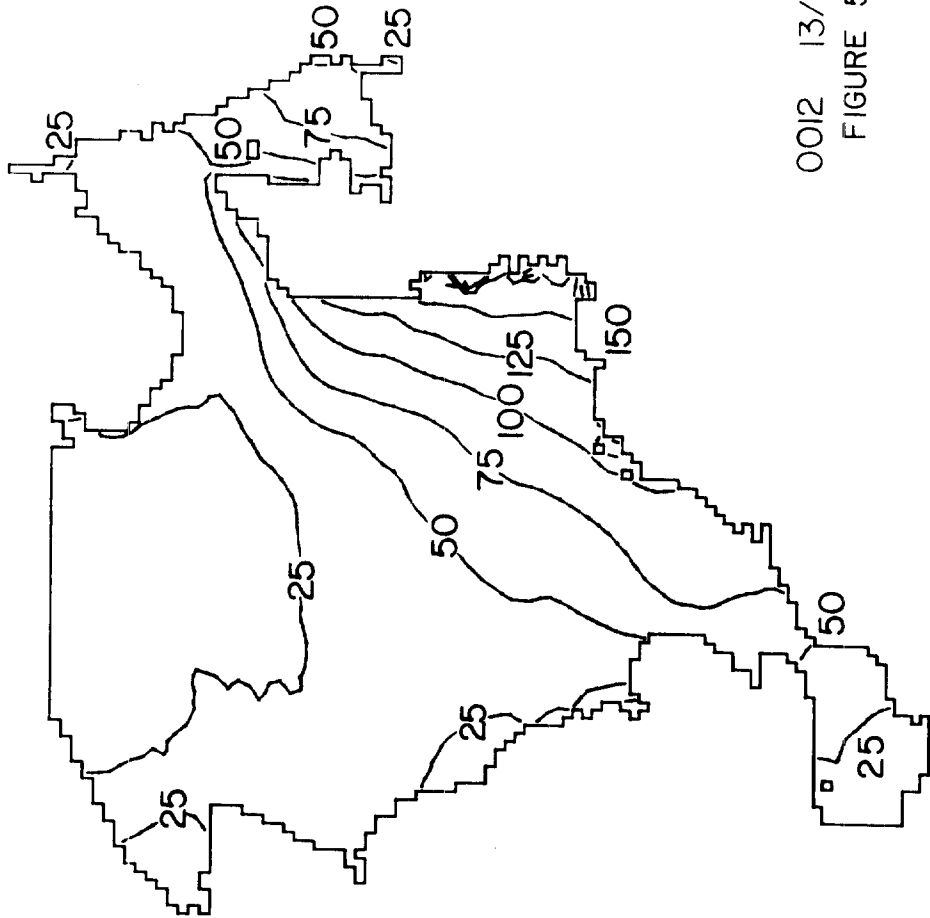
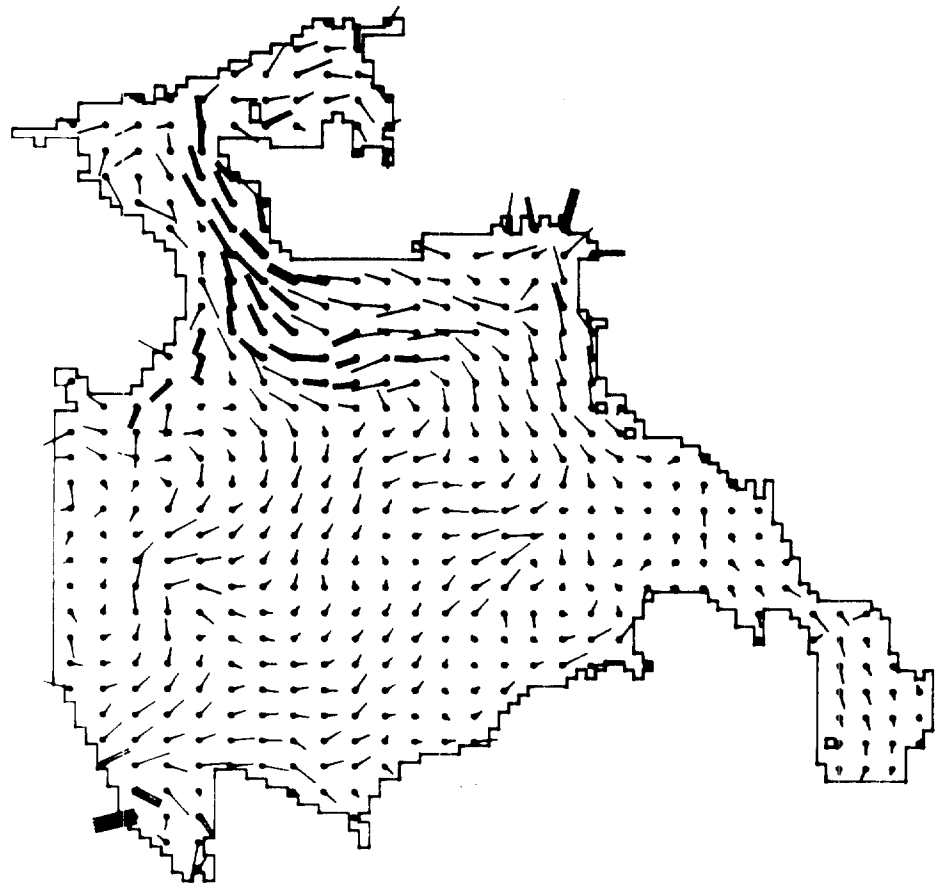
1800 12/11/73
FIGURE 5d



0000 13/11/73
 FIGURE 5e



0006 13/11/73
FIGURE 5f



0012 13/11/73
FIGURE 5g

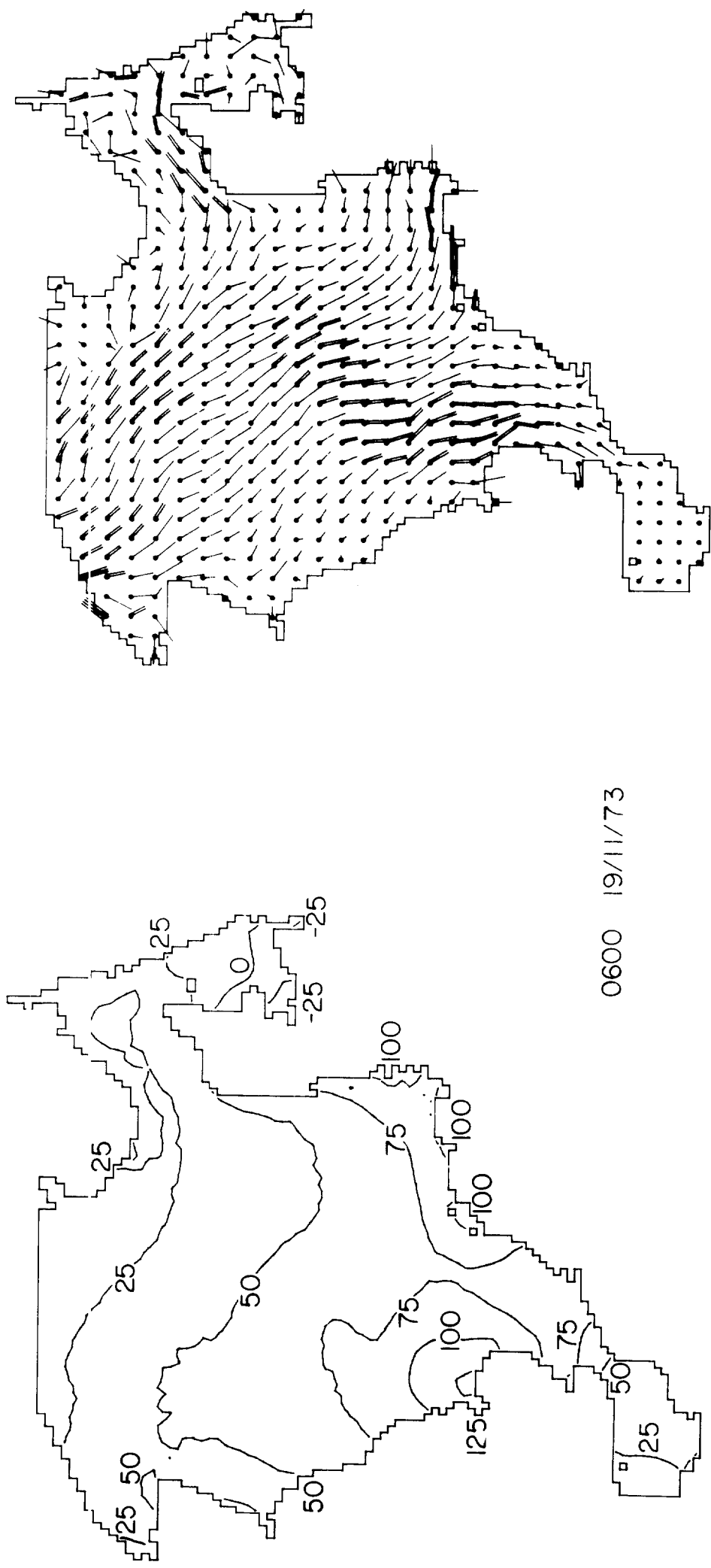
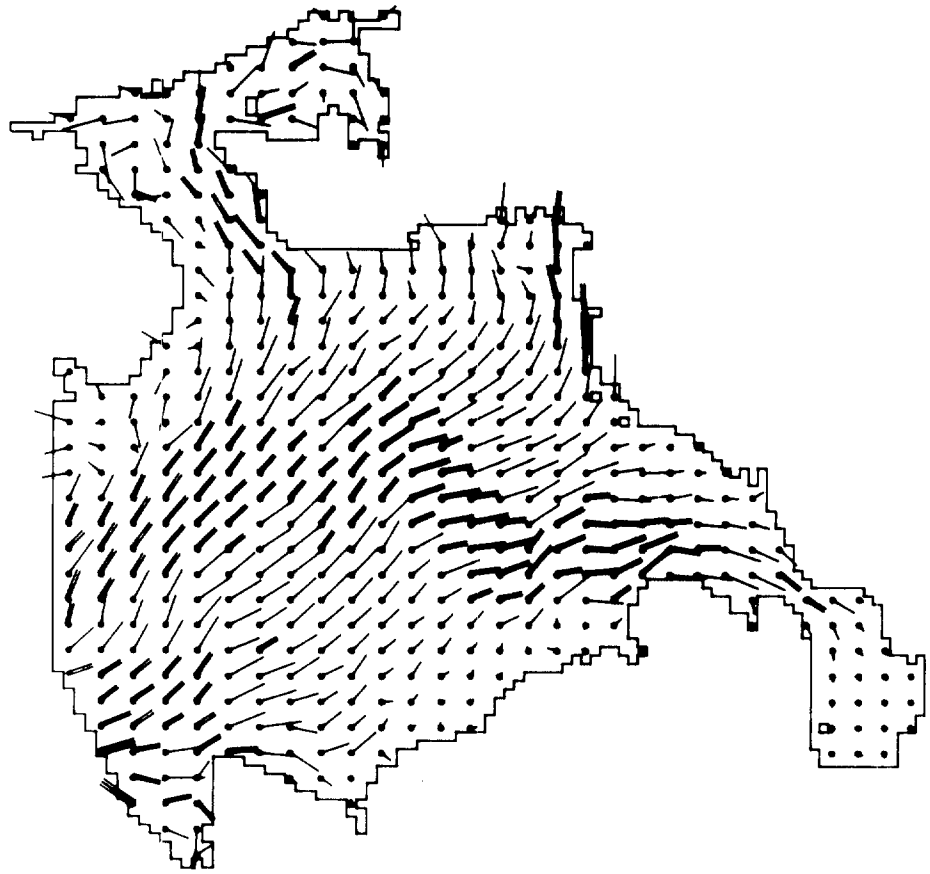
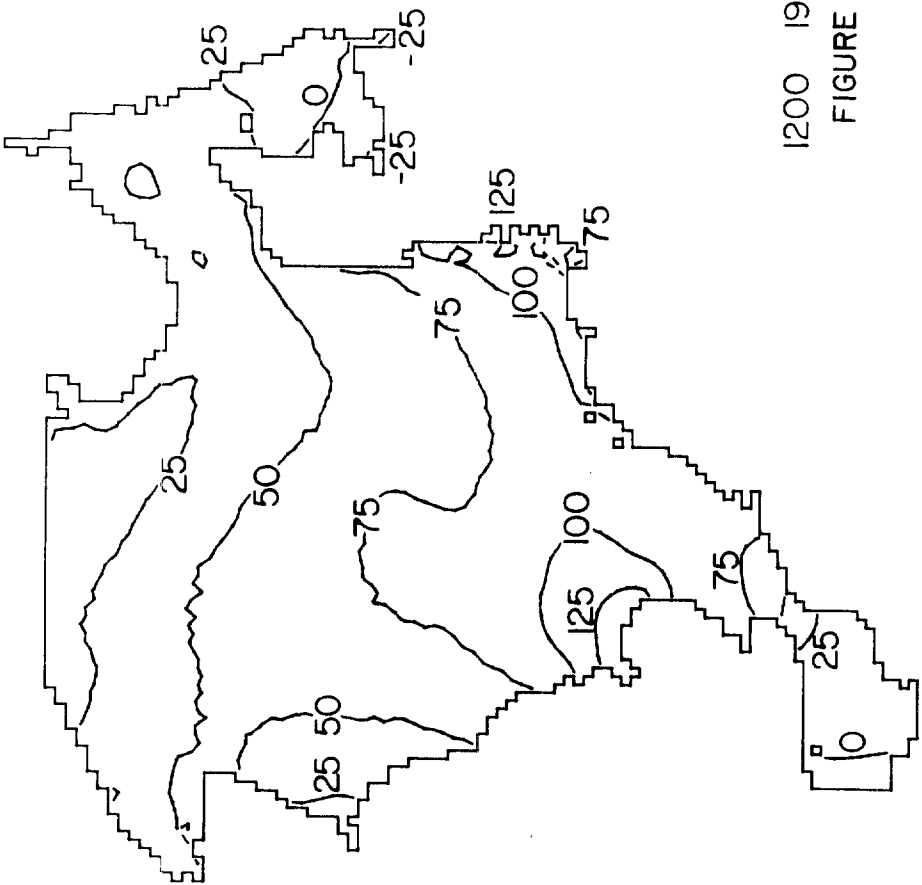
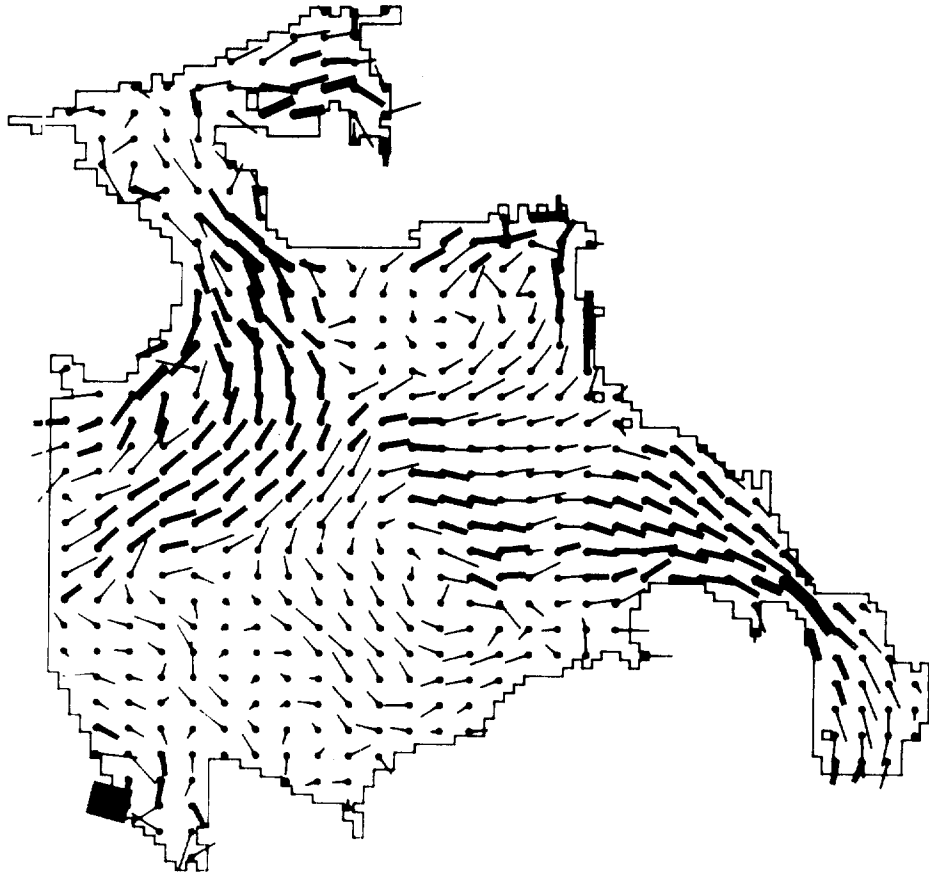
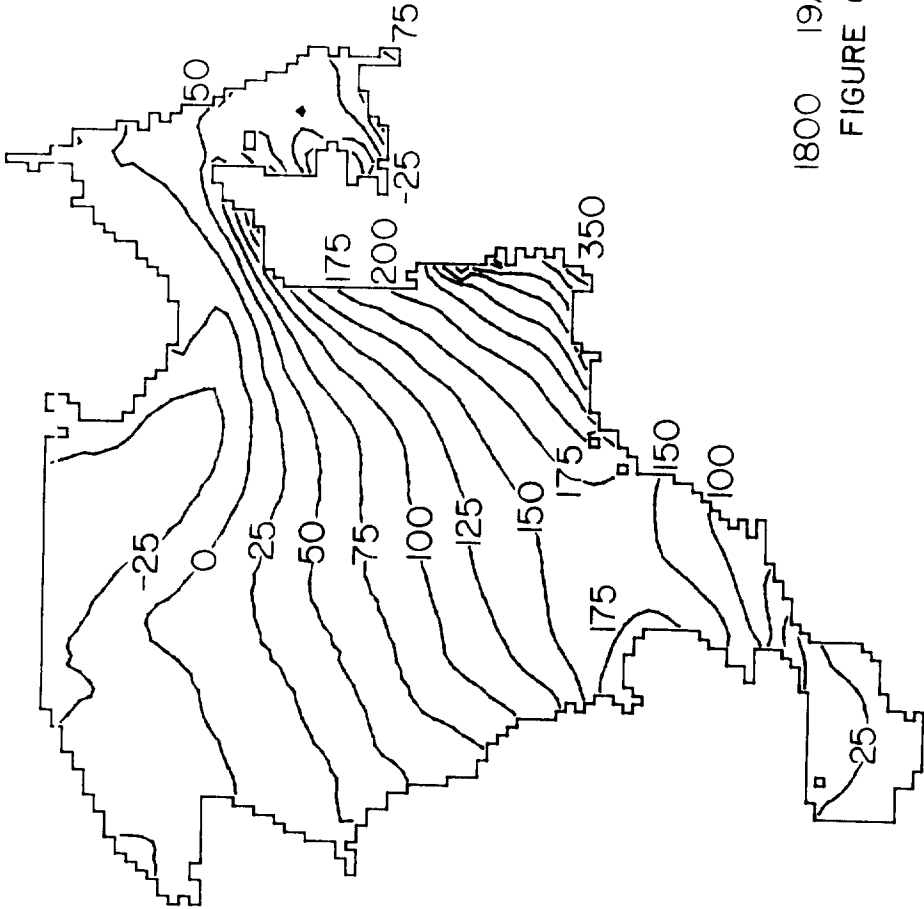


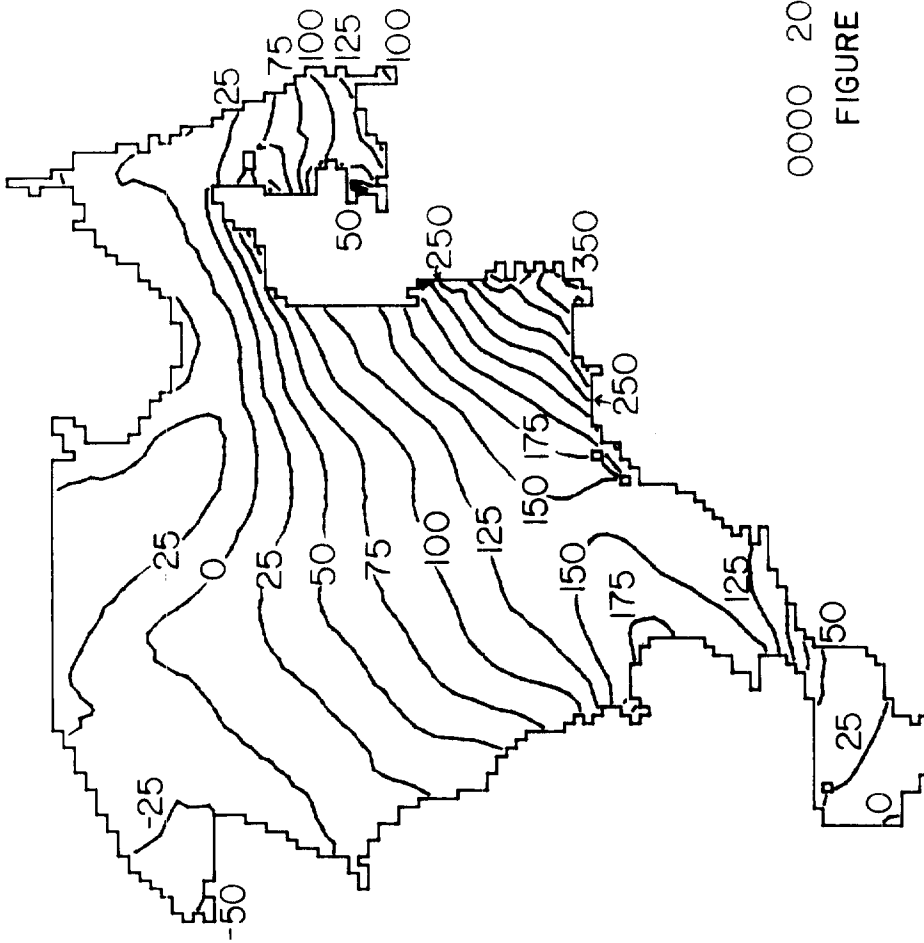
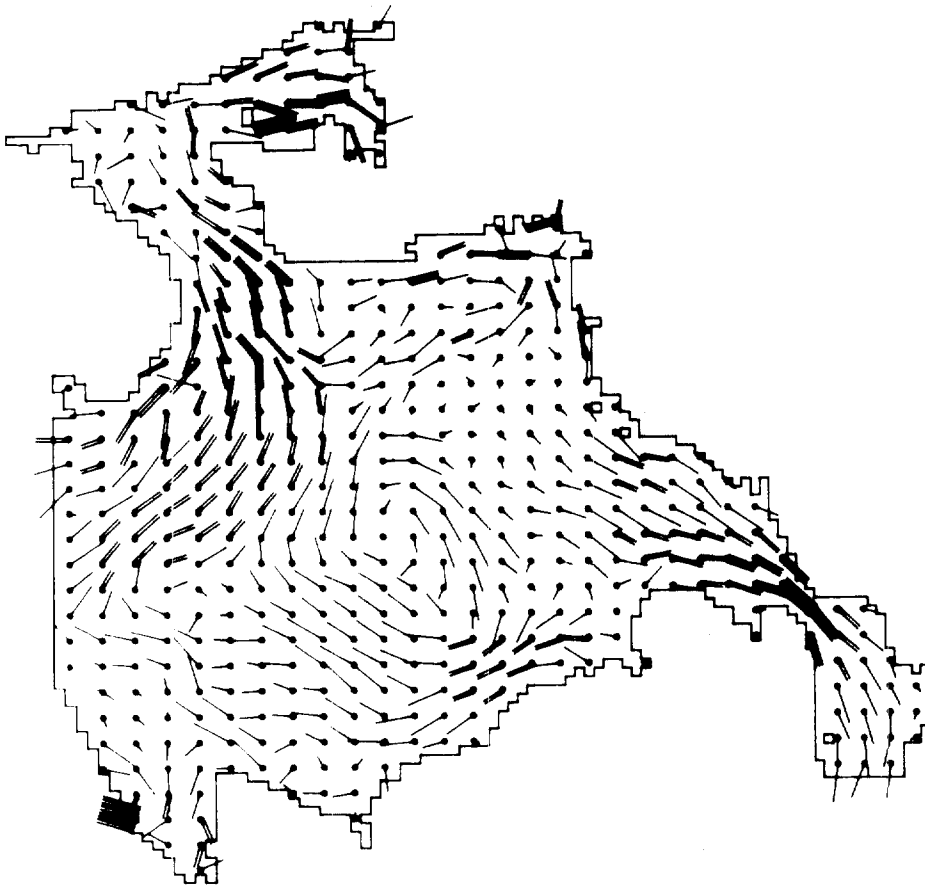
FIGURE 6a: CONTOURS OF SURFACE ELEVATION (cm.) AND CURRENT VECTORS FOR THE STORM SURGE 19-20/11/73



1200 19/11/73
FIGURE 6b

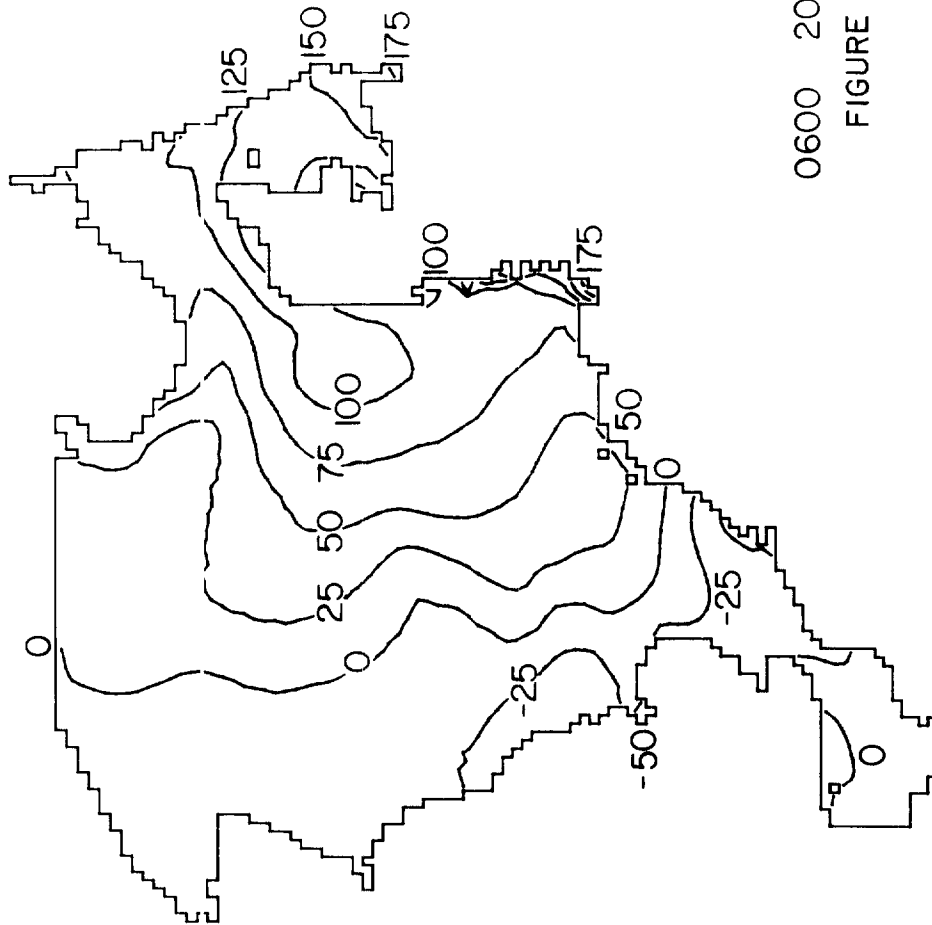
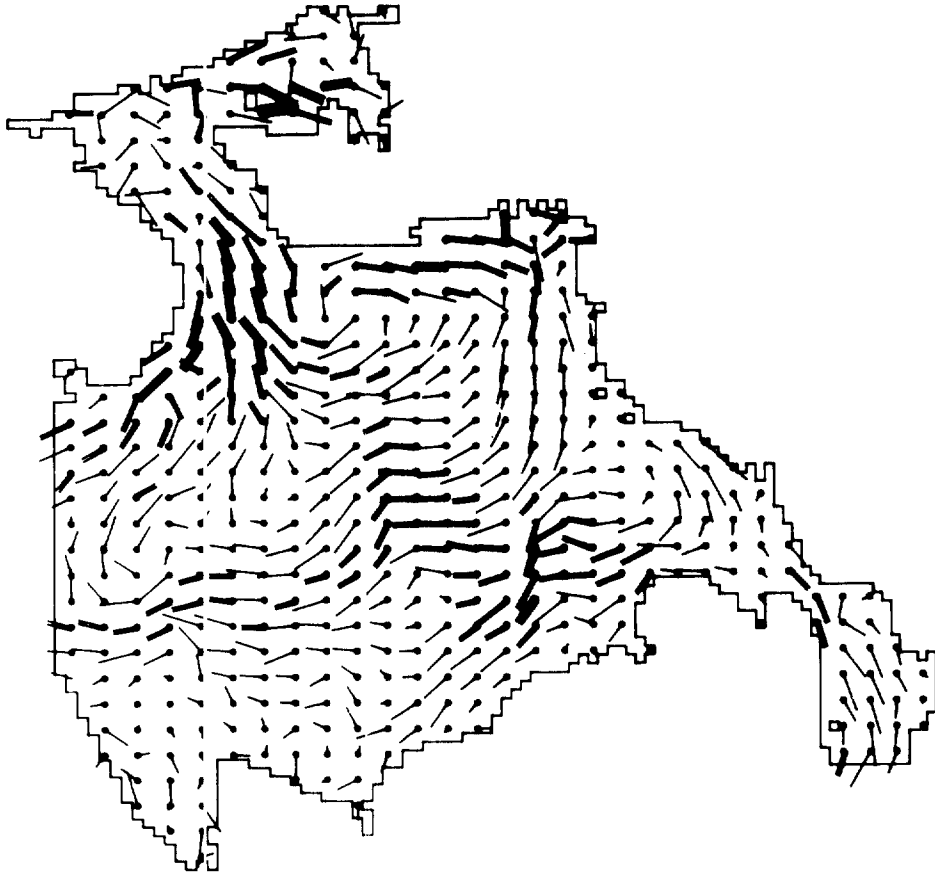


1800 19/11/73
FIGURE 6c

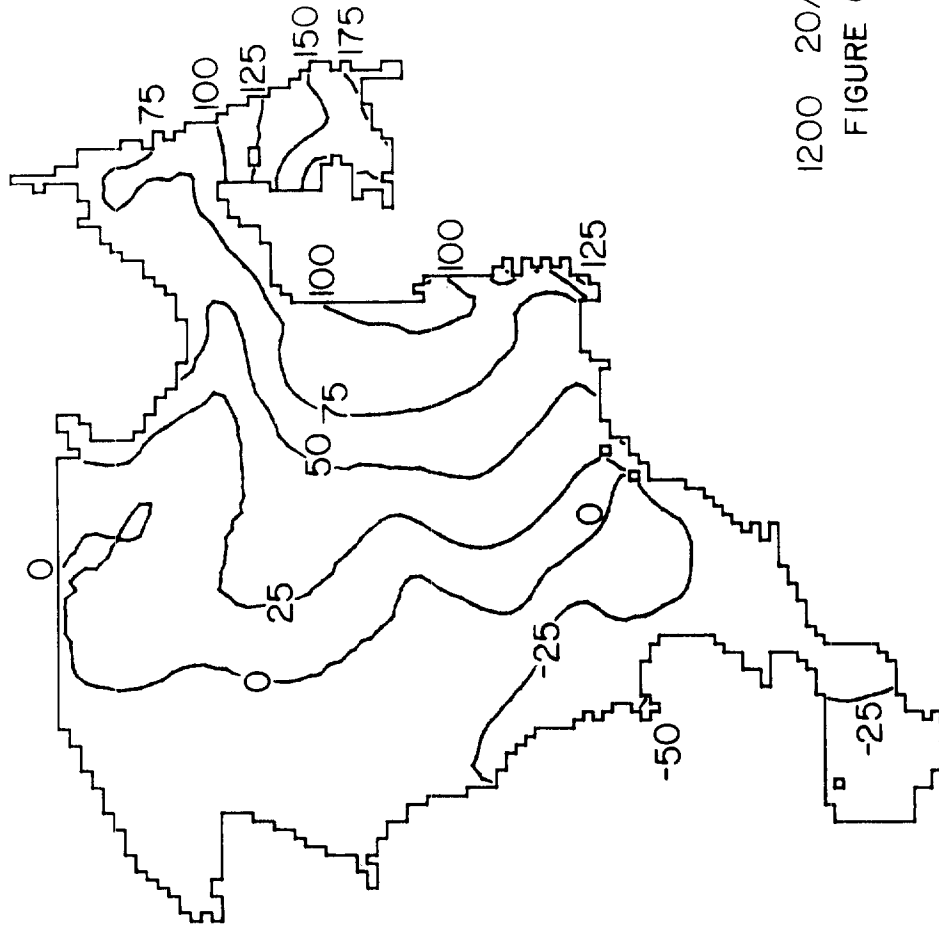
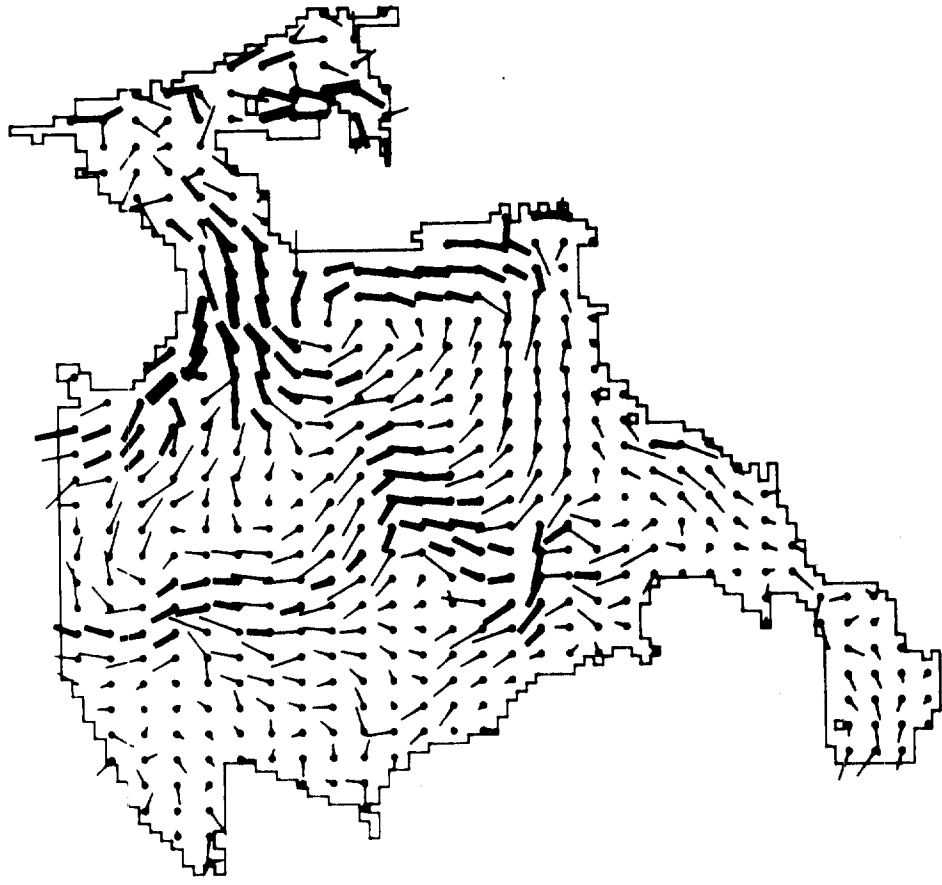


0000 20/11/73

FIGURE 6d

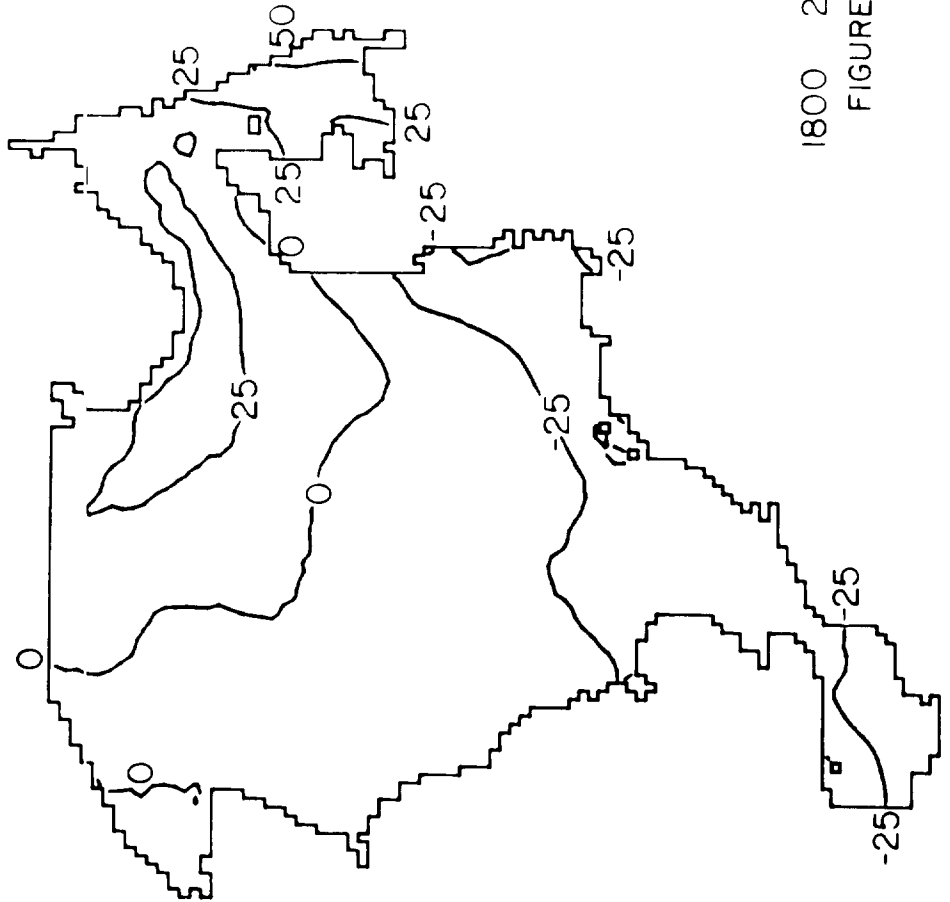
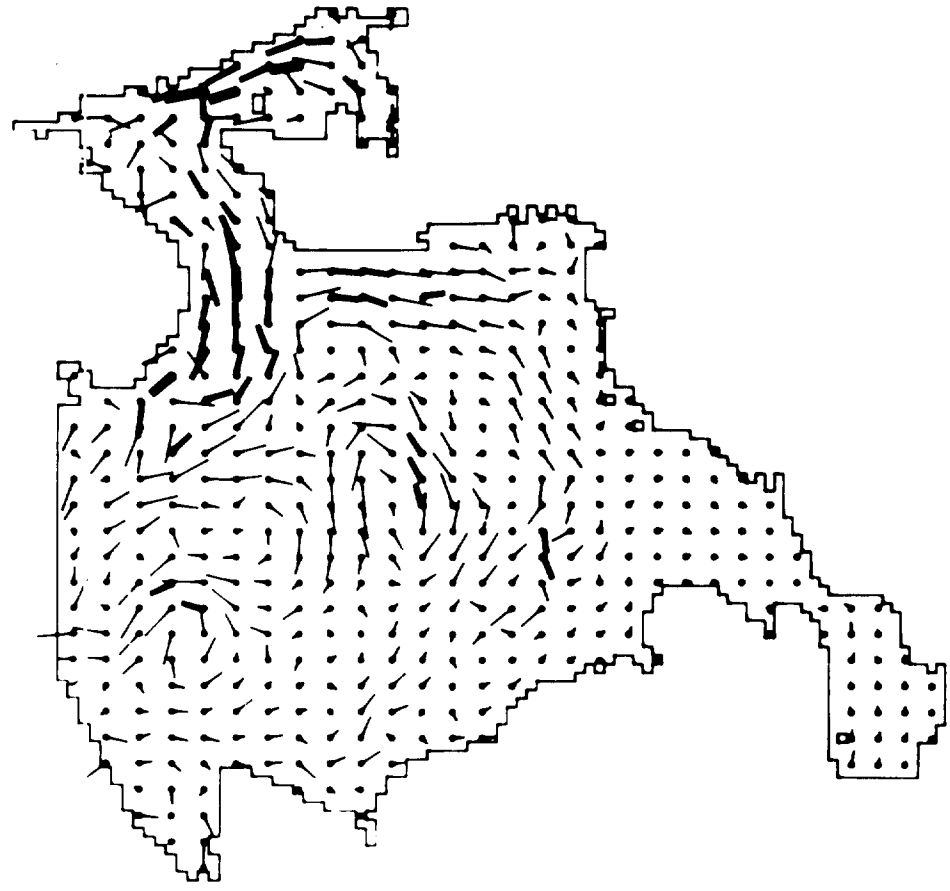


0600 20/11/73
FIGURE 6e



1200 20/11/73

FIGURE 6f



1800 20/11/73

FIGURE 6g

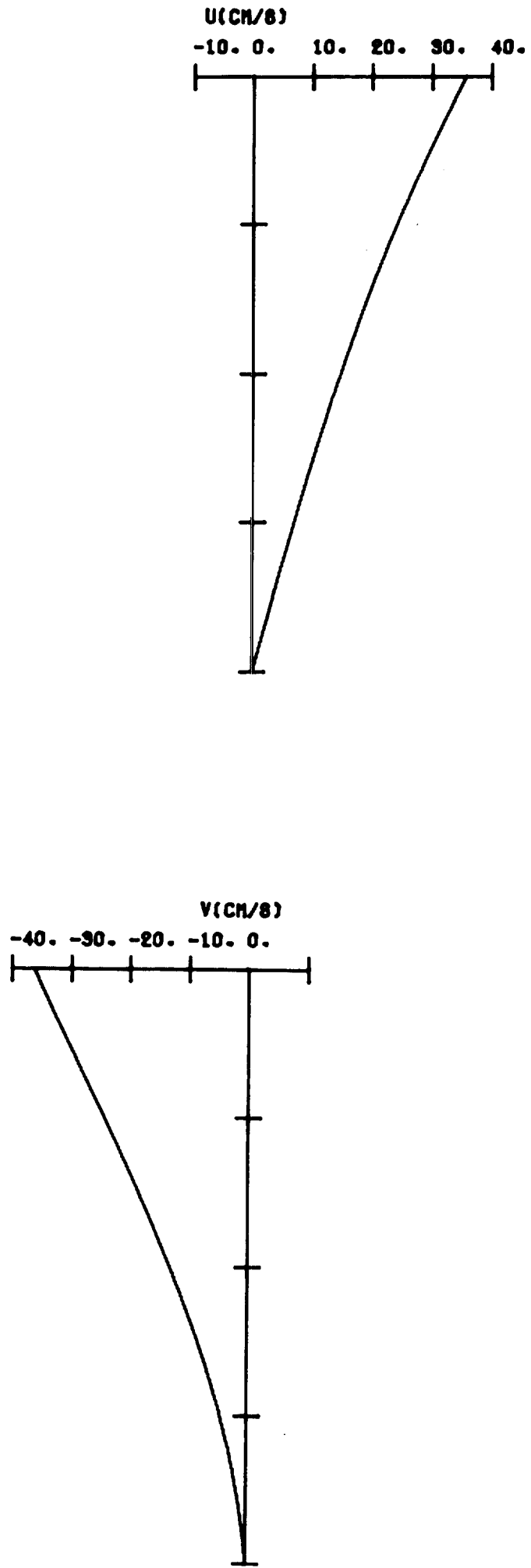


FIGURE 7a: VERTICAL PROFILES OF STORM SURGE INDUCED CURRENTS

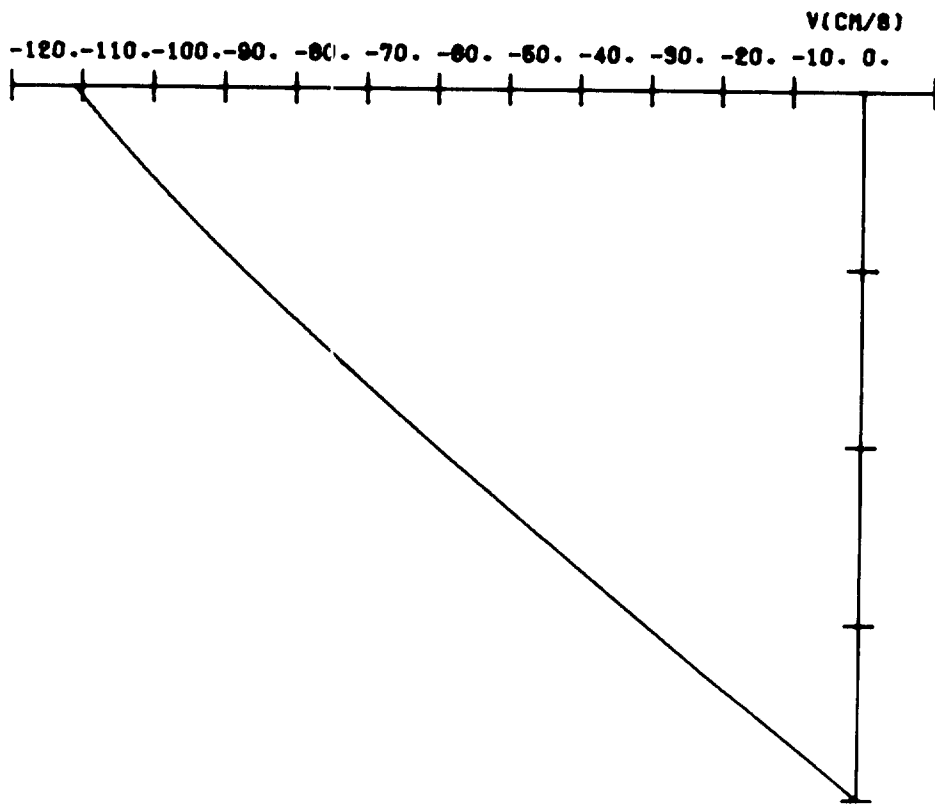
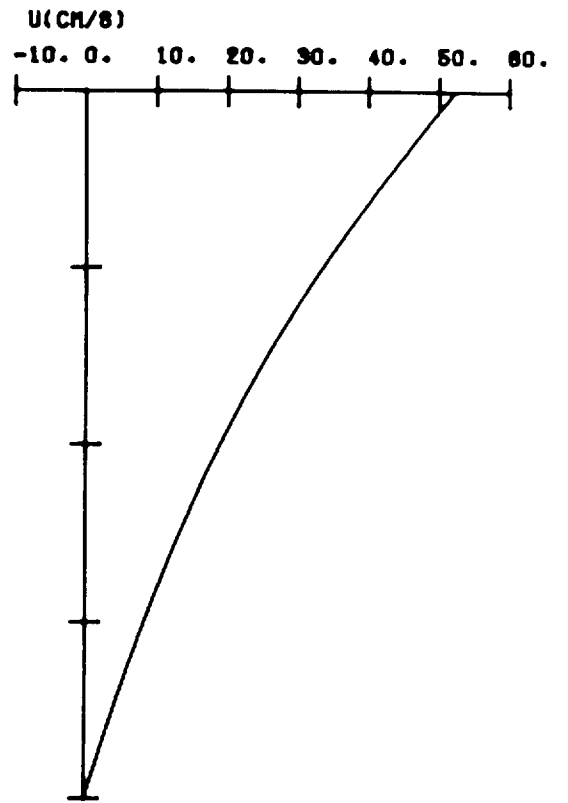


FIGURE 7b

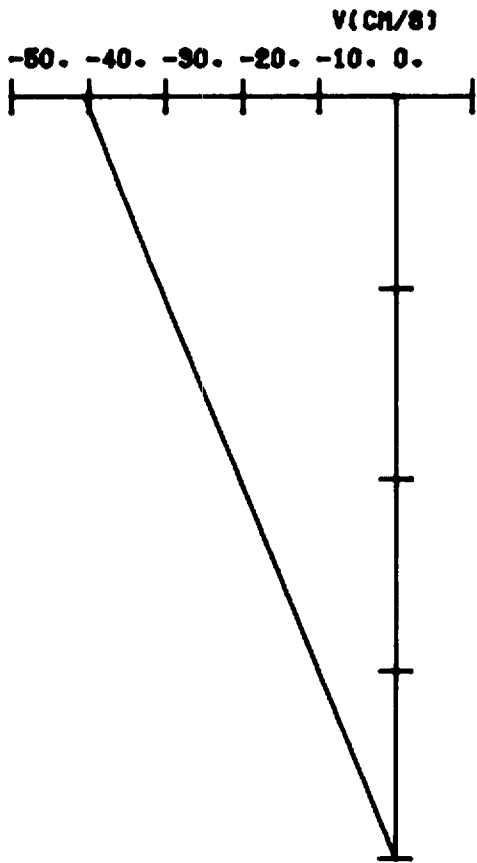
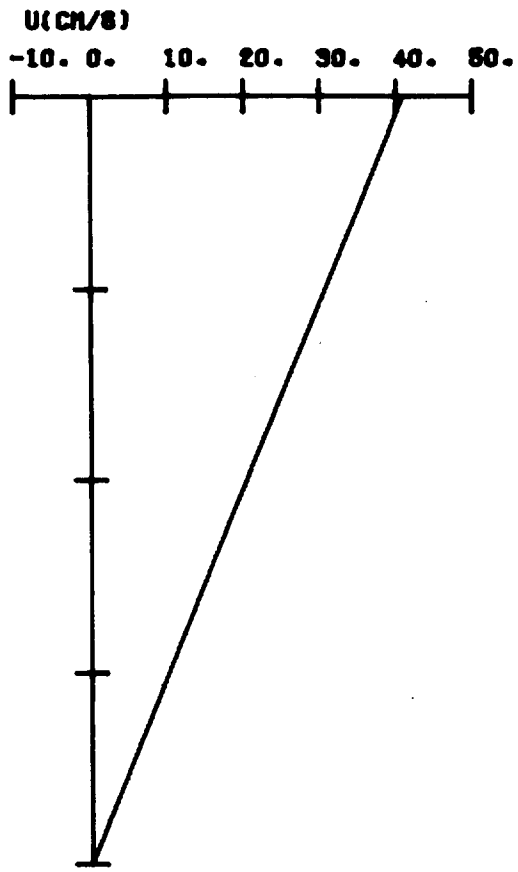


FIGURE 7c

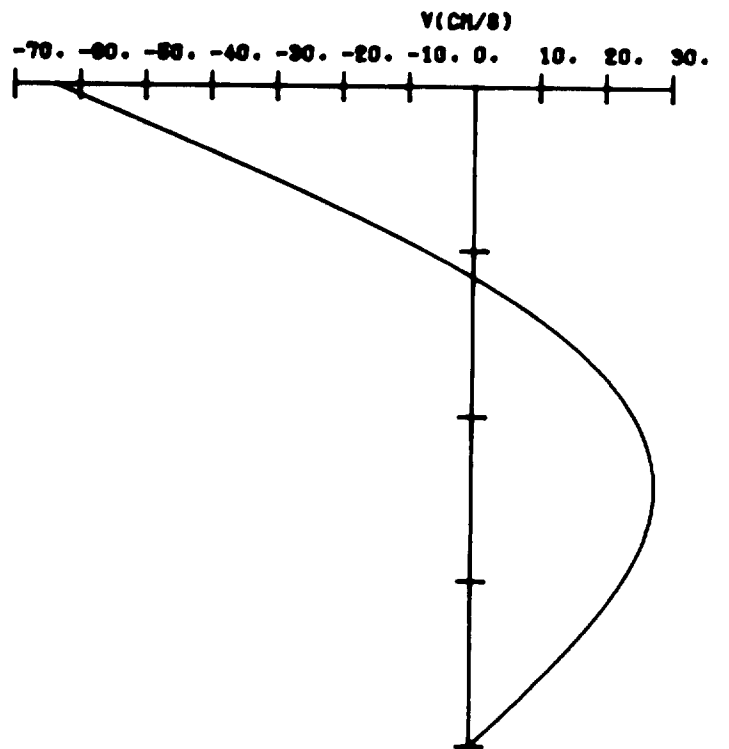
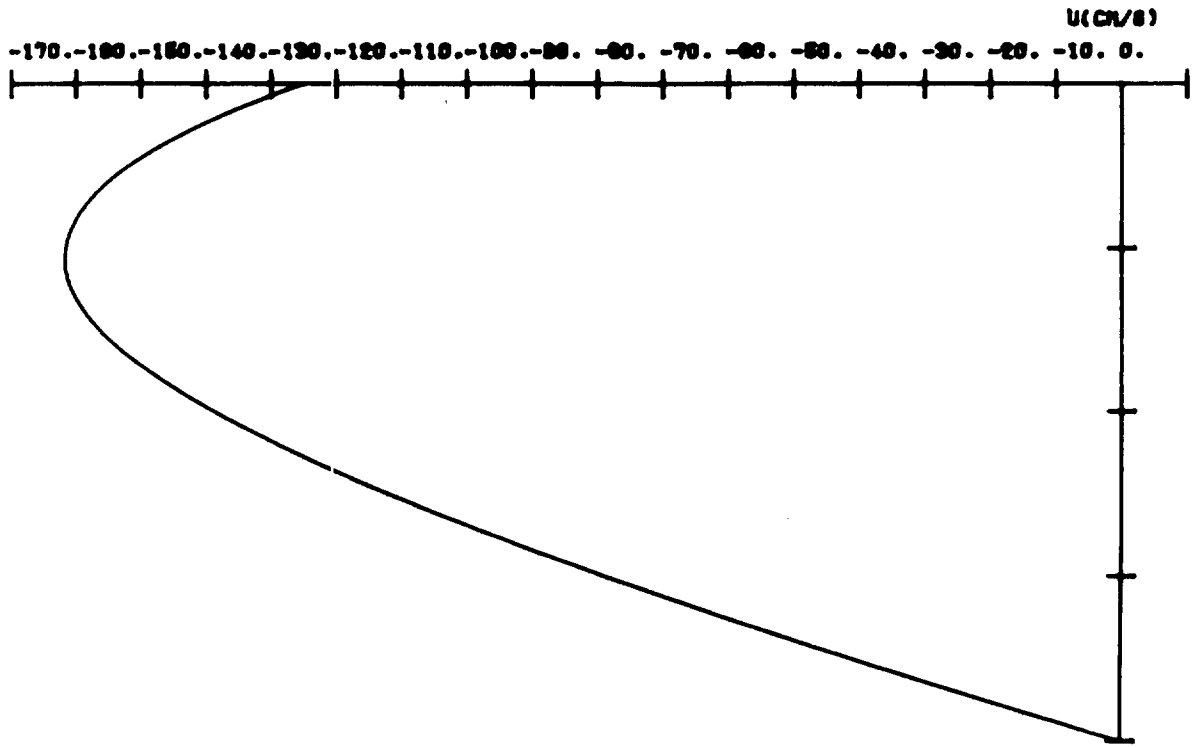


FIGURE 7d